NUREG/CR-5583
KEI No. 1656

Prediction of Check Valve Performance and Degradation in Nuclear Power Plant Systems -- Wear and Impact Tests

Final Report
September 1988 – April 1990

Prepared by M. S. Kalsi, C. L. Horst, J. K. Wang, V. Sharma

Kalsi Engineering, Inc.

Prepared for
U.S. Nuclear Regulatory Commission

AVAILABILITY NOTICE

Availability of Reference Materials Cited in NRC Publications

Most documents cited in NRC publications will be available from one of the following sources:

1. The NRC Public Document Room, 2120 L Street, NW, Lower Level, Washington, DC 20555

2. The Superintendent of Documents, U.S. Government Printing Office, P.O. Box 37082, Washington, DC 20013-7082

3. The National Technical Information Service, Springfield, VA 22161

Although the listing that follows represents the majority of documents cited in NRC publications, it is not intended to be exhaustive.

Referenced documents available for inspection and copying for a fee from the NRC Public Document Room include NRC correspondence and internal NRC memoranda; NRC Office of Inspection and Enforcement bulletins, circulars, information notices, inspection and investigation notices; Licensee Event Reports; vendor reports and correspondence; Commission papers; and applicant and licensee documents and correspondence.

The following documents in the NUREG series are available for purchase from the GPO Sales Program: formal NRC staff and contractor reports, NRC-sponsored conference proceedings, and NRC booklets and brochures. Also available are Regulatory Guides, NRC regulations in the *Code of Federal Regulations*, and *Nuclear Regulatory Commission Issuances*.

Documents available from the National Technical Information Service include NUREG series reports and technical reports prepared by other federal agencies and reports prepared by the Atomic Energy Commission, forerunner agency to the Nuclear Regulatory Commission.

Documents available from public and special technical libraries include all open literature items, such as books, journal and periodical articles, and transactions. *Federal Register* notices, federal and state legislation, and congressional reports can usually be obtained from these libraries.

Documents such as theses, dissertations, foreign reports and translations, and non-NRC conference proceedings are available for purchase from the organization sponsoring the publication cited.

Single copies of NRC draft reports are available free, to the extent of supply, upon written request to the Office of Information Resources Management, Distribution Section, U.S. Nuclear Regulatory Commission, Washington, DC 20555.

Copies of industry codes and standards used in a substantive manner in the NRC regulatory process are maintained at the NRC Library, 7920 Norfolk Avenue, Bethesda, Maryland, and are available there for reference use by the public. Codes and standards are usually copyrighted and may be purchased from the originating organization or, if they are American National Standards, from the American National Standards Institute, 1430 Broadway, New York, NY 10018.

DISCLAIMER NOTICE

NUREG/CR-5583
KEI No. 1656
RG, RV

Prediction of Check Valve Performance and Degradation in Nuclear Power Plant Systems -- Wear and Impact Tests

Final Report
September 1988 – April 1990

Manuscript Completed: May 1990
Date Published: August 1990

Prepared by
M. S. Kalsi, C. L. Horst, J. K. Wang, V. Sharma

W. S. Farmer, NRC Project Manager

Kalsi Engineering, Inc.
745 Park Two Drive
Sugar Land, TX 77478

Prepared for
Division of Engineering
Office of Nuclear Regulatory Research
U.S. Nuclear Regulatory Commission
Washington, DC 20555
NRC FIN D2510

ABSTRACT

Check valve failures in nuclear power plants have led to safety concerns as well as extensive damage and loss of plant availability in recent years. Swing check valve internals may experience premature deterioration if the disc is not firmly held open against its stop. At the present time no guidelines exist for the prediction of degradation trends and the determination of suitable inspection intervals.

This research is aimed at developing a reliable quantitative wear and fatigue prediction model for swing check valves which can be used to improve the safety and reliability of their operation. Additionally, the predictive techniques can be used to augment check valve preventive maintenance programs by providing the plant engineer with quantitative and conservative estimates of damage potential for check valve internals.

TABLE OF CONTENTS

	Page
EXECUTIVE SUMMARY	1
INTRODUCTION	2
Background	2
Overall Research Objectives	2
Phase I Research	2
Phase II Research	3
WEAR PREDICTION	5
Theoretical Wear Equation	5
Wear Coefficient, K	5
Sliding Distance	5
Load	6
ACCELERATED WEAR TESTS	7
General	7
Valve and Hinge Pin Modifications for Wear Testing	9
Selection of Materials to Accelerate Wear	9
Preliminary Wear Tests, Accuracy of Measurements, and Eliminating Effects of Corrosion and Erosion	12
Matrix of Accelerated Wear Tests	13
WEAR TEST RESULTS AND DISCUSSION	15
Accelerated Wear Test Results	15
Normalized Wear Rates	19
Comparison Between Theoretical Wear Prediction and Tests	20
WEAR PREDICTION METHODOLOGY - SUMMARY AND CONCLUSIONS	22
IMPACT AND FATIGUE PREDICTIONS	23
Theoretical Prediction Techniques	23
Disc Natural Frequency Approach	23
Pipe Eddy Frequency Approach	24
Mean and 3σ Disc Speed Approach	24
IMPACT AND FATIGUE TESTING	25
General Methodology	25
Test Valve	25
Calibration of Strain Gaged Valve Disc	29
Instrumentation	29

TEST RESULTS 30
Typical Impact Signature 30
Discussion of Impact and Disc Motion Signals 32
Discussion of Disc Motion Measurements and Modified Disc 33
Use of 3σ Disc Speed for Disc Impact Force Estimates 34
Rate of Occurrence of Impacts 35

CORRELATION OF IMPACT TEST DATA TO THEORY 37
Kinetic Energy Conversion Approach 37
Disc Oscillation Amplitude and Frequency Approach 37

IMPACT FORCE AND FATIGUE PREDICTION METHODOLOGY – SUMMARY AND CONCLUSIONS 40

CORRELATION AGAINST PLANT DATA 41
Plant Correlation Example 1: 41
18-Inch Swing Check Valves with Excessive Hinge Pin Bushing Wear
Plant Correlation Example 2: 44
18-Inch Swing Check Valves with Low Hinge Pin Bushing Wear
Plant Correlation Example 3: 44
4-Inch Tilting Disc Check Valve Modifications to Reduce Hinge Pin Wear
Plant Correlation Example 4: 45
10" Swing Check Valve Disc Stud Fatigue Failure

SUMMARY OF CHECK VALVE REVIEW METHODOLOGY 47
Overview of Check Valve Review and Analysis Procedure 47
V_{min} Calculation 47
Calculation of Modified V_{min} using C_{up} 50
Wear and Fatigue Calculations 51
Conclusions 51

REFERENCES 52

APPENDIX A: Impact and Fatigue Prediction Methods
APPENDIX B: Calculation of V_{min}, Flow Velocity, and Wear Rate for Plant Correlation Example 1
APPENDIX C: Correlation of Fatigue Analysis with Available Plant Data for Plant Correlation Example 4
APPENDIX D: Plots of Mean Disc Speed and 3-Sigma Disc Speeds for the 3-Inch and 6-Inch Test Swing Check Valves

LIST OF FIGURES

Figure No.		Page
1	Typical Swing Check Valve Geometry	4
2	Instrumented Test Valve	7
3	Valve Modifications for Accelerated Wear Tests	10
4	Modified Hinge Pin for Accelerated Wear Tests	11
5	Typical Aluminum Hinge Pin and Bushings Used in Wear Tests	11
6	Multihole Orifice Plates Used to Generate Turbulence	12
7	Typical Hinge Pin Wear Results for the 3-Inch Swing Check Valve (Upstream Disturbance: 36 x 3/16-Inch Hole Turbulence Plate at 2.5 D)	15
8	Accelerated Wear Test Results for the 3-Inch Valve	17
9	Accelerated Wear Test Results for the 6-Inch Valve	18
10	Comparison of Accelerated Wear Test Results to Theoretical Predictions	21
11	Instrumented Disc Cross Section	25
12	Strain Gage Bridge Schematics	26
13	Strain Gaged Check Valve Disc	26
14	Detail of Strain Gage Installation	27
15	Disc Showing Sealed Wire Exit	27
16	Wire Exit from Disc	28
17	Completion of Pressure Boundary Using Hermetic Connector	28
18	Impact Signature, Upstream Turbulence Source	31
19	Impact Signature, Upstream Elbow	31
20	Impact Signature, Upstream Turbulence (Modified Disc)	31
21	Raw and Filtered Impact Force Signatures	32
22	Disc Displacement Plot Corresponding to Impact Event of Figure 21	33
23	Impact Measurement Assembly	34
24	Impact Force Survey (Based on Filtered Signal, lbs)	36
25	Impact Force Survey (Based on Filtered Signal, lbs)	36
26	18-Inch Swing Check Valve Installation Used in Example 1	42
27	Hinge Pin Bushing Wear in 18-Inch Valves (Example 1)	43
28	Severe Hinge Pin Wear in 4-Inch Tilting Disc Check Valve	44
29	Minimum Velocity Formula Comparison Against Test Results	48
30	Significance of Disc Projection (Y/D) on Performance	49

LIST OF TABLES

Table No.		Page
1A	Data for 3-Inch Valve	8
1B	Data for 6-Inch Valve	8
2	Matrix of Hinge Pin Accelerated Wear Tests	14
3	Summary of Hinge Pin Accelerated Wear Tests	14
4	Summary of Test Parameters and Wear Rates Results of Hinge Pin Accelerated Wear Tests	16
5	Disc Assembly Resonant Frequencies, hz	30
6	Impact Force Ranges (After Low-Pass Filtering)	35
7	Comparison of Theoretical and Measured Impact Forces 6-Inch Modified Disc Assembly; High Turbulence Source at 1.5 Diameters Upstream	39

ACKNOWLEDGEMENTS

We are greatful for the funding provided by the Small Business Innovation Research program of the U. S. Nuclear Regulatory Commission which made this research possible. Special thanks are due William S. Farmer of the NRC for his guidance and encouragement throughout the project.

The authors would also like to pay special recognition to Daniel Alvarez for the development of the load cell concept employed in these tests, and to Bobbie Lambert for patiently working through many revisions and for her painstaking attention to detail in preparing this manuscript.

EXECUTIVE SUMMARY

Check valve failures at nuclear power plants in recent years have led to serious safety concerns, and caused extensive damage to other plant components which had a significant impact on plant availability. In order to understand the failure mechanism and improve the reliability of check valves, a systematic research effort was proposed by Kalsi Engineering, Inc. to U.S. Nuclear Regulatory Commission (NRC) under their Small Business Innovation Research (SBIR) program. The overall goal of the research was to develop models for predicting the performance and degradation of swing check valves in nuclear power plant systems so that appropriate preventive maintenance or design modifications can be performed to improve the reliability of check valves.

Under Phase I of this research, a large matrix of tests was run with instrumented swing check valves to determine the stability of the disc under a variety of upstream flow disturbances (elbows, reducers, butterfly valves, and multiple hole orifice plates as high turbulence sources), covering a wide range of disc stop positions (50 to 75 degrees) and flow velocities (up to 20 ft/sec) in two different valve sizes (3- and 6-inch). Phase I research led to the development of upstream flow disturbance factors which should be taken into account to determine the minimum velocity required to achieve a stable, full open disc position. The matrix of tests also quantified the severity of the disc fluctuations that can be expected when these minimum velocity requirements are not met. The results of Phase I research were published in NUREG/CR-5159.

The goals of Phase II research were to develop predictive models which quantify the anticipated degradation of swing check valves that have flow disturbances closely upstream of the valve and are operating under flow velocities that do not result in full disc opening. Two major causes of swing check valve failure are premature degradation due to hinge pin wear and fatigue of the disc stud connection to the hinge arm. A matrix of accelerated wear tests were performed using aluminum hinge pins and bushings in the 3- and 6-inch valves to quantify wear experienced in the hinge pin area. A special disc instrumented with strain gages was used in the 6-inch valve to measure the impact forces and their rate of occurrence to quantify the fatigue damage caused by tapping of the disc against the stop. Based on this theoretical and experimental research, wear and fatigue prediction models have been developed which show good correlation against laboratory test results as well as against a limited number of check valve failures at the plants which had been sufficiently documented in the past.

This research allows the inspection/maintenance activities to be focussed on those check valves that are more likely to suffer premature degradation. The quantitative wear and fatigue prediction methodology can be used to develop a sound preventive maintenance program. The results of the research also show the improvements in check valve performance/reliability that can be achieved by certain modifications in the valve design.

INTRODUCTION

Background

A review of check valve failures in nuclear power plants shows that severe degradation of the internals during normal plant operation is responsible for most of the failures (Refs. 1 through 8). Ideally, check valves should be sized to provide full disc lift under normal flow conditions, and should be located sufficiently away from upstream flow disturbances to avoid premature degradation. Where these ideal conditions are not met, all check valves can be expected to experience some degradation. However, the level of degradation may vary from negligible to very severe, depending upon a number of factors relating to the design, installation, operating conditions, usage, and maintenance practices. Previous surveys have shown that, even though over 70 percent of the check valve installations do not meet the "ideal" requirements of minimum flow velocity and distance from upstream flow disturbances (Ref. 9), serious problems do not exist with this large population of valves. In fact, the actual percentage of check valves that fail in service due to premature degradation is estimated to be only 1 to 2 percent (Refs. 2, 3). This shows that the previous classification of "misapplied" check valves (based on failing minimum velocity and proximity of the upstream disturbance criteria) is too coarse, and better screening techniques are need to truly identify the valves that are most likely to suffer from premature degradation.

Overall Research Objectives

In order to accomplish this goal of better identifying swing check valves that are most likely to suffer premature degradation, Kalsi Engineering, Inc. proposed a systematic research program to the U.S. Nuclear Regulatory Commission under the Small Business Innovation Research (SBIR) program. The major objective of the proposed research was to develop *quantitative* techniques for predicting swing check valve performance and degradation in nuclear power plant systems. These predictive techniques can be integrated into preventive maintenance programs with the aim of identifying the few valves most likely to be suffering from accelerated degradation and ensuring that maintenance efforts are expended first on those valves with the greatest need. The proposed research was selected and funded by NRC in two phases. Phase I was completed in April 1988, the results of which were published in Reference 1. Since the details of Phase I research are important for a complete understanding of the overall predictive techniques developed under Phase I and II, the reader is encouraged to familiarize himself with the contents of Reference 1 which are briefly summarized here.

Phase I Research

The major objective of Phase I research was to investigate the stability of the swing check valve disc at different flow velocities in piping systems that have significant flow disturbances within 10 pipe diameters upstream of the check valve. The effects of elbows, reducers, and turbulence sources of varying degrees of severity on the disc stability were investigated. A matrix of over 2,000 flow tests was completed to determine the disc stability of three-inch and six-inch swing check valves. Under these upstream flow disturbances, the minimum flow velocity requirements to achieve full disc opening, as well as the maximum disc fluctuations (when the flow velocities are less than the minimum requirements), were determined for a wide range of test conditions.

Phase II Research

The objective of Phase II research was to develop quantitative techniques for predicting the degradation of internals of swing check valves operating under velocities insufficient to fully open the disc. Figure 1 shows a typical swing check valve. There are two major areas in swing check valves that are subject to premature degradation: the hinge pin, and the disc stud connection to the hinge arm. Hinge pin failures are caused by excessive wear, and disc stud connection failures occur because of impact related fatigue.

The overall goals of Phase II research were accomplished by the development of appropriate theoretical models supported by necessary laboratory testing, and then correlation to actual plant data that were available. Accelerated wear testing using aluminum hinge pins and bushings was done on three-inch and six-inch instrumented test valves for a number of upstream flow disturbance configurations. Impact force measurements were made in the six-inch test valve using a disc that had been modified to incorporate strain gages.

As a result of this extensive theoretical and experimental research, predictive methodology for quantifying degradation of the check valve internals caused by hinge pin wear or disc stud impact has been developed. The predictions were found to be in reasonable agreement with the actual performance at the operating plants, as shown in the plant correlation examples. For reliable predictions based on the methodology developed, a detailed knowledge of the geometry and design of the check valve internals, its installation details, operating conditions, and usage is required. The predictions should be compared with the actual performance history, whenever possible, to refine various assumptions used in the analytical methodology. When properly implemented and integrated with the preventive maintenance activities, the quantitative degradation prediction techniques developed under Phase I and II research have the potential of significantly improving the overall reliability of the check valves in nuclear power plants.

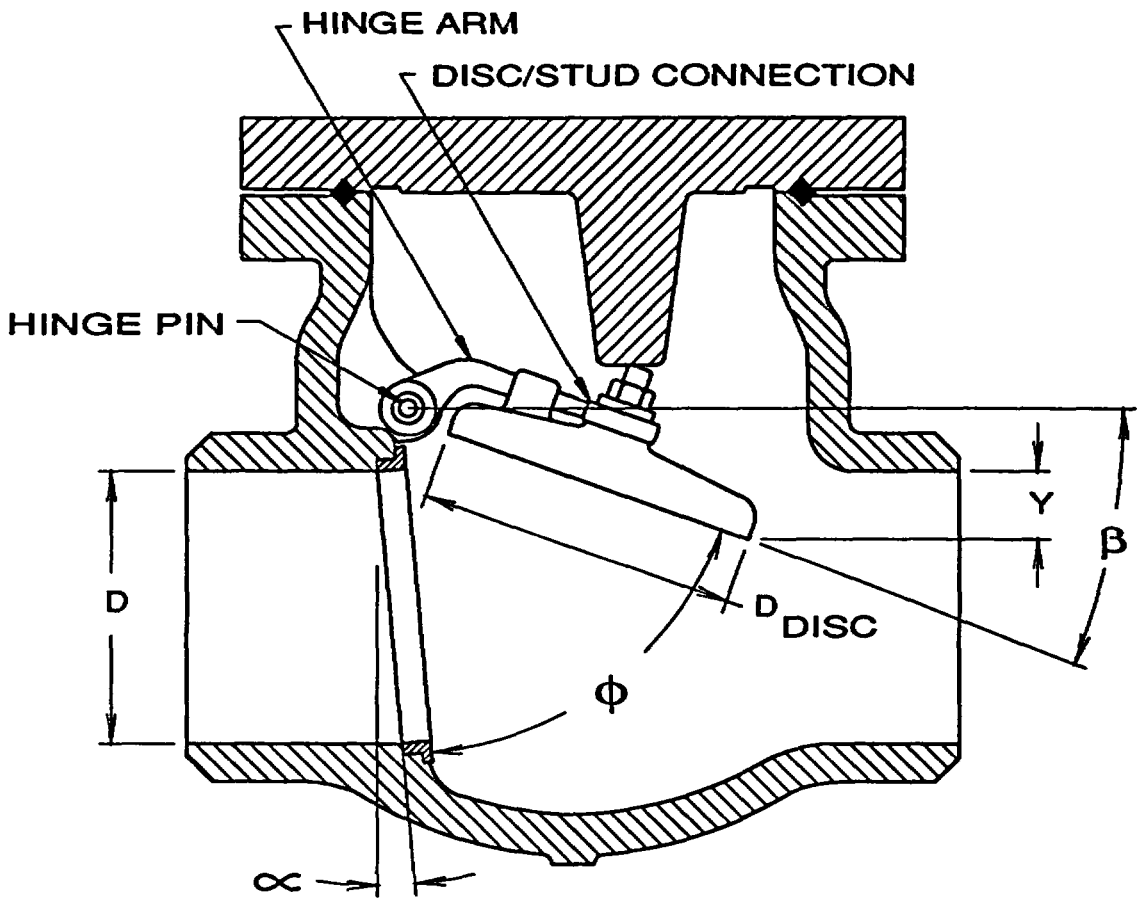

Figure 1

Typical Swing Check Valve Geometry

WEAR PREDICTION

Theoretical Wear Equation

Excessive hinge pin wear is a common cause of many swing check valve and tilting disc check valve failures. Adhesive wear is the most commonly encountered and least preventable form of wear in sliding contacts. Hinge pin wear, whether it is caused by a two-body adhesive mechanism in which wear particles escape the rubbing interface or a three-body abrasive wear mechanism in which wear particles remain entrapped at this interface, can be predicted by a simple equation which has the same form for both types of wear mechanisms (Ref. 10):

$$W = \frac{K L V t}{H}$$

where W = Volume of material worn away

L = Load between the two bodies in sliding contact

V = Relative velocity between sliding surfaces

t = Time over which sliding occurs

H = Penetration hardness of the surface of material being worn away

K = Nondimensional "wear coefficient" for the sliding pair of materials

Wear Coefficient, K

Ideally, an experimentally determined value of the wear coefficient for the sliding material combination under the actual environmental conditions should be used to make accurate wear predictions. The wear coefficient can be determined experimentally by using any of the standard wear test machines described in Reference 10. In the absence of an experimentally determined wear coefficient for the exact material combination and environmental conditions of interest, a reasonable choice can be made by judicious use and interpolation of available data from various sources. The use of previously published data for wear coefficients requires a careful consideration of several factors such as compatibility of the alloying elements used in the metal pair, the degree of lubrication provided by the fluid, and the operating temperature. Adhesive wear coefficients span a range from 3×10^{-6} to 1500×10^{-6} for various combinations of metal surfaces sliding under varying degrees of lubricity provided by water and steam to no lubrication. Extensive work has been done in this area by Rabinowicz (Refs. 10, 11) to develop a table of wear coefficients for adhesive wear, which can be used within its statistical bounds of uncertainty to make wear estimates. However, it is important to note that the individual behavior of a specific tribological pair of metals may be higher or lower than the average of the category into which they fall (Ref. 11). Actual data for the specific metal combinations, therefore, remains the best choice for accurate wear predictions.

Sliding Distance

In the wear equation (1), the term V t can be equated to d, the total distance the two wear surfaces have slid relative to each other. For check valves, this total sliding distance can be estimated from the disc oscillation frequency and its amplitude. The amplitude of disc

fluctuation depends upon the type of upstream disturbance and its proximity. The results of extensive testing on three-inch and six-inch valves under Phase I in which disc fluctuations were measured under a variety of common upstream disturbances are documented in Ref. 1. Evaluation of the disc motion data obtained from the Phase I tests shows that in general the disc does not oscillate at a well-defined single frequency. However, an estimate of the dominant frequency at which the disc is likely to oscillate can be made by calculating the disc natural frequency based on one of three methods: fluid spring stiffness, pendulum frequency, and eddy frequency approaches as described in Appendix A. Alternatively, the mean disc speed can be used directly in making wear calculations, if it is known. Appendix D includes the results of Phase I test data which were processed to obtain the mean and 3σ disc speeds as a function of flow velocity, upstream disturbances, and full disc opening angles for the three- and six-inch test valves. These data span a range of flow velocities and upstream disturbances and their proximity to the check valve. These disc speeds can be used directly or for reference and comparison against the frequency- and amplitude-based disc speed estimates.

Load

The load, L, between the hinge pin and the bushing is the result of disc weight and fluid dynamic lift and drag components on the disc. A free body diagram analysis of the complete force system shows that this resultant load remains within ± 20 percent of the effective disc weight for swing check valves over a wide range of disc opening angles. Since the uncertainty in wear coefficients is much larger than this, the effective disc weight, which includes the hinge arm weight contribution ($W_{eff} = W_{disc} + 0.5\ W_{arm}$), can be used as the total reaction load in making wear estimates for swing check valves. However, in tilting disc check valves, since the disc remains in the flow stream, fluid dynamic drag forces at very high fluid velocities and for non-aerodynamically shaped discs will be much higher than for swing check valves. The total hinge pin reaction load can therefore be significantly higher than the disc weight alone. Fluid dynamic drag forces should, therefore, be considered in determining total load estimates for tilting disc check valves.

ACCELERATED WEAR TESTS

General

Accelerated wear tests were performed using aluminum hinge pins and bushings in the three-inch and six-inch swing check valves under a number of upstream flow disturbance configurations and flow velocities to validate and support the development of a reliable wear prediction model. Aluminum wear parts have been primarily used by others in determining relative wear trends in double disc and swing check valves; however, no attempt was made in these studies to achieve correlation against absolute wear rate predictions (Refs. 13, 14). By substituting soft aluminum for the hardened carbon steel or stainless steels normally used as hinge pin/bushing materials, significant amounts of wear can be produced within a few hours that normally take several months or years of actual operation in the plant. The ability to run many tests allowed the important parameters to be varied in a systematic manner in a matrix of accelerated wear tests, discussed in the following sections.

Figure 2 shows the three-inch test valve with a Plexiglass bonnet and a displacement transducer for continuous disc motion monitoring. Dimensional and weight data for the three-inch and six-inch test valves used in Phase I and II tests are included in Tables 1A and 1B.

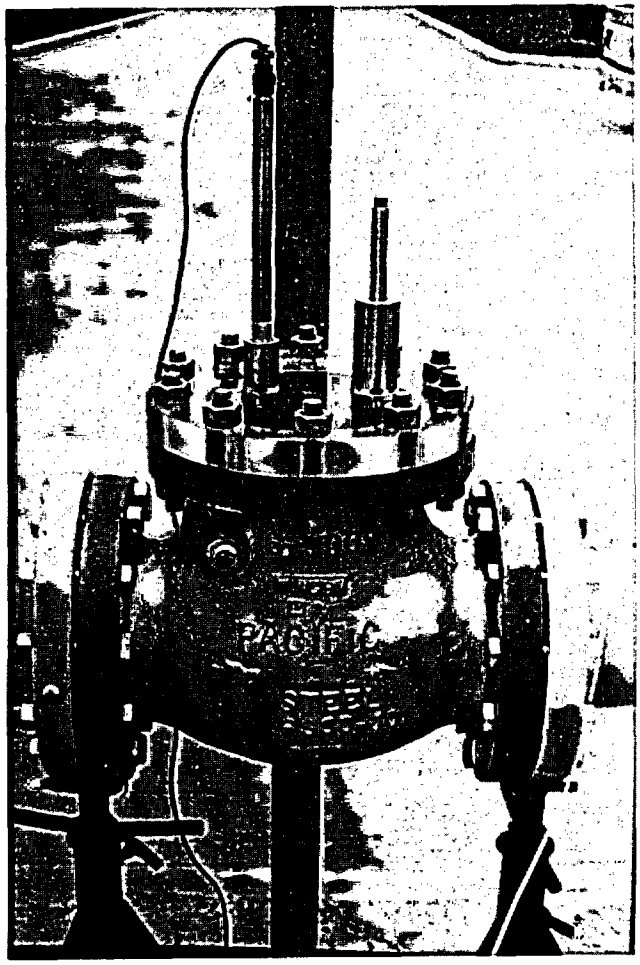

Figure 2
Instrumented Test Valve

Valve Type	3", 300# Swing Disc Check
Manufacturer	MCC Pacific Valve Company
Weight and Dimensional Data	
Disc Weight (incl. nut), W_{disc}	1.94 lbs.
Hinge Arm Weight, W_{hinge}	0.72 lbs.
Hinge Pin Diameter, d_{hinge}	0.375"
Disc O.D., D_{disc}	3.90"
Seat Bore Diameter, D	3.0"
Seat Tilt From Vertical, α	3°
Full Open Angle From Vertical, $\alpha + \phi$	73°
Fluid Impingement Angle, θ	17°*
Hinge Pin to Disc Stud Distance, R	2.85"
Disc Projection, Y	0.0"

Table 1A
Data for 3-Inch Valve

Valve Type	6", 300# Swing Disc Check
Manufacturer	MCC Pacific Valve Company
Weight and Dimensional Data	
Disc Weight (incl. nut), W_{disc}	8.94 lbs.
Hinge Arm Weight, W_{hinge}	3.38 lbs.
Hinge Pin Diameter, d_{hinge}	0.500"
Disc O.D., D_{disc}	6.90"
Seat Bore Diameter, D	6.0"
Seat Tilt From Vertical, α	3°
Full Open Angle From Vertical, $\alpha + \phi$	70°
Fluid Impingement Angle, θ	20°*
Hinge Pin to Disc Stud Distance, R	5.12"
Disc Projection, Y	0.8"

Table 1B
Data for 6-Inch Valve

* See discussion on the effect of valve geometry on fluid impingement angle θ in section entitled "Summary of Check Valve Review Methodology."

Valve and Hinge Pin Modifications for Wear Testing

Figures 3, 4, and 5 show the modifications made in the hinge pin and the hinge arm bushing area of the test valves to incorporate certain key features. The hinge pin wear area was reduced to relatively narrow bands, approximately 1/16-inch wide, so that reduction in the wear diameter could be accurately measured to within ± .0001-inch. Even though actual weight loss measurement (within ± 0.2 milligrams accuracy) was used as the primary method of wear quantification, the diametrical measurements were used as an independent check on the location and magnitude of wear. In order to ensure that wear took place at the same location on the wear bands, an indexing slot and tang arrangement was used on one end of the pin to prevent rotation of the pin and ensure the correct angular orientation after disassembly and reassembly to make intermediate weight loss measurements. Pin rotation was prevented to ensure that all of the wear occurred between the wear bands on the aluminum hinge pin and the aluminum bushing and that no sliding took place between the aluminum hinge pin and the carbon steel body.

To allow for easy removal of the hinge pin for frequent weight-loss measurements, a dummy pin could be inserted which pushed out the test pin and simultaneously supported the hinge arm. The hinge pin was provided with generous chamfers so it would slide in and out smoothly.

Selection of Materials to Accelerate Wear

A thorough investigation of the type of aluminum to be used was done to ensure that reliable wear data could be developed. Heat treatable aluminum alloys such as 6061-T6, 7075-T6, etc., were ruled out to avoid possible problems caused by continuing change in their mechanical properties due to their age hardening characteristics. To achieve high wear rates and maintain reasonably constant material properties, commercially pure aluminum (Alloy 1100F) was selected because of its low hardness and its freedom from age hardening phenomenon. After machining, the aluminum hinge pin was fully annealed to develop the desired mechanical properties. In this condition, the hardness of the material was tested to be 23 Brinell. The material had a yield strength of 3,600 psi, tensile strength of 12,000 psi with 51 percent elongation, and 93 percent reduction of area. In order to guarantee consistency of material behavior from pin to pin, all test pins of the same size were made from the same bar, even though different bars were used for different sizes.

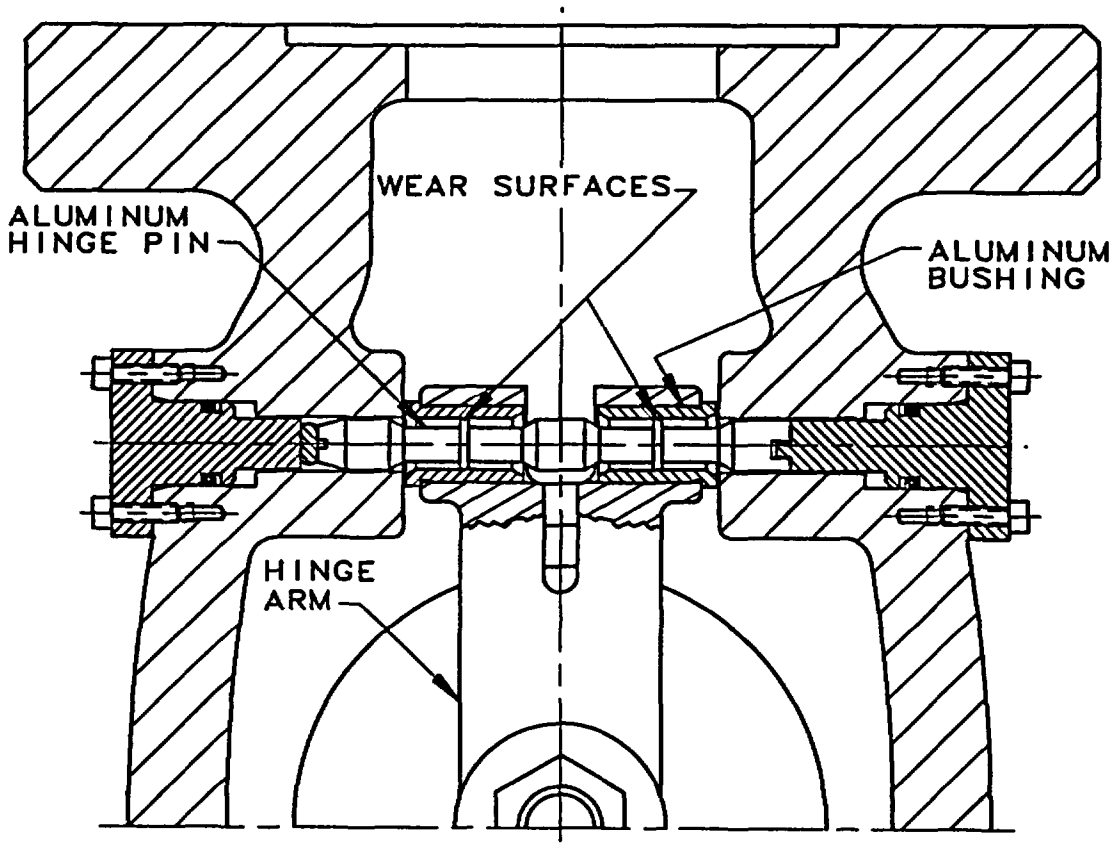

Figure 3

Valve Modifications for Accelerated Wear Tests

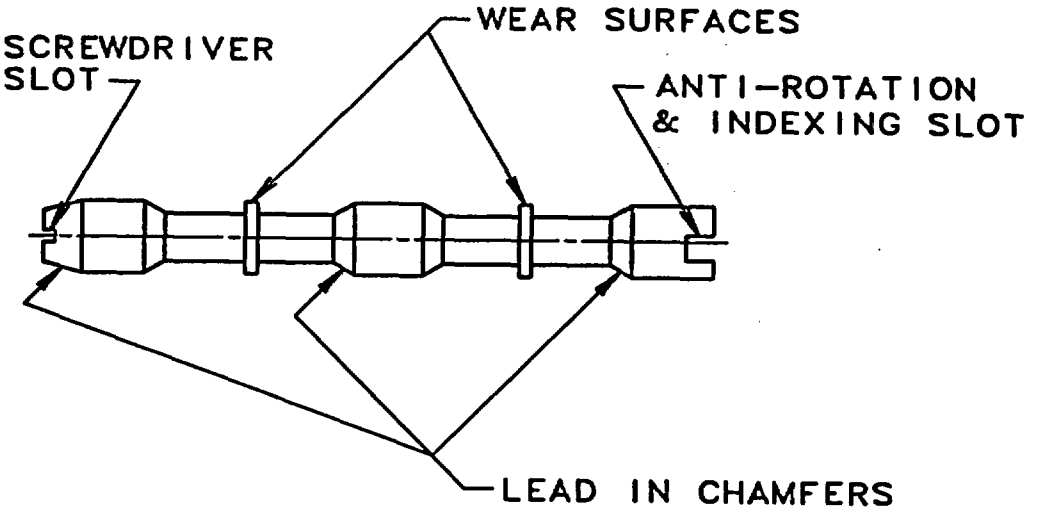

Figure 4

Modified Hinge Pin for Accelerated Wear Tests

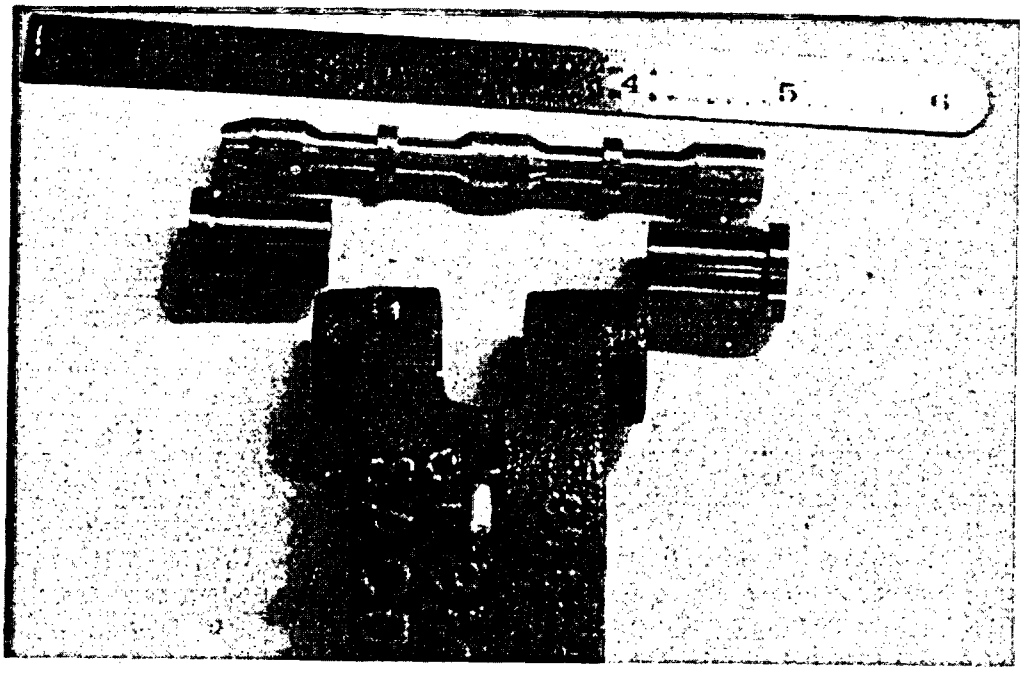

Figure 5

Typical Aluminum Hinge Pin and Bushings Used in Wear Tests

Preliminary Wear Tests, Accuracy of Measurements, and Eliminating Effects of Corrosion and Erosion

All of the preliminary wear tests were performed on the three-inch Pacific swing check valve with a multi-hole orifice plate placed 2.5 diameters upstream. A number of multi-hole orifice plates were used in Phase I tests (Fig. 6); the specific orifice plate used in Phase II tests had 36 holes of 3/16-inch diameter, which was determined to be the most severe turbulence source during the Phase I tests. The flow velocity chosen for these tests was 7 ft/sec, which corresponds to a zone of operation where the mean disc speed of the fluctuating disc was near its maximum value (around 22°/sec), but the disc stud was not tapping against the backstop. These test conditions were chosen to create maximum wear rates for the three-inch valve during preliminary testing.

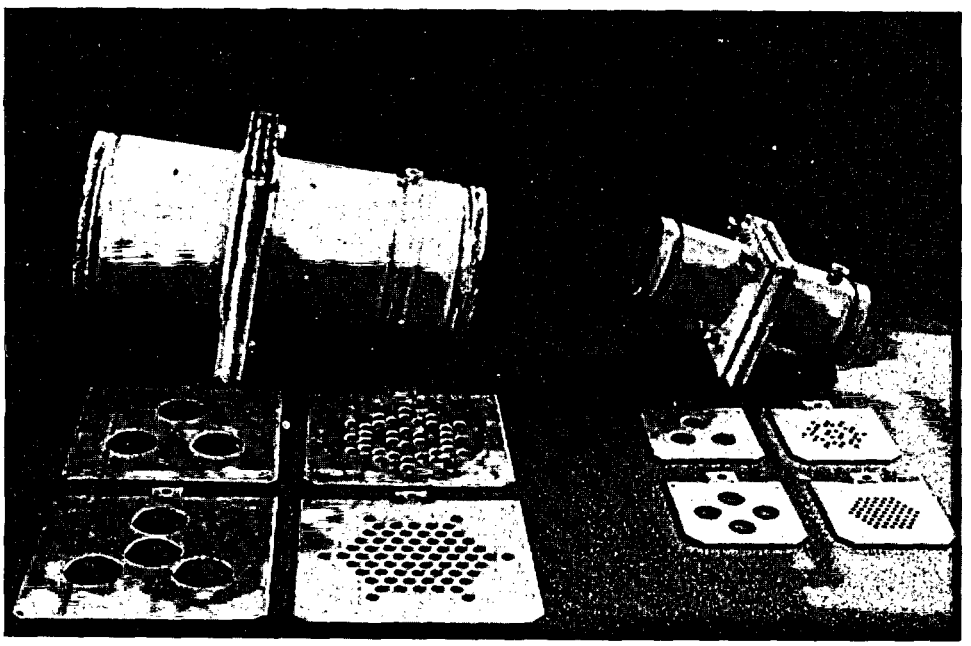

Figure 6
Multihole Orifice Plates Used to Generate Turbulence

A series of tests were run with the objective of accurately quantifying wear rates and separating them from other effects such as corrosion or erosion which can also cause a material loss from the hinge pin. Initial tests were run with the aluminum hinge pin being run against 17-4 PH stainless steel bushings. In order to separate the contribution of material loss caused by sliding wear from that caused by corrosion and erosion, a series of tests was run: one in which the disc was allowed to oscillate, the second in which the disc was prevented from fluctuating by bringing the backstop down to the appropriate position,

and another with pins immersed in still water. These tests revealed that the material loss due to corrosion was not an insignificant part of the total hinge pin weight loss for the three-inch valve hinge pin. From these results, it was concluded that provisions will need to be made to reduce the corrosion material loss so that it is well below the levels encountered in these tests.

It was decided to anodize the aluminum hinge pin to eliminate corrosion related material loss, leaving the wear band areas on the hinge pin unanodized by masking them during the anodizing process. The next series of tests run with the anodized aluminum hinge pin against 17-4 PH stainless steel bushings confirmed that corrosion wear effects were virtually eliminated, and practically all of the weight loss encountered was attributable to sliding wear. However, it was also found that the actual wear rates obtained by using the aluminum hinge pin against 17-4 PH stainless steel bushings were less than our goal to accomplish accelerated wear testing within 20 to 30 hours average for any given set of conditions being tested.

Since it is well documented (Refs. 10, 11) that the wear coefficients using an identical pair of materials (e.g., Al vs Al) at the sliding contact are on the average three times higher than those obtained with compatible material (e.g., Al vs. Fe), the next series of tests were run with the aluminum hinge pin sliding against aluminum bushings. The specific aluminum alloy selected for the bushings was 7075-T6, which is harder than the 1100F alloy used for the hinge pin. This was done to ensure that wear would occur predominantly on the hinge pin. As expected, this change produced higher wear rates, thus permitting typical test durations of 20 to 30 hours during subsequent tests. As described in more detail later, the actual test duration for any given configuration ranged from 6 hours to 40 hours. The minimum duration of each test was governed by our goal of reducing the overall error to less than 10 percent in the weight loss measurements considering the accuracy and repeatability of the laboratory balance used, and the amount of material that could be lost while removing and inserting the hinge pin for intermediate measurements.

This concluded the preliminary debugging stage of the wear tests. All of the subsequent long-term wear tests were done with the aluminum hinge pin (with the non-wearing surface anodized) sliding against the aluminum bushing.

Matrix of Accelerated Wear Tests

Table 2 shows the matrix of accelerated wear tests that were run on the three- and six-inch valves. Two types of disturbances at varying upstream distances were used in a judicious manner to cover the anticipated range in the mean disc speed, which, as predicted by the fundamental wear equation, should directly affect the wear rates in a linear manner. The turbulence plates with small holes used in Phase I tests that produced the most severe disc oscillations were used as one of the upstream flow disturbances, with upstream distances ranging up to 10 diameters. An "elbow up" configuration at different upstream distances was used as the second source of flow disturbance. Table 2 identifies flow disturbance, flow velocity, test number, and the total hours of testing for each configuration.

For each valve size, the flow velocities chosen corresponded to the approximate range of maximum disc fluctuations. In some tests, the flow velocity was intentionally selected to be different to determine if the wear behavior followed the predictions based on the fundamental wear equation. In one of the tests, a combination of the two flow disturbances

(elbow up plus turbulence plate) was used to study its combined effect on the wear rates. All together, a total of eight unique test configurations identified by A-1 through A-8 were tested for the three-inch valve, and seven configurations identified by B-1 through B-7 were tested for the six-inch valve. As summarized in Table 3, the average duration of tests was 30.6 hours and 19.7 hours respectively for the three-inch and six-inch valves. Each test was spanned by several intermediate segments to inspect the wear surfaces and make intermediate weight measurements. The test segments averaged 5.1 hours and 7.7 hours respectively for the three-inch and six-inch valves.

Valve Size	*Disturbance Source*	*Flow Velocity*	*Test Number*						*Total Test Hours*
			Distance To Disturbance Source						
			0D	*1.5D*	*2.5D*	*3D*	*4.5D*	*10D*	
3"	36 x 3/16" Turbulence Plate	7 fps		A-8	A-1 A-3		A-2	A-4	138
	Elbow Up	7.5 fps	A-5			A-6			76
	Elbow Up + 36 x 3/16" Turbulence Plate	7.5 fps		A-7					8
6"	36 x 3/8" Turbulence Plate	5.5 fps		B-1	B-6		B-5		58
	Elbow Up	5.5 fps	B-4			B-7			53
	Elbow Up	9.0 fps	B-2						21
	Elbow Up, (w/worn pin)	5.5 fps	B-3						6

Table 2
Matrix of Hinge Pin Accelerated Wear Tests

Test Valve Size	*Number of Tests*	*Total Number of Testing Hours*	*Average Duration of Test per Configuration (Hours)*	*Average Duration of Each Test Segment (Hours)*
3"	8	222	27.8	6.3
6"	7	138	19.7	7.7

Table 3
Summary of Hinge Pin Accelerated Wear Tests

WEAR TEST RESULTS AND DISCUSSION

Accelerated Wear Test Results

Figure 7 shows a typical plot obtained from the accelerated wear test (Test No. A-1) on the three-inch test valve, with a severe turbulence source (orifice plate with 36 holes of 3/16-inch diameter each) located 2.5 diameters upstream of the check valve. Intermediate measurements after each test segment show that the hinge pin wear follows a linear trend as predicted by the wear equation. The number of intermediate weight measurements was different for each test, but in each case no significant deviations from a linear trend was noted. The average wear rate for this test configuration is found to be 0.95 mg/hr.

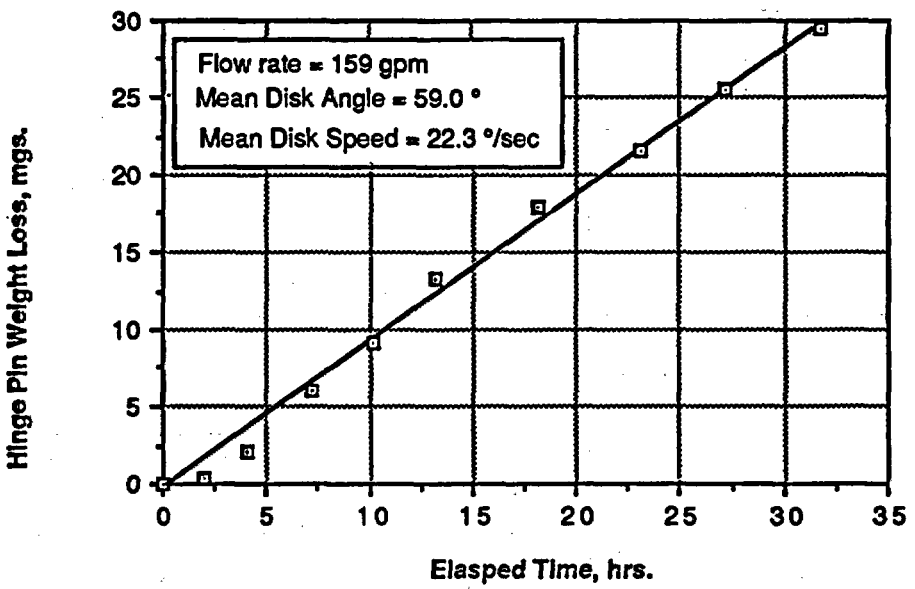

Figure 7

Typical Hinge Pin Wear Results for the 3-Inch Swing Check Valve (Upstream Disturbance: 36 x 3/16 Inch Hole Turbulence Plate at 2.5 D)

The overall results of all the accelerated wear tests performed on the three-inch and six-inch test valves are summarized in Table 4. The wear rates were found to span a range from 0.11 mg/hr to 0.95 mg/hr for the three-inch valve and 0.37 mg/hr to 2.8 mg/hr for the six-inch valve, depending upon the upstream disturbance source and its proximity.

Valve Size	*Test No.*	*Number of Hours of Testing*	*Mean Disc Angle (°)*	*3σ Disc Fluct. (°)*	*Mean Disc Speed (°/sec)*	*3σ Disc Speed (°/sec)*	*Wear Rate (mgs/hr)*
3"	A-1	32	59.0	12.8	22.3	50.8	0.95
	A-2	30	60.6	7.8	15.1	34.8	0.39
	A-3	8	60.5	11.2	20.0	47.1	0.51
	A-4	31	60.9	3.8	6.3	14.4	0.16
	A-5	36	60.0	5.4	10.7	25.0	0.33
	A-6	40	60.8	3.4	6.1	14.3	0.11
	A-7	8	60.8	14.0	27.9	63.4	0.86
	A-8	37	59.6	11.6	20.3	47.5	0.70
6"	B-1	13	58.1	13.8	17.0	42.4	2.80
	B-2	21	66.1	6.0	9.9	23.6	2.48
	B-3	6	60.3	5.2	4.9	13.2	1.04
	B-4	29	60.3	5.8	6.4	15.3	0.37
	B-5	23	58.2	9.6	11.6	26.3	1.38
	B-6	22	53.4	13.0	14.6	32.7	2.52
	B-7	24	60.5	4.4	5.5	12.9	0.47

Table 4
Summary of Hinge Pin Wear Test Results

To provide better insight into the overall results from accelerated wear tests, wear rates are plotted as a function of mean disc speed for the three-inch and six-inch valves in Figures 8 and 9 respectively. The tables in these figures are arranged in order of decreasing mean disc speed, regardless of the type of upstream disturbance and its proximity.

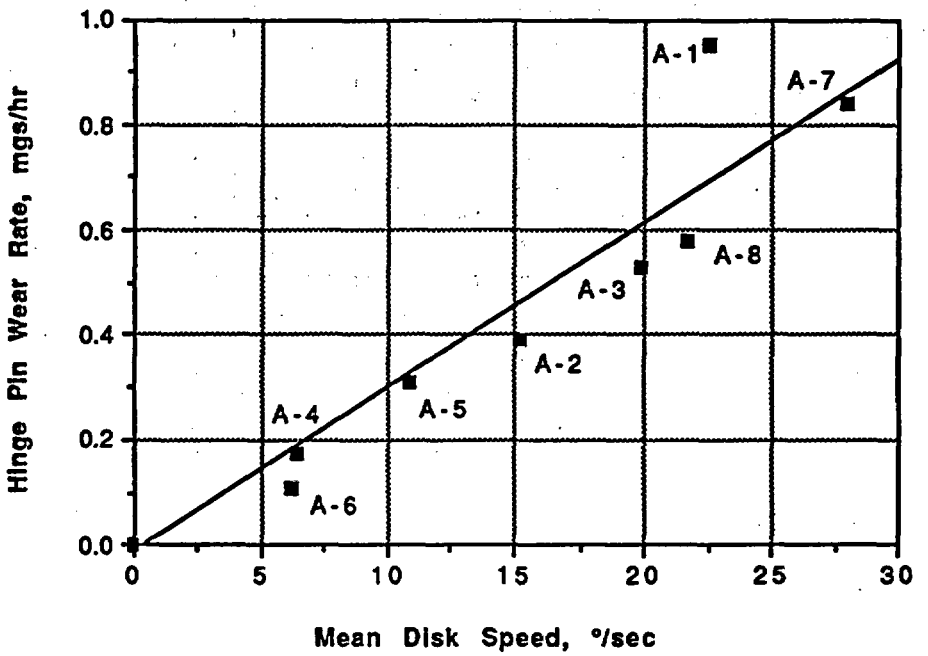

Upstream Disturbance	*Upstream Distance*	*Mean Disk Speed degrees/second*	*Wear Rate mgs/hr*	*Test Number*
Elbow Up + Turbulence Plate	1.5D	27.9	0.86	A-7
Turbulence Plate	1.5D	20.3	0.70	A-8
Turbulence Plate	2.5D	20.0	0.51	A-3
		22.3	0.95	A-1
Turbulence Plate	4.5D	15.1	0.39	A-2
Elbow Up	0D	10.7	0.33	A-5
Turbulence Plate	10D	6.3	0.16	A-4
Elbow Up	3D	6.1	0.11	A-6

FIGURE 8

Accelerated Wear Test Results for the 3-Inch Valve

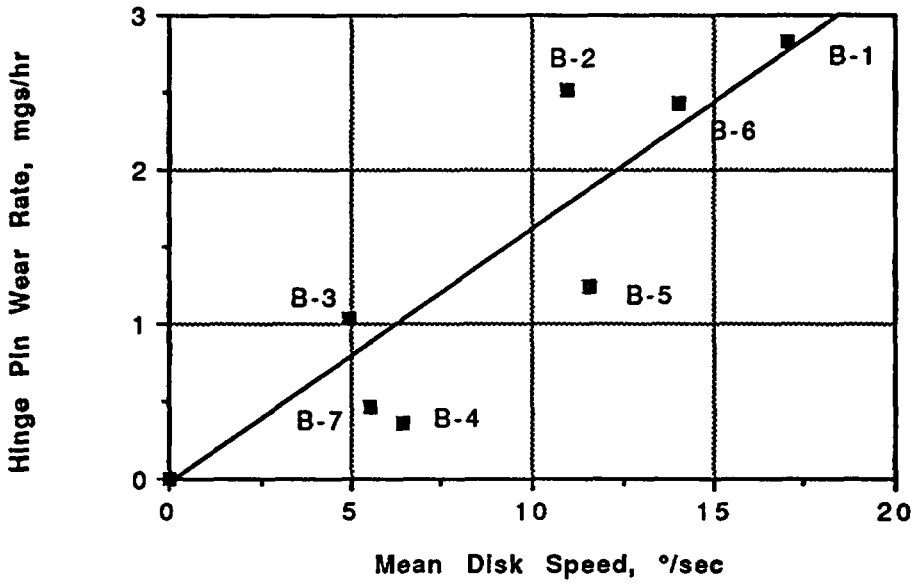

Upstream Disturbance	*Upstream Distance*	*Mean Disk Speed degrees/second*	*Wear Rate mgs/hr*	*Test Number*
Turbulence Plate	1.5D	17.0	2.80	B-1
Turbulence Plate	2.5D	14.6	2.52	B-6
Turbulence Plate	4.5D	11.6	1.38	B-5
Elbow Up / Increased Velocity	0D	9.9	2.48	B-2
Elbow Up	0D	6.4	0.37	B-4
Elbow Up	3D	5.5	0.58	B-7
Elbow Up / Worn Hinge Pin	0D	4.9	1.04	B-3

Figure 9

Accelerated Wear Test Results for the 6-Inch Valve

The most important conclusion from these plots is that the wear rate depends upon the mean disc speed, regardless of the type and proximity of the upstream disturbance responsible for it. This confirms that the fundamental wear equation is a valid qualitative form of predictive model for hinge pin wear in swing check valves. The quantitative correlation between the predicted and the actual wear rates will be discussed next.

Normalized Wear Rates

To facilitate a comprehensive comparison between theoretical predictions and test results, the fundamental wear Equation (1) can be rearranged to express wear rates in a normalized form as shown below. The volume of the material worn away is given by Equation (1) and is repeated here for convenience:

$$W = \frac{K L V t}{H} \tag{1}$$

For a material weight density of ρ, the above equation can be converted to give the weight, m, of the material lost:

$$m = \frac{\rho K L V t}{H} \tag{2}$$

Therefore, wear rate can be expressed as

$$\dot{m} = \frac{m}{t} = \frac{\rho K L V}{H} \tag{3}$$

The average sliding speed, V, at the hinge pin of diameter d_{hinge} can be related to the angular mean disc speed, $\dot{\theta}$ (degree/sec) as follows:

$$V = 0.5\, d_{hinge} \left(\dot{\theta} \times \frac{\pi}{180}\right) 3{,}600 \tag{4}$$

$$V = 10\pi \dot{\theta}\, d_{hinge} \text{ in/hr}$$

From Equations (3) and (4),

$$\dot{m} = \frac{\rho K L \left(10\pi \dot{\theta}\right) d_{hinge}}{H}$$

Rearranging

$$\boxed{\overline{M} \equiv \left(\frac{\dot{m}}{L\, d_{hinge}}\right) = \frac{\rho K \left(10\pi \dot{\theta}\right)}{H}} \tag{5}$$

where

$\overline{M}$ = Defined as normalized wear rate in mg/hr/lb/in

$\dot{m}$ = Wear rate in mg/hr

L = Load at the sliding surfaces, lb

d_{hinge} = Diameter of the hinge pin, in

ρ = Weight density of material, mg/in^3

K = Nondimensional wear coefficient for the sliding pair of materials

$\dot{\theta}$ = Mean angular disc speed, degrees/sec

H = Penetration hardness of the surface of the material being worn

Comparison Between Theoretical Wear Prediction and Tests

All of the accelerated wear test data for the three-inch and six-inch test valves were reduced to a plot of normalized wear rate, $\overline{M}$, vs. mean disc speed, $\dot{\theta}$, using Equation (5). The effective disc weight was used for the load on the sliding surfaces in this equation. Data for the weights and hinge pin diameters shown in Tables 1A and 1B were used.

Theoretical wear calculations were done by using a density of 44,452 mg/in^3 for aluminum and a surface hardness of Brinell 23, which corresponds to 32,700 psi. Wear coefficients for adhesive wear for identical metals range from $K = 3 \times 10^{-4}$ for poor lubrication to $K = 15 \times 10^{-4}$ for no lubrication. Wear coefficients for abrasive wear are typically an order of magnitude lower (Refs. 10, 11, 12).

Figure 10 shows an overall comparison between all the wear test data and theoretical predictions. Theoretical predictions based on the generic table of wear coefficients for adhesive wear for identical metal sliding pairs with poor lubrication to no lubrication nicely bound all the test results. This confirms the wear mechanism to be the adhesive one and the quantitative validity of the predictive approach.

A more precise prediction can be made if the actual wear coefficients for aluminum vs. aluminum, instead of the generic value for identical metals was used. However, no data for this specific material combination were found in the available published literature. Further research into the wear coefficients of aluminum against aluminum revealed that aluminum has a higher wear coefficient than the average. Unpublished data by the leading tribologist Rabinowicz shows that K for aluminum vs. aluminum is two to three times higher than the generic average for identical metal pairs, and the use of a geometric average (log scale) between the poorly lubricated and unlubricated values was recommended* . This gives a value of $K = 6.7 \times 10^{-4}$. With this specific wear coefficient, experimental results and theoretical predictions were found to be in excellent agreement.

From this laboratory comparison, it is concluded that the wear model presented in this report is a valid approach for predicting hinge pin wear in swing check valves. The application of the model and its correlation against limited plant data that were available will be presented in a separate section.

---

* Private communication between Prof. Ernest Rabinowicz, Massachusetts Institute of Technology, and M. S. Kalsi (principal investigator, NRC/SBIR project), May 8, 1990.

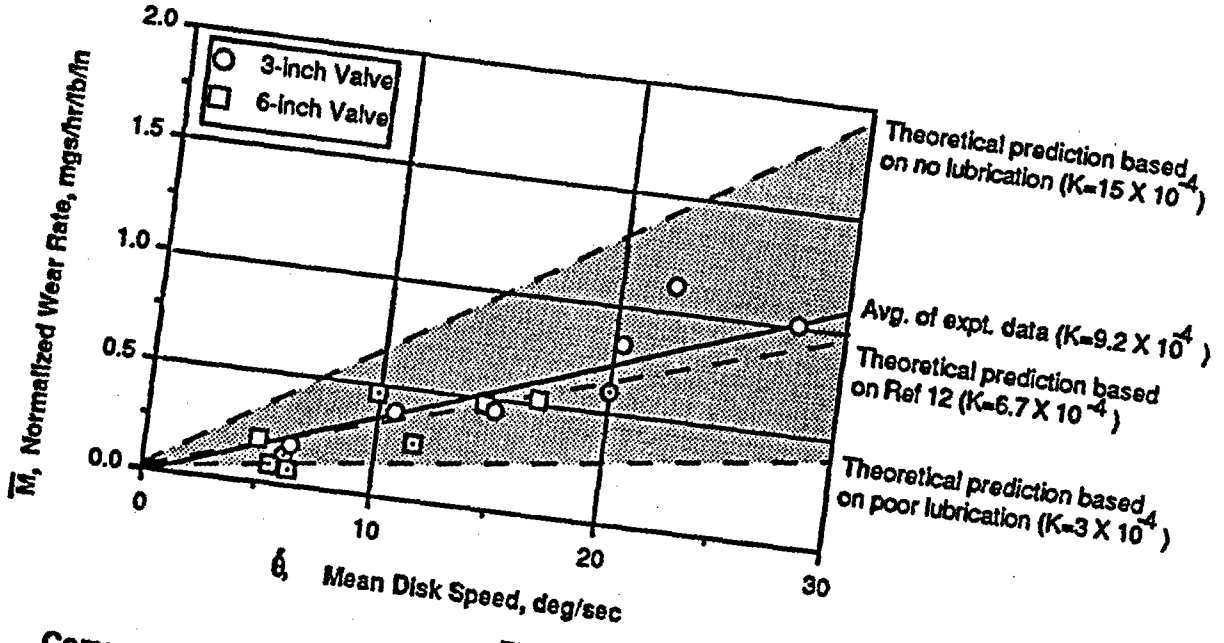

Figure 10

Comparison of Accelerated Wear Test Results to Theoretical Predictions

WEAR PREDICTION METHODOLOGY - SUMMARY AND CONCLUSIONS

The overall results and conclusions from the swing check valve hinge pin wear prediction research are summarized below:

1. The wear mechanism causing hinge pin wear is adhesive wear.
2. The fundamental wear equation predictions were found to provide excellent correlation with the accelerated wear test results for the three-inch and six-inch test valves under a total of 15 different test configurations that were tested.
3. Mean disc speed can be used to predict wear rates, regardless of the upstream disturbance source that is responsible for causing the disc motion.
4. Data from the large matrix of tests performed under Phase I research have been processed and included in Appendix D to provide mean disc speeds for a large number of upstream disturbances at varying proximities. Where applicable, this matrix of wear disc speed results can be used in hinge pin wear analysis.
5. The combined effect of more than one upstream flow disturbance was determined in only one test (A-7). A high turbulence orifice plate and an elbow were tested at 1.5 diameters upstream. The wear rate for this combined disturbance was found to be approximately the same as would be expected with the more severe source alone.
6. The use of appropriate adhesive wear coefficient requires a detailed knowledge of the tribological system to make accurate wear predictions. The actual wear coefficients for different metal sliding pairs under various environmental conditions span a very wide range. A number of factors, such as compatibility of the alloy elements in both of the metals, environmental fluid, and operating temperature, should be considered in selecting wear coefficients from previously published wear data. For best prediction, experimentally determined wear coefficient for the specific combination of sliding metals of interest should be used.
7. Even though hinge pin wear was found to follow linear predictions, excessive wear can cause the wear rates to increase nonlinearly. This can result from increases in hinge pin load due to possible impact between the sliding parts due to increased clearances.
8. Differences in the range of factors of 2 to 3 between the actual wear rates and the prediction based on a sound application of tribological principles are considered normal (Refs. 10, 11). If the differences are larger than this range, the assumption used or the actual conditions warrant a closer scrutiny.
9. Measurements of the actual parts in service obviously provide the most reliable information regarding actual wear rates. Whenever practically possible, these data should be used to refine future wear predictions and to determine suitable maintenance intervals.

This summary concludes our discussion on the accelerated wear test research on the three-inch and six-inch valves in the laboratory. Application of this prediction methodology to actual plant conditions and their correlation are presented in a separate section.

IMPACT AND FATIGUE PREDICTIONS

When the flow velocity through a check valve is insufficient to cause the disc to reach the fully open position, disc oscillation and tapping can occur. Tapping against the backstop can generate significant impact forces that may result in fatigue failure of the disc stud. This section describes an analytical approach developed to predict these impact forces as well as documents the results of impact force measurements made on a specially modified and instrumented check valve disc during actual flow operation. Theoretical predictions are compared to the measurements for model verification.

Theoretical Prediction Techniques

The kinetic energy of the oscillating disc assembly is assumed to be completely converted into strain (potential) energy of the impacting members at the instant contact occurs. Since the stiffness of the elements involved in the impact (disc, disc stud, valve bonnet) is either known or can be calculated, this strain energy can be used to determine the peak force delivered during impact. It can be shown that the stiffness of the disc and bonnet is considerably higher than that of the disc stud; therefore, the strain energy will be absorbed principally by the much softer disc stud. This system model assumes that the disc stud behaves as a linear spring element and that no other losses occur that would decrease the net amount of energy delivered to the disc stud.

The most important element in this model becomes the determination of the disc velocity and, therefore, the kinetic energy of the disc at the moment of impact. Several approaches were developed which can be used to predict the disc velocity at impact. Each method relies on determining a characteristic frequency of disc motion and corresponding amplitude from which an estimate of linear velocity can be derived. Briefly, these approaches for determining velocity before impact are:

1. Disc natural frequency based on fluid spring stiffness,
2. Pipe eddy frequency,
3. Mean and 3σ disc speed from Phase I test data.

Each of these techniques will be described more fully in the following sections. For a complete derivation of the velocity and impact force equations presented below, refer to Appendix A.

Disc Natural Frequency Approach

This approach is based on the assumption that the disc behaves as a single degree of freedom vibratory system and will therefore oscillate at its natural frequency when subjected to the random fluctuating forces present in the turbulent flow. The disc weight at any opening angle is supported by the fluid impingement force, which has a nonlinear force vs. opening angle characteristic (Ref. 3.). Due to this nonlinear force deflection characteristic, the disc natural frequency will vary as a function of disc position defined by angle, θ, which in turn depends upon the flow velocity (Appendix A). The disc velocity can be calculated as follows:

$$V_{disc} = V R \frac{\Delta\theta}{2}\left[\frac{2K\rho A_{disc} V^2 Z}{R W}\right]^{1/2} \qquad (6a)$$

where

$$Z = \left[\cos\theta \sin\frac{\theta}{2} + \frac{1}{2}\cos\frac{\theta}{2}\sin\theta\right] \tag{6b}$$

The impact force can be directly calculated using the method described in Appendix A if the disc fluctuation angle, $\Delta\theta$, is known. The best available data for disc fluctuation angle under a variety of upstream flow disturbances and their proximities were developed under Phase I of this program and are reported in Reference 1.

Pipe Eddy Frequency Approach

This estimate of disc velocity is based on the eddy frequencies observed in fully developed turbulent flow in a pipe (Refs. 17, 18, 19). Since disc oscillations in water (or other liquids) were found to be highly damped in our Phase I tests, the disc has a tendency to respond to the disturbing frequencies present in the turbulent flow stream. The disc velocity based on its response at this frequency is given by:

$$\boxed{V_{disc} = 0.2513\frac{V\,R\,\Delta\theta}{D_{pipe}}} \tag{7}$$

Again, the impact force can be directly calculated using the method described in Appendix A.

Mean and 3σ Disc Speed Approach

The disc motion data gathered during the Phase I portion of this program was extensively reviewed to ascertain the characteristic disc oscillation frequencies for the many tests performed. However, this analysis showed that only a small percentage of test cases had an energy peak near a dominant frequency. Typically, the oscillation energy was spread over a range of frequencies up to approximately 6 hz. Therefore it appears that the disc does not behave as a simple single degree of freedom system that would respond at its single natural frequency, but is able to respond over a range of frequencies contained in the input flow stream. Considering the chaotic nature of the turbulent flow stream, this response seems reasonable.

In order to characterize the disc motion and velocity in some usable way, a numerical technique was developed which considered the randomness of the disc response. The result is a parameter we call the Mean Disc Speed which is, in effect, the average disc angular velocity taken over a time long enough to average out instantaneous variations which would otherwise skew the velocity in one direction or another. When fatigue calculations are to be performed, the maximum velocity attained prior to impact is of particular interest because the highest velocity impacts, even though relatively infrequent, will account for the majority of fatigue damage. To this end, a second parameter is calculated by taking the standard deviation of the disc velocity data. When multiplied by three, we have the 3σ disc speed which will bound the highest 0.3 percent of the disc velocities. A discussion of how these parameters are calculated is contained in Appendix D. Also contained in this appendix is a complete set of the mean and 3σ disc speed plots derived from the Phase I work for both the three- and six-inch valves.

IMPACT AND FATIGUE TESTING

In order to measure the impact forces generated when disc tapping occurs, a test program was devised in which a specially modified check valve could be subjected to a variety of flow conditions known to cause the disc to tap against the full open stop. By instrumenting the valve disc with strain gages, actual disc stud impact forces could be captured in real time and compared to theoretical predictions.

General Methodology

The six-inch valve was installed in the flow loop and tested with two different upstream disturbances. An elbow was used to generate low levels of turbulence and a perforated plate was used for high levels of turbulence. Tests were performed with the disturbances at two proximities and flow velocities were varied over a range from 2 to 18 feet per second. During the tests, data from the instruments were recorded on a wide-band FM tape recorder for subsequent review and signal processing.

Test Valve

Modifications were made to the six-inch swing check valve to permit direct measurement of disc stud impact loads. This was accomplished by building a special disc with provisions for mounting strain gages in a machined recess in the disc (Fig. 11). A thin diaphragm (0.125-inch thick) was created so that mechanical amplification of the strain caused by impact would produce adequate strain signals. Extensive finite element analyses were conducted to optimize the load measuring characteristics of the disc and to provide a relatively constant strain field at the gage locations.

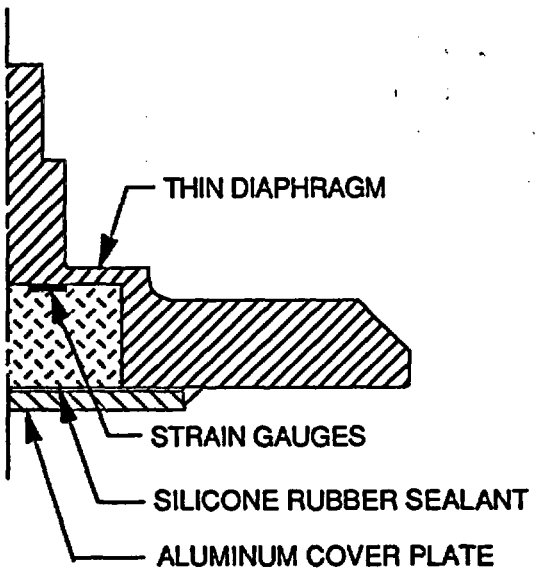

Figure 11
Instrumented Disc Cross Section

The disc was instrumented with three separate strain gage bridges as shown in Fig. 12. Eight gages were mounted in the recessed cavity, four of which were used in a full bridge

configuration for axial load measurement. Two additional full bridges, each with two active arms, were built to measure bending loads along two orthogonal axes (Figs. 13, 14). The gages were protected from moisture penetration by various epoxy and silicone coatings. The remaining cavity volume was then filled with a special silicone potting compound, covered with an aluminum plate, and again sealed from the environment with an adhesive coating (Fig. 15).

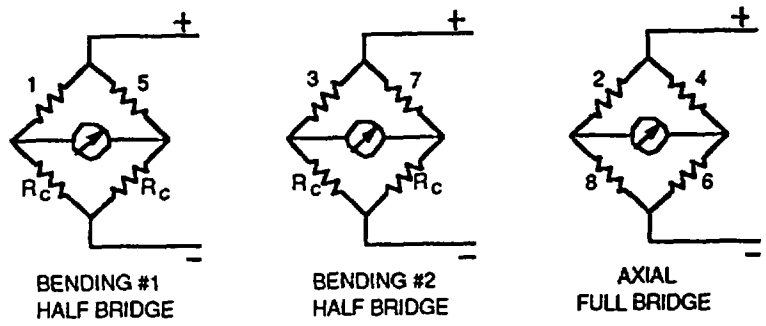

Figure 12

Strain Gage Bridge Schematics

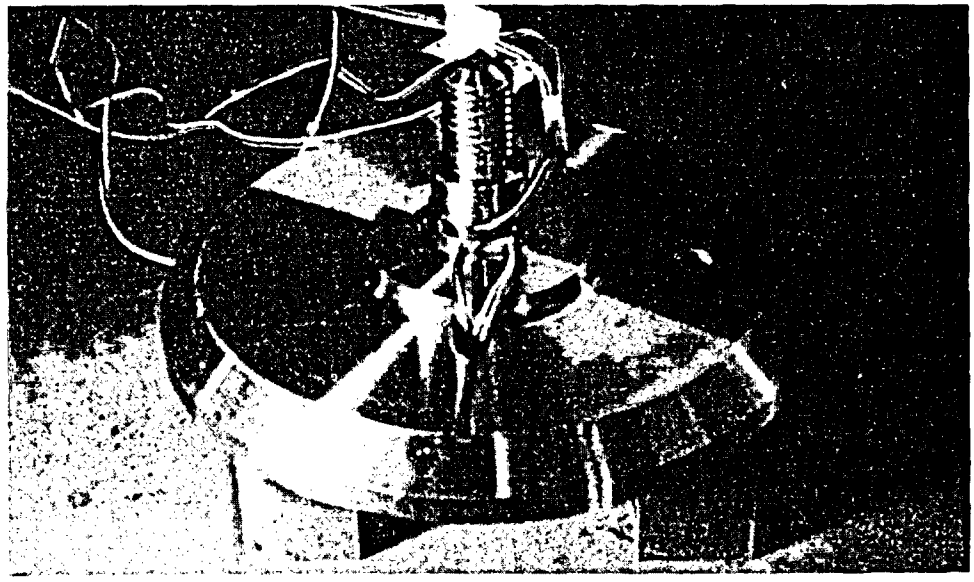

Figure 13

Strain Gaged Check Valve Disc

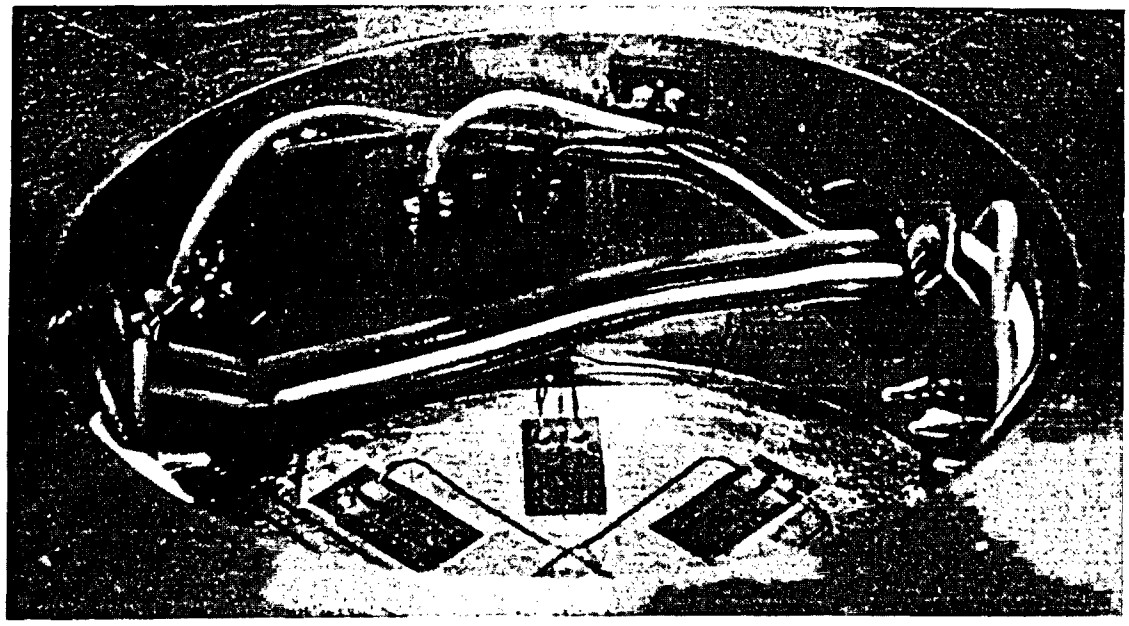

Figure 14
Detail of Strain Gage Installation

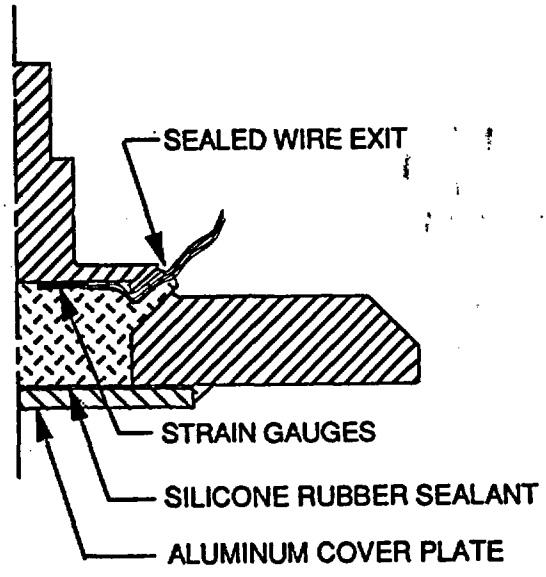

Figure 15
Disc Showing Sealed Wire Exit

Wires from the gages were routed through a drilled passage to the top of the disc and routed along the hinge arm with appropriate strain relief. The wire exit was also thoroughly potted in silicone adhesive and potting compounds to preclude moisture penetration (Fig. 16). Finally, the wires were terminated in a special glass sealed hermetic connector mounted on the valve bonnet which served as part of the valve body pressure boundary as well as an exit to the outside world for the strain signals (Fig. 17).

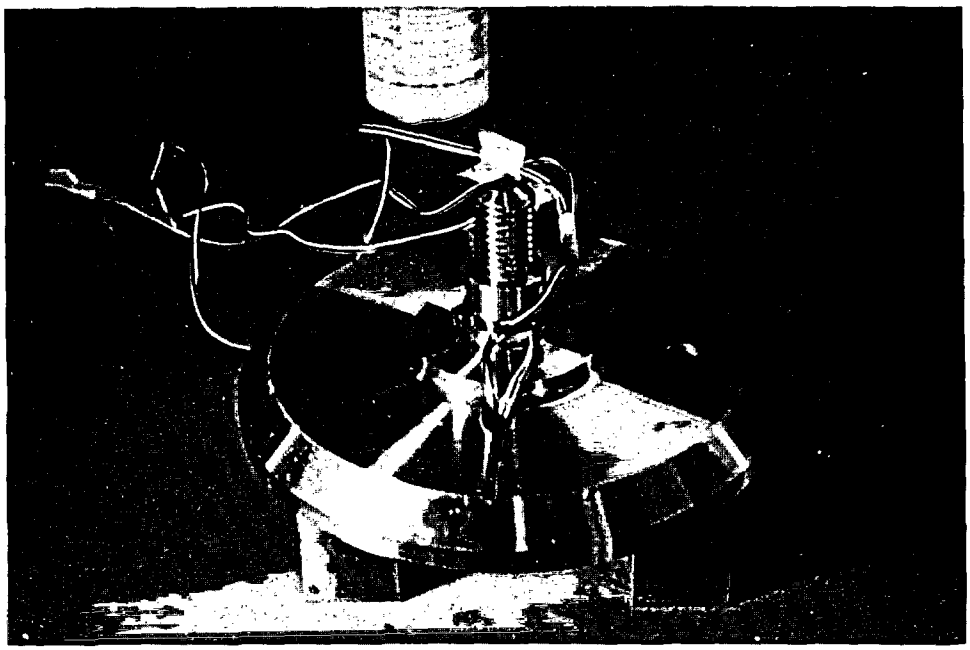

Figure 16

Wire Exit from Disc

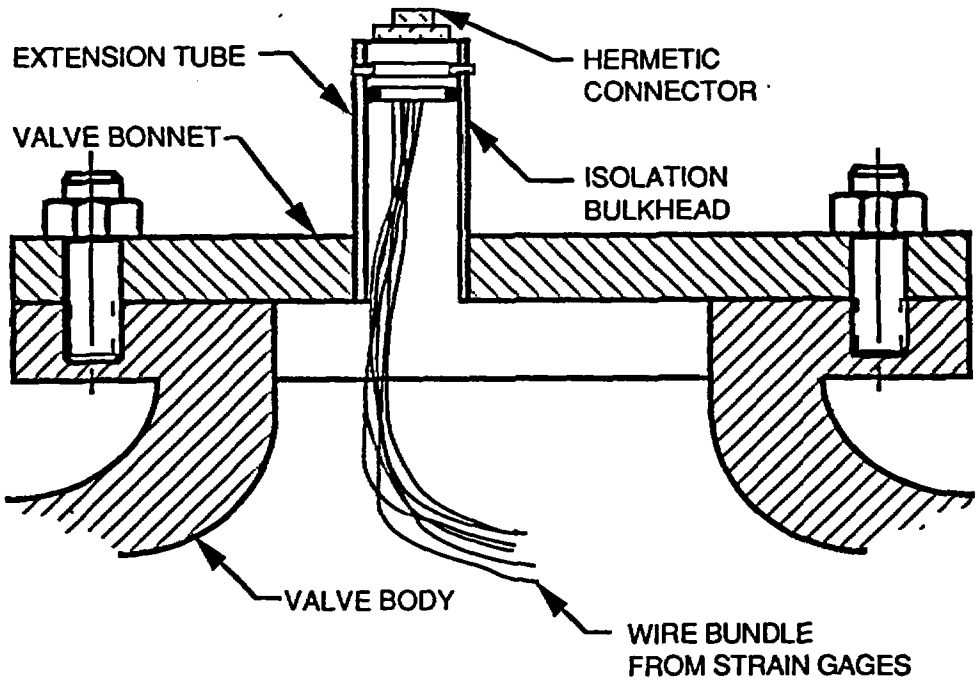

Figure 17

Completion of Pressure Boundary Using Hermetic Connector

Calibration of Strain Gaged Valve Disc

Each of the three strain gage bridges was calibrated before starting the impact tests. The bridges were found to respond in a very linear fashion, and the amplified axial bridge output was 2,900 lb/volt. During the course of testing, the bending bridges were damaged and became unusable. A check of the axial bridge found it to be operating satisfactorily with no detectable change in output scale factor. After completing the test series, the axial bridge output was found to have decreased somewhat to 2,288 lbs/volt; but the bridge behavior remained very linear and repeatable. Since the shift in output scale factor could not be traced to a particular point in time, all data reduction has used an average of these two values, or $\frac{2{,}900 + 2{,}288}{2}$ = 2,594 lbs/volt. Therefore, the maximum error in the force measurements reported here is approximately bounded by ± 12 percent.

Instrumentation

Much of the instrumentation used in the course of the impact testing was the same as that used in the Phase I research (Ref. 1). The additional equipment used consisted of the following:

1. Strain gage amplifiers and signal conditioners,
2. Seven-channel FM tape deck,
3. Two-channel spectrum analyzer,
4. Two-channel digital storage oscilloscope,
5. Digital signal processing and filtering software.

An important aspect of the force measurement instrumentation was to ensure adequate instrument frequency response for capturing the impact load signatures. Measurements of impacts made during the Phase I effort showed that the load event duration was approximately three milliseconds. Since a stiffer steel bonnet was being used in the Phase II tests than the one made of polycarbonate used in the Phase I tests, even shorter impact durations could be expected. Therefore, the strain gage amplifiers and tape deck used to record these events were capable of measuring signals from DC to 10 khz ± 0.5 db.

TEST RESULTS

The impact tests were divided into two areas of investigation. First, the impact load signature was characterized in terms of its amplitude, duration, and shape. This information, gathered for different upstream disturbances and flow velocities, would be used for correlation to the impact force prediction techniques. Second, the frequency at which these impacts happen was determined. The number of impacts of a given magnitude that occur over the "tapping zone," which is defined as the range of flow velocities over which tapping takes place, was determined for a very large number of impact events. This information combined with the data about impact magnitudes provides the basis for performing disc stud fatigue calculations.

Typical Impact Signature

Shown in Figs. 18 to 20 are impact load signatures generated with the strain-gaged disc assembly. Figures 18 and 19 are impacts recorded with the high turbulence source and elbow located 1.5 diameters and 3 diameters upstream of the valve respectively. Figure 20 is also for the high turbulence source, but includes additional modifications to the disc and hinge arm assembly to be discussed later. The plots show that the characteristic shape of the impact signal is independent of the type and proximity of the upstream disturbance as well as the flow velocity. The principal difference among the signals is the amplitude, which depends on the velocity of the disc at the time of impact. The plots also show that the impact excites various resonant frequencies in the load measuring disc. These frequencies are superimposed on the basic impact load signature and, because they are relatively high in magnitude compared to the impact force itself, result in a low signal-to-noise ratio. In addition, the resonant frequencies are of the same order as the frequency of the impact event itself, further heightening the difficulty of extracting the signal of interest.

Before we could attempt to filter out the high frequency information from the impact force signals, the resonant frequencies had to be identified. A separate series of controlled impact tests were performed to determine the natural frequencies of the load measuring disc. The measured natural frequencies are shown in Table 5:

Test Case	*f1*	*f2*
Disc Assembly in Air	4123	2000
Disc Assembly in Water	3875	1875

Table 5

Disc Assembly Resonant Frequencies, hz

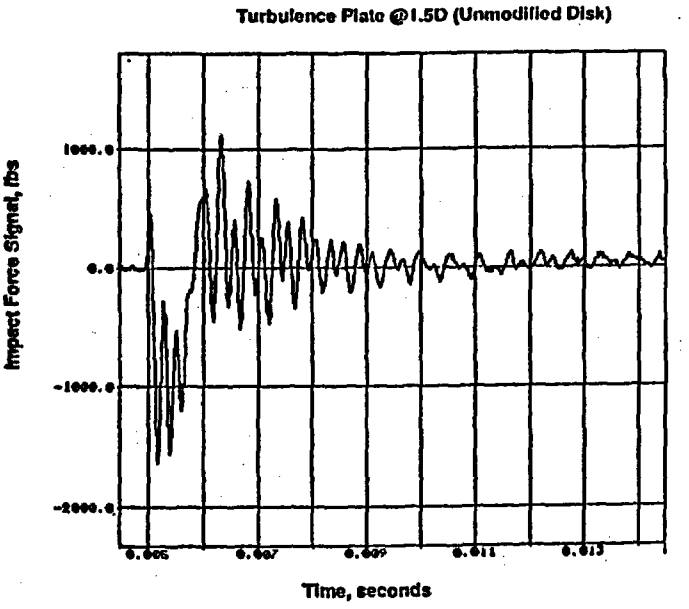

Figure 18

Impact Signature, Upstream Turbulence Source

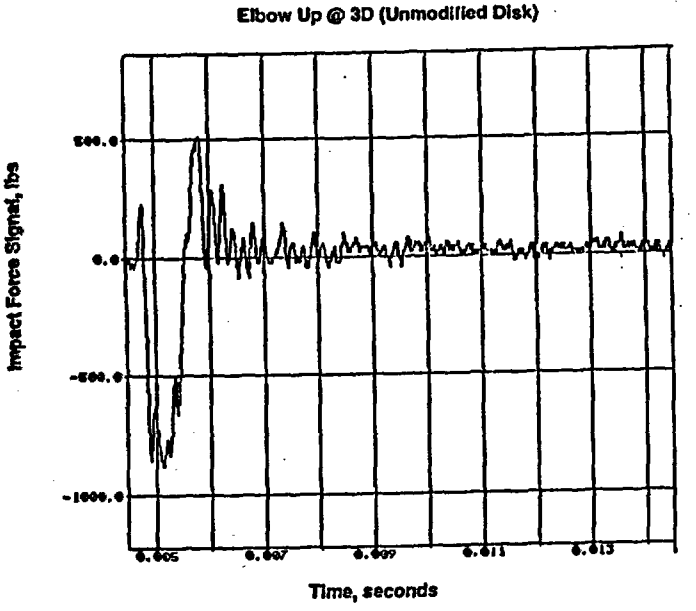

Figure 19

Impact Signature, Upstream Elbow

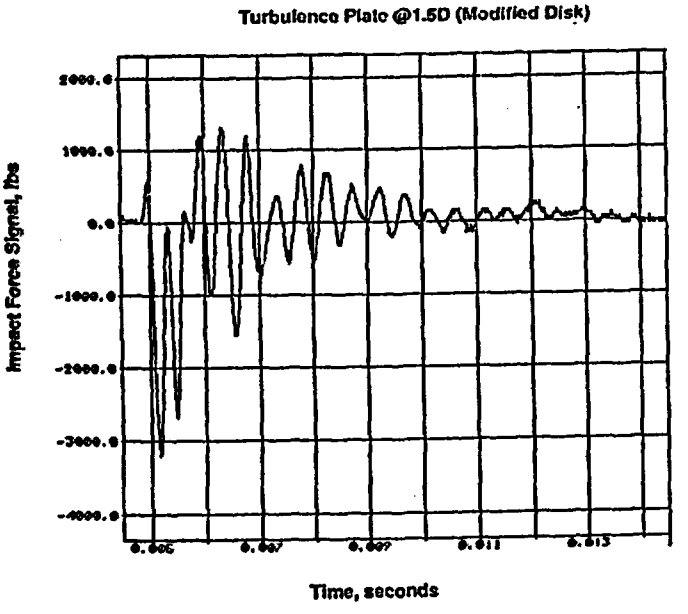

Figure 20

Impact Signature, Upstream Turbulence (Modified Disc)

By performing the tests in and out of water, we were able to quantify the added mass effect of the water, which increases the effective weight of the dynamic portion of the strain gaged assembly by 14 percent. Spectral analysis of the test data also confirmed our qualitative observation that the impact energy was concentrated below 1000 hz. Since the disc assembly natural frequencies are higher than the effective frequency of the impact event, a digital low pass filter was implemented to remove these unwanted frequencies from the impact force signal. The result is shown in Figure 21 where the original and filtered signals are shown superimposed. The remaining impulse is now clearly visible and the amplitude and duration can be easily extracted.

Discussion of Impact and Disc Motion Signals

Examples of an impact signal (filtered and un-filtered) and the corresponding disc motion signal are shown in figures 21 and 22. The peak force can be measured directly from the plot as 950 pounds. Since both signals were recorded on tape simultaneously, the disc excursion that resulted in the impact event can be identified and the average velocity at impact determined as 10.5 inches per second. This velocity is used to calculate the kinetic energy of the disc at impact which is then converted to the peak impact force for later comparison.

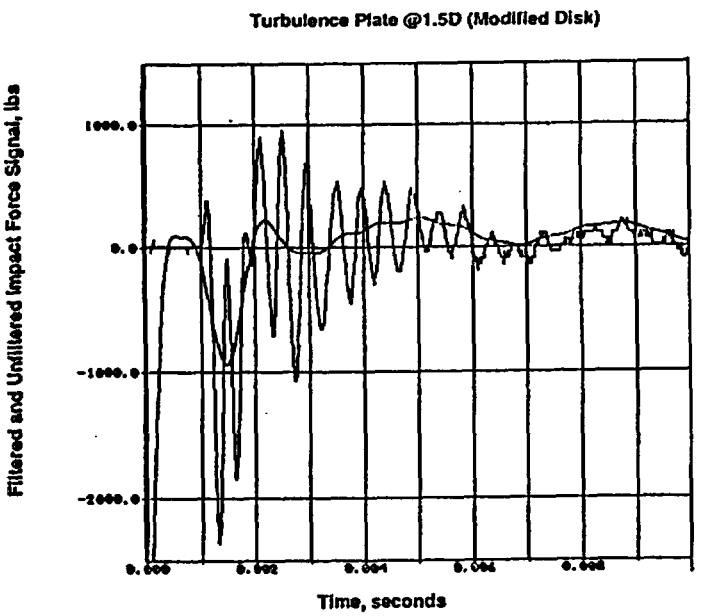

Figure 21

Raw and Filtered Impact Force Signatures

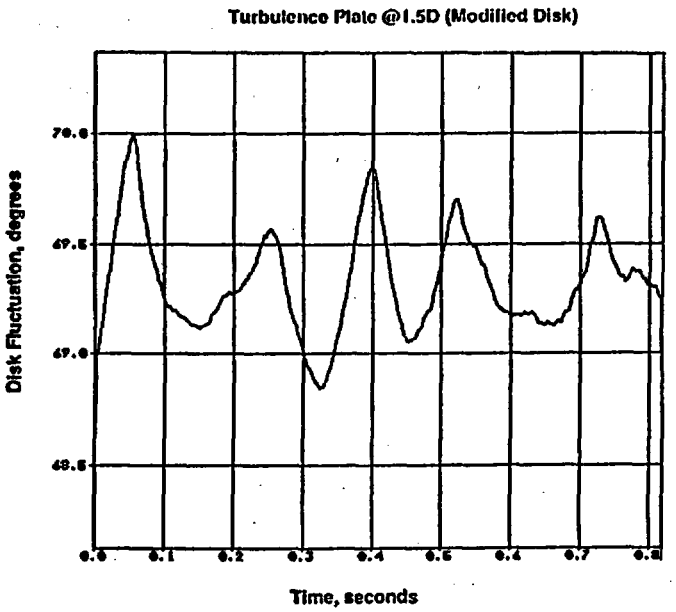

Figure 22

Disc Displacement Plot Corresponding to Impact Event of Figure 21

Discussion of Disc Motion Measurements and Modified Disc

The technique used to measure disc motion is illustrated schematically in Figure 23. As can be seen, the physical connection from the displacement transducer is made to the hinge arm which moves with the disc in response to the fluid flow. While this system has served very well in previous test programs, certain limitations became apparent in this project. The important variable in the force calculation is the impact velocity *of the disc.* Since the measurement connection is actually made to the hinge arm, the disc velocity is, in effect, inferred from the motion (hence, velocity) of the hinge arm. The clearance, C_1, between the disc stud and hinge arm allows the disc a small but significant amount of freedom independent of the hinge arm. To eliminate this problem, the disc was modified by rigidly pinning it to the hinge arm so that the two behaved as a single entity. While this helped the situation, impact force calculations, based on instantaneous hinge arm motion, remained in disagreement with the measurements.

We believe that, although minimized as far as practicable, the remaining clearances shown in the illustration, namely those between the hinge arm and pin, C_2, and clevis and hinge arm, C_3, still prevent the LVDT from following the disc motion to the degree of accuracy needed for these measurements to provide instantaneous correlation between velocity and impact.

This can be quantified as follows. The measured clearance, C_3, is 0.005-inch. At disc velocity, V, of 3 in/sec, the time required to traverse clearance C_3 is

$$t = \frac{C_3}{V} = \frac{0.005\,\text{inch}}{3\,\text{in/sec}} = 0.0017 \text{ seconds}$$

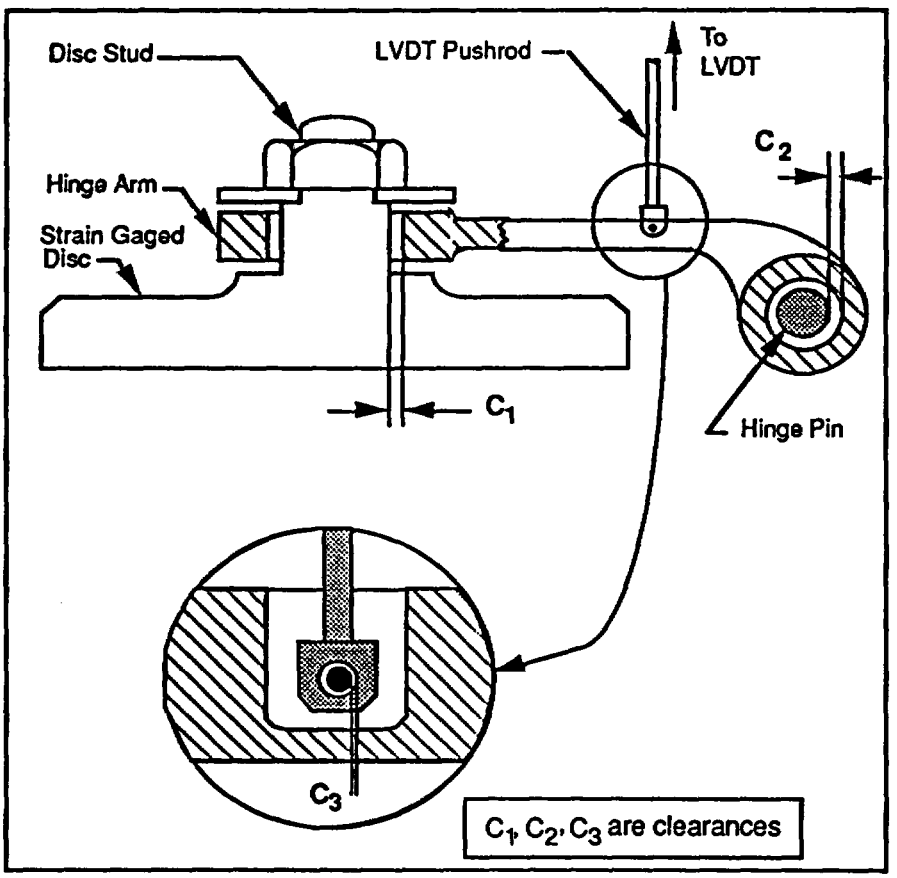

Figure 23
Impact Measurement Assembly

This length of time is almost twice the duration of the impact events themselves. Therefore, the actual *disc impact force* measured by the disc mounted strain gages could easily occur out of complete time synchronization with the *hinge arm* motion/velocity measurement. The only way to eliminate this problem and get true disc motion measurement would be to attach an accelerometer directly to the disc stud and use this signal as the basis for disc motion and velocity. This was not easily achievable; therefore, emphasis was put on comparing measurements with the upper-bound predictions discussed earlier.

Use of 3σ Disc Speed For Disc Impact Force Estimates

The problems associated with determining the instantaneous disc impact velocity from the disc motion signals caused us to reexamine the 3σ disc speed data presented in Appendix D as an alternate measure of the disc velocity. The 3σ disc speed, which has proven a good measure of the maximum disc velocity, should establish an upper bound on the impact velocity, and therefore on the calculated impact force. In reviewing the data presented in Appendix D, one can see that as the flow velocity increases through the tapping zone, the disc speed begins to decrease. For the purpose of calculating the bounding values, the maximum 3σ disc speed has been used and no credit taken for any decrease. This measure of disc velocity has been taken from data collected during the Phase I portion of this work and reduced as part of the Phase II program.

Rate of Occurrence of Impacts

In order to perform a fatigue analysis of the disc stud, the frequency of occurrence of impacts of a given magnitude must be known. To quantify this factor, the six-inch valve flow test data was surveyed and the number of impacts above a given threshold force were counted and recorded. The test data were divided into the impact force ranges presented in Table 6:

Range ID	*Elbow Up @ 3 d*	*High Turbulence Source @ 1.5 d*
A	130 - 260 lbs	260 - 520 lbs
B	260 - 325 lbs	520 - 780 lbs
C	325 - 390 lbs	780 - 1040 lbs
D	390 - 520 lbs	1040 - 1170 lbs
E	520 - 650 lbs	1170 - 1575 lbs
F	650 - 780 lbs	1575 - 1950 lbs
G	780 - 1040 lbs	1950 - 2080 lbs

Table 6

Impact Force Ranges
(After Low-Pass Filtering)

At forces below the lowest incremental level (Range A), the impact frequency was so high (about four impacts per second) that manually counting them was unfeasible. Since the stresses developed in the stud at these lower force levels are well below the endurance limit of the stud material, their contribution to cumulative fatigue damage can be neglected. The method used to identify these impacts used the raw, or un-filtered strain gage signals containing the high amplitude ringing due to resonant excitation. For comparison to the impact force data presented earlier, which had been processed with the digital low pass filter to eliminate the ringing effects, the forces reported in this section have been reduced by a factor of two, which was the typical reduction observed after filtering the raw impact force signals.

Data from the high turbulence and elbow up surveys is presented in Figures 24 and 25. In both sets of data, as the impact force decreases, the number of impacts rises quickly. This agrees with observed valve behavior where the statistical occurrence of low velocity excursions that would result in low impact forces is greater than high velocity excursions that would create high impact forces. Another observation is that the number of impacts that occur at a given load range is much greater for the high turbulence source than for the elbow up. For example, impact forces between 130 and 260 pounds occur at a rate of about 0.7 impacts per second with the elbow disturbance, whereas the turbulence source generates forces between 1,040 to 1,170 pounds at roughly the same rate. This is in keeping with the data gathered during Phase I where the amplitude of disc motion generated with the turbulence source was much greater than with the elbow.

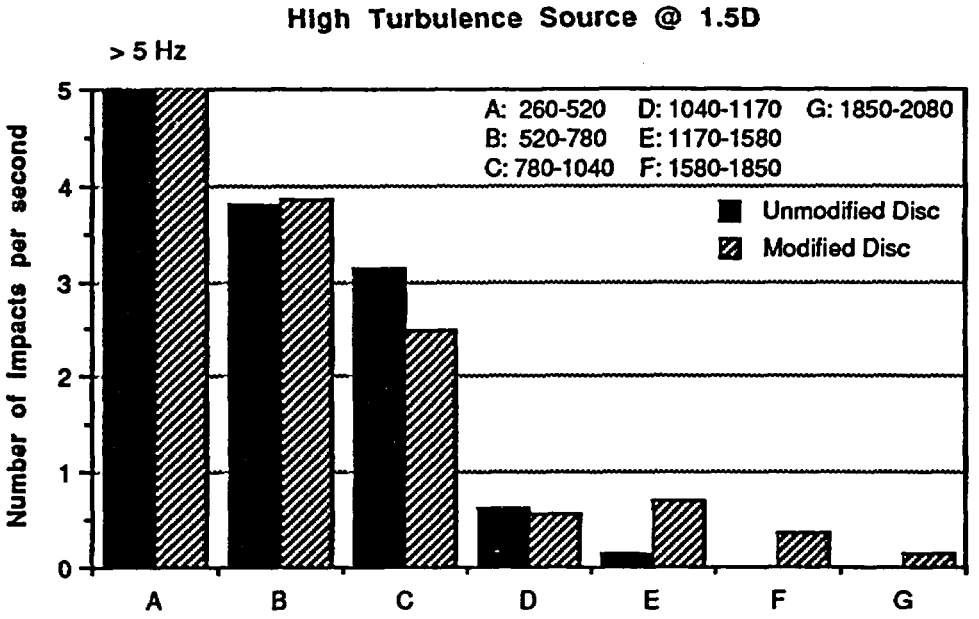

Figure 24

Impact Force Survey
(Based on Filtered Signal, lbs)

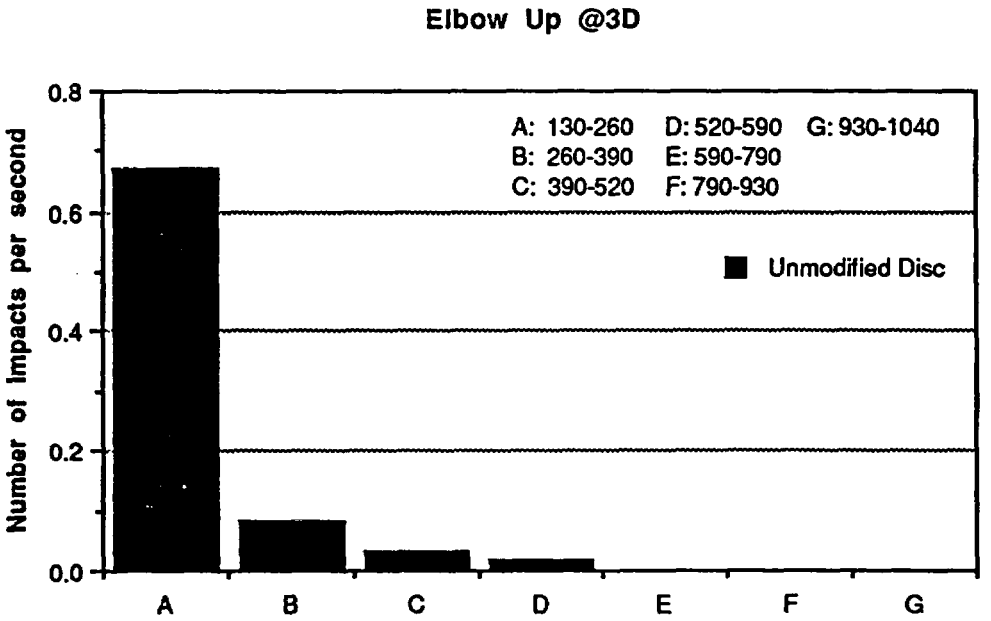

Figure 25

Impact Force Survey
(Based on Filtered Signal, lbs)

CORRELATION OF IMPACT TEST DATA TO THEORY

A total of twelve impact events have been analyzed for comparison to theoretical predictions of impact force. The data is presented in Table 7. All tests were performed with the modified disc assembly previously described. The upstream disturbance used was the high turbulence source located 1.5 diameters upstream. Flow velocities ranged from 6 fps (start of tapping) to 18 fps. It is important to note that cavitation begins at approximately 10 fps and increases in intensity to 18 fps. Cavitation will increase the level of turbulence as well as create higher frequency disturbances in the flow stream to which the disc may respond.

Kinetic Energy Conversion Approach

Using the 3σ disc speed to estimate the maximum disc impact velocity, the conversion to kinetic energy yields predicted impact forces that are within 80 percent of the measured loads up to a flow velocity of 9.5 fps. Beyond this flow velocity, where cavitation begins, the difference grows larger, reaching about 250 percent at 14 fps. Beyond this point, the level of cavitation is quite high, and the predictive technique falls short of the measured loads by a large margin.

Disc Oscillation Amplitude and Frequency Approach

A second predictive technique involves use of the disc natural frequency estimation method along with the appropriate disc oscillation amplitude data gathered during Phase I of this project. (Refer to Appendices A and C for the methodology used.)

Impact Force Calculations for Six-Inch Instrumented Disc

Flow Condition	:	Water @ 8 f/s ≈ 70°F
Upstream Disturbance	:	Perforated plate at 1.5D upstream
Disc Oscillation Angle	:	16° before tapping
Disc Equilibrium Angle	:	63°

Disc Natural Frequency:

$$f_n = \frac{1}{2\pi}\sqrt{\frac{K_{stiff}}{W/g}}$$

$$= \frac{1}{2\pi}\sqrt{\frac{2KA\rho V^2 Z}{RW}}$$

where

$K = 2.0$

$A = \left(\frac{6.9}{12}\right)^2 \times \frac{\pi}{4} = 0.26\ ft^2$

$\rho = 62.4\ lb/ft^3$

$$V^2 = 8 \text{ ft/sec}$$

$$R = \frac{5.04}{12} = 0.42 \text{ ft}$$

$$W = W_{disc} + \frac{1}{2} W_{hinge} + \frac{1}{3} \rho (d_{disc})^3$$

$$= 10.19 + \frac{1}{3} \times 62.4 \times \left(\frac{6.9}{12}\right)^3$$

$$= 14.14 \text{ lb}$$

$$Z = \cos\theta \sin\frac{\theta}{2} + \frac{1}{2} \cos\frac{\theta}{2} \sin\theta$$

$$= \cos 27° \sin 13.5° + \frac{1}{2} \cos 13.5 \sin 27°$$

$$= 0.429$$

$$\therefore \quad f_n = \frac{1}{2\pi} \sqrt{\frac{2 \times 2 \times 0.26 \times 62.4 \times 8^2 \times 0.429}{0.42 \times 14.14}}$$

$$= 2.757 \text{ hz} \quad \leftarrow$$

Maximum Disc Velocity at
2.757 hz and 16° Amplitude (peak to peak)

$$V_{max} = R \times \frac{\theta}{2} \times 2\pi f$$

$$= 5.04 \times 8 \times \frac{\pi}{180} \times 2\pi \times 2.757$$

$$= 12.19 \text{ in / sec}$$

Maximum Disc Impact Force

$$F_{max} = 162.4 \, V_{max}$$

$$= 1{,}980 \text{ lb} \quad \leftarrow$$

The highest force measured in the tapping zone was 1,276 lbs. As can be seen by examining the measured impact loads in Table 7, the theoretical value of 1,980 lbs bounds this value by a comfortable margin.

Flow Velocity ft/sec	*Average Velocity at Impact* deg/sec	*3 Sigma Disc Speed* deg/sec	$F_{theoretical}$ *based on 3 Sigma Disc Speed* lbs	$F_{measured}$ lbs	*Ratio of* $F_{measured}$ *to* $F_{theoretical}$
6.0	7.8	78	1,063	916	0.86
7.9	19.5	60	818	998	1.22
8.5	13.2	55	750	920	1.23
9.0	16.4	50	682	1,276	1.87
9.5	12.3	45	613	1,098	1.79
10.0	18.8	40	545	1,407	2.58(2)
11.0	5.9	33	450	1,148	2.55(2)
12.0	12.2	25	560	894	1.60(2)
13.0	14.7	20	341	792	2.32(2)
14.1	5.6	15	204	971	4.75(2)
16.0	4.7	7	96	795	8.28(2)
17.1	3.6	6	82	530	6.50(2)

(1) Modified disc is rigidly connected to the hinge arm to eliminate excess clearance

(2) This data affected by onset of cavitation

Table 7
Comparison of Theoretical and Measured Impact Forces
6-Inch Modified Disc Assembly (1)
High Turbulence Source @ 1.5 Diameters Upstream

IMPACT FORCE AND FATIGUE PREDICTION METHODOLOGY – SUMMARY AND CONCLUSIONS

The overall results and conclusions from the six-inch swing check valve impact and fatigue prediction research are summarized below:

1. Impact forces as high as 1,276 pounds can occur when the valve is operating at flow velocities in the tapping zone. Testing shows that, as the disc enters the tapping zone, the impact forces increase in magnitude to a maximum and then diminish as the flow velocity increases.

2. Measured impact forces are bounded by predicted values based on the disc frequency and oscillation amplitude method discussed earlier in this section.

3. Impact forces calculated using the disc velocity inferred from hinge arm motion were within 80 percent of the theoretical values in the flow range of 6.0 ft/sec to 9.5 ft/sec where other factors such as cavitation were not present.

4. To make valid comparisons of predicted versus measured impact forces, an accurate measurement of the instantaneous disc motion (instead of the hinge arm motion) is required.

5. Experimental measurement of the number of impacts occurring at a given load is bounded by predictions made using the disc natural frequency method.

6. Higher amplitude impacts occur less frequently than lower level impacts.

7. As discussed later in Plant Correlation Example 4, the techniques described in this report adequately predict actual disc-stud fatigue failure.

CORRELATION AGAINST PLANT DATA

As discussed in detail in other sections of this report, wear and fatigue/impact predictive models were found to be in good agreement with the laboratory tests conducted under Phase II research. This section presents the correlation between model predictions and actual plant test data for some important, well-documented cases of premature degradation or failure of check valves. Also included are some examples of correlations where relatively low degradation was predicted for valves used in long-term service with the disc not fully open. Separate correlation examples are given for failures of each type: those resulting from excessive hinge pin wear and one caused by fatigue of the disc stud nut. The fatigue example is the San Onofre Unit 1 check valve failure event in November, 1985 that caused the NRC and the nuclear industry to focus their attention on check valve problems (Refs. 5, 6, 7).

It should be pointed out that this part of the project was limited in scope because specific tasks in our original proposal to obtain detailed performance data from several operating plants under the NRC (SBIR Phase II) research could not be funded. Despite this, our literature search, review of previously published plant data, and our involvement with utilities in root cause analyses of check valve failures provided us with some excellent examples against which the validity of the predictive methodology could be established. As additional plant data with sufficient details are obtained in the future, further validation and refinements of the predictive model will be made.

Plant Correlation Example 1:
18-Inch Swing Check Valves with Excessive Hinge Pin Bushing Wear

This is one of the best cases for wear correlation against the predictive model because all the pertinent valve design data, installation data, dimensional inspections, and operating and maintenance history records for a large population of valves for many years of operation are well documented (Refs. 15, 16).

Sixteen 18-inch, Class 900 swing check valves (CV-3) installed in the primary loop of the core discharge system of the pressurized water reactor operated by UNC Nuclear Industries, Inc. for the U.S. Department of Energy near Richland, Washington were found to have high hinge pin bushing wear. Excessive wear of the hinge pin bushings had caused some of the bushings to completely wear through, and the debris of the worn-through bushings for some valves were found downstream. Figures 26 and 27 show installation details and the typical hinge pin bushing wear observed. These valves were installed within two feet downstream of a side discharge dead-end line tee. The average wear rate was found to be 0.022"/year for these valves based on the first detailed inspection in 1973 after approximately eight years of operation. In a subsequent surveillance inspection program, the wear rates were more precisely monitored and found to be 0.027"/year of service. At this rate, the 3/16-inch thick bushing wears through in about seven years, necessitating massive change-out of components. It should be noted that both the hinge pin and the bushing are made of cobalt-based alloys (Haynes Stellite #25 and Stoody #6 respectively). These materials are known to have relatively good wear characteristics.

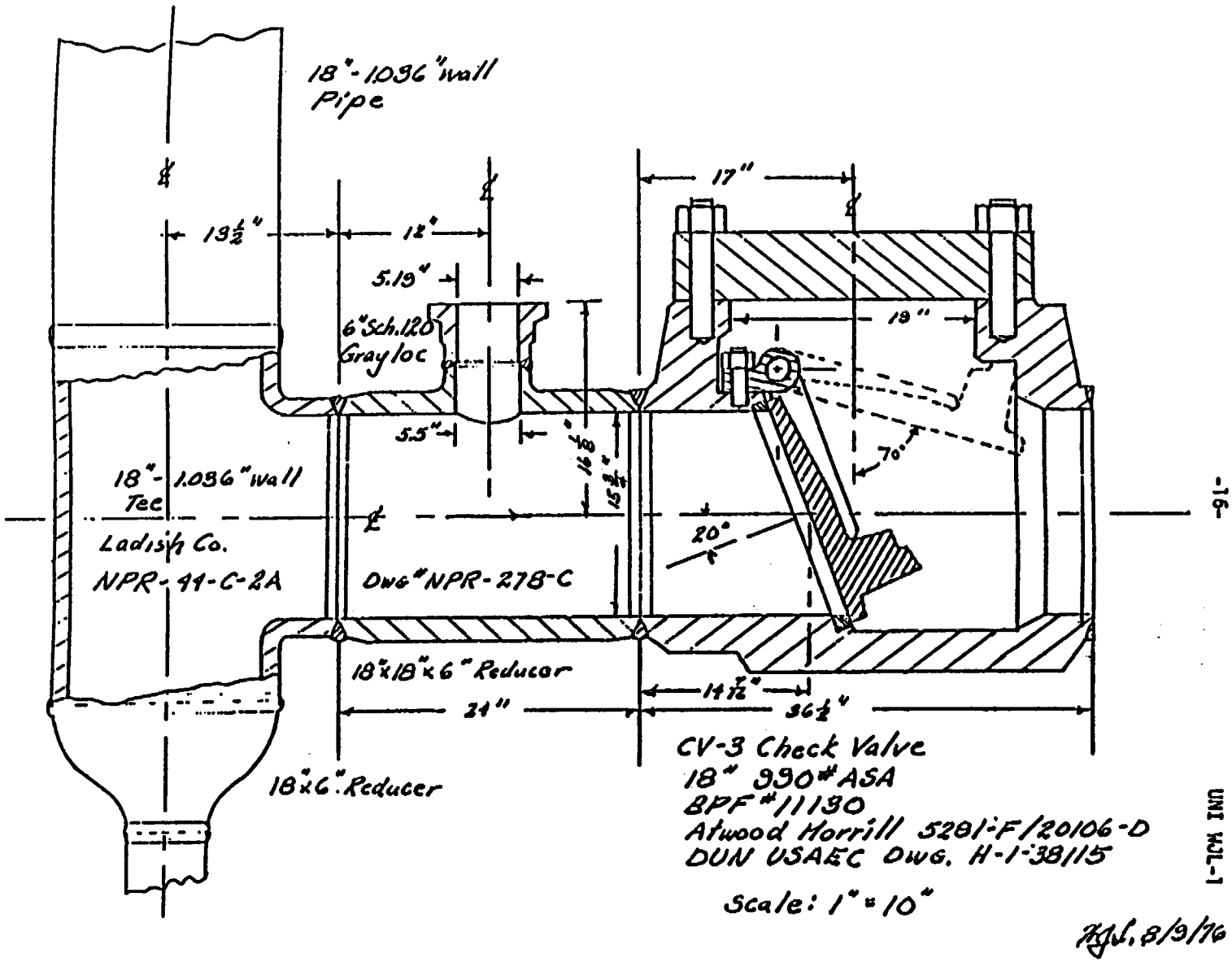

Figure 26
18" Swing Check Valve Installation Used In Example 1

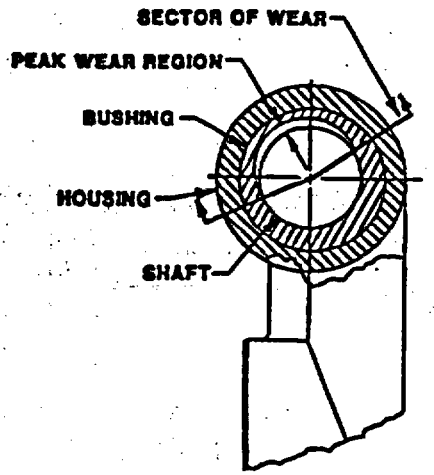

Figure 27
Hinge Pin Bushing Wear in 18" Valves (Example 1)

Appendix B contains the pertinent data and analysis details for these valves based on the predictive models developed under this NRC-sponsored research. The results show that the minimum velocity required to fully open the valve without any upstream disturbance is 19 ft/sec; however, when the effect of the upstream disturbance is accounted for as described in the Phase I report, the minimum velocity to fully open goes up to 22.8 ft/sec. The actual flow velocity during normal operation was 20 ft/sec, thus showing that the valve disc will be oscillating in the tapping zone. Since the valve disc and hinge arm are of an integral cast design that eliminates the disc stud connection to the hinge arm, the typically fatigue-prone area is not present in this design, and no fatigue problems were found.

The upstream flow disturbance is a tee connection with one end dead-end on the main run. The intensity of this flow disturbance is estimated to be more severe than an elbow, but less severe than the high turbulence source. This gives a (3σ) disc fluctuation angle of approximately eight degrees, based on Phase I research. The natural frequency of disc oscillation is calculated to be 2.0 hz based on Appendix A approach. The overall sliding motion is shared by the two bushings between the disc and shaft, and two bushings between the support trunnions and shaft, within which the shaft is free to rotate.

Because the bushing was made of a cast Stoody-6 (Co-CR-W alloy) and the shaft was made of wrought Haynes Stellite-25 (Co-Cr-W-Ni alloy), the sliding pair of metals can be classified as compatible. The value of the wear coefficient for this combination for water at high temperature is estimated to fall between 1×10^{-4} (for poor lubrication) and 5×10^{-4} (for no lubrication). The average (on a logarithm scale) of these two values is 2.24×10^{-4}, which is our best estimate of the applicable wear coefficient in lieu of actual tests on the exact material combination.

The theoretical wear rate prediction based on this value of K is calculated to be 0.0335-inch per year, compared to the measured wear rate of 0.022 to 0.027 inch/year. Based on our predictive methodology, the 3/16-inch thick bushing will be expected to wear through

completely in a little less than six years of operation. This is in excellent agreement with the actual experience which caused a number of the bushings to wear through in eight years of operation.

Plant Correlation Example 2:
18-Inch Swing Check Valves with Low Hinge Pin Bushing Wear
This is an extension of Example 1 because the only difference between the two is that these sixteen 18-inch valves (CV-5) of identical design were installed in the core inlet side at the end of a long run of approximately 70 feet of pipe. The operating flow conditions and their durations are the same as for the valves in Example 1.

In the absence of an upstream flow disturbance, the disc fluctuations are predicted to be in the range of baseline 3σ disc fluctuation of 1.5 to 2 degrees (instead of the 8 degrees for Example 1) as shown in the Phase I report.

These low levels of disc oscillations are predicted to result in bushing wear rates of .006-inch to .008-inch per year, which corresponds to a bushing wear-out life of 22.8 to 31.2 years. This correlates well with actual wear rates, which were reported to be "negligible" based on eight years of actual operation for these valves in Ref. 16.

Plant Correlation Example 3:
4-Inch Tilting Disc Check Valve Modifications to Reduce Hinge Pin Wear
Severe hinge pin wear was observed in two four-inch, Class 600 tilting disc check valves used in the auxiliary feedwater turbine steam supply system after one year of operation at San Onofre Unit 2 in 1986 (Ref. 8). The valves are normally closed, but the system had been recently modified to permit a small flow of 600 to 800 lb/hr of steam through these valves to avoid condensation and accumulation of water in the downstream piping. In one year of operation, the 0.5-inch diameter 410 stainless steel hinge pins had almost completely worn through due to the disc oscillation caused by the low rate of steam flow (Fig. 28). In this case, the 410 SS hinge pins were sliding against the bushings made from Stellite 6 material.

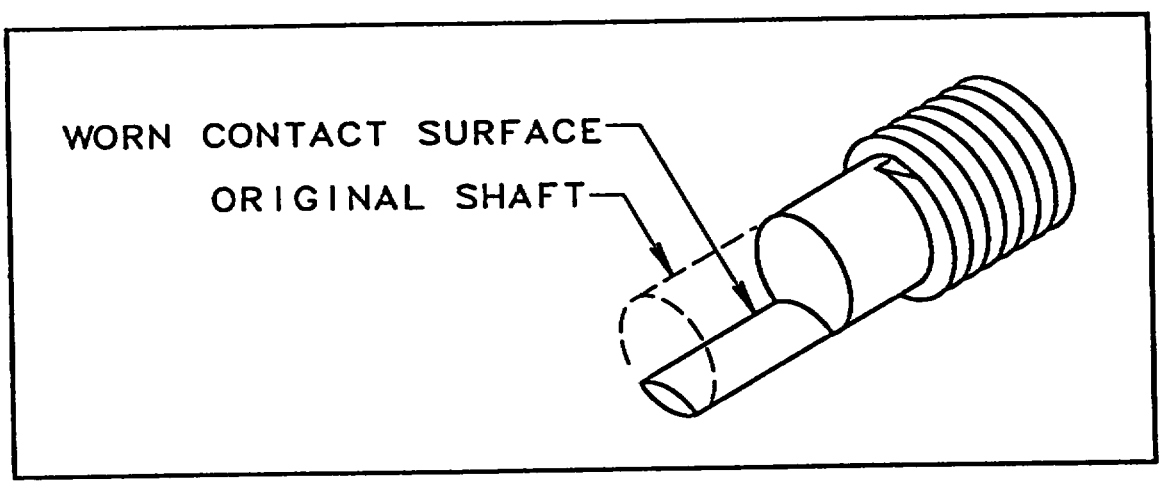

Figure 28

Severe Hinge Pin Wear in 4-Inch Tilting Disc Check Valve

Wear analysis for this valve was performed using the pendulum frequency approach because the disc is oscillating near the closed position due to low flow conditions. Disc oscillation frequency was calculated to be 2.9 hz, and mean disc oscillation angle of ± 10 degrees was used in wear analysis. The upper bound of disc oscillations found in the Phase I tests with water was around 16 degrees, and somewhat higher values are anticipated in steam due to lower damping. Wear coefficient for the 410 stainless steel (Fe-Cr-Ni alloy) hinge pin and Stellite-6 (Co-Cr-Ni alloy) bushing, a compatible metal sliding pair in steam (unlubricated surfaces) is estimated to be 5.0×10^{-4}. The hardness of the pin was approximately 275 Brinell.

Analysis predicted severe wear of 0.36-inch in one year of operation, which is more than 70 percent of the hinge pin diameter. Under such high wear conditions, wear depth rate increases rapidly after half the hinge pin diameter is worn due to reduction in the bushing area. These analytical estimates were found to be in agreement with actual inspection results from the two valves.

Even though absolute wear predictions based on assumptions made in the analysis should be considered accurate only within a factor of two or three (Refs. 10, 11), relative improvements by making material modifications can be predicted more accurately. Modifications were made in the hinge pin area by changing to Stellite-6 vs. Stellite-6 materials, which was predicted to reduce the wear rate to between 0.007-inch and 0.030-inch per year. Actual measurements made on the modified arrangement after five months of operation showed a wear rate of 0.010"/year, which is in good agreement with the predicted improvement, and about 30 times less than the original design!

Plant Correlation Example 4:
10-Inch Swing Check Valve Disc Stud Fatigue Failure

At San Onofre Nuclear Generating Site Unit 1, a water hammer event occurred in the pressurized water reactor horizontal feedwater line caused by failed check valves in November 1985 (Ref. 7). The disc stud/nut connection in these check valves had fractured due to repeated impact against the open stop, which had allowed the disc to separate from the hinge prior to this water hammer event. These valves had operated satisfactorily for several years at full power conditions. Fifteen months prior to this event, the plant was operated at approximately 85 percent reduced power. This resulted in insufficient flow velocity to fully open the disc, causing disc tapping and eventually fatigue failure of the threaded connection. Root cause analysis of this failure is documented in earlier reports (Refs. 6, 7); however, the root cause analysis did not attempt to quantify the fatigue failures.

Using the predictive fatigue/impact model developed under this research, this failure was reexamined quantitatively from a fatigue standpoint. The details of the analysis approach are contained in Appendix C. The important results from this analysis are presented here.

The minimum flow velocity to fully open the valve with no upstream disturbance is calculated to be 14.6 ft/sec. When adjusted for the upstream disturbance effect of the severe turbulence source (control valve) that is present immediately upstream, the minimum flow velocity requirements increase to approximately 17.5 ft/sec to 20.4 ft/sec. The actual flow velocity at full power is 18.5 ft/sec which is in the same range as the minimum flow

requirements. Therefore, the disc is estimated to be only marginally seated even at full power. At 85 percent power, the actual flow velocity is 16.5 ft/sec, which is just below the minimum requirements. Therefore, severe disc tapping is predicted to occur in this zone of operation.

Disc oscillation magnitude for this installation, which has a severe turbulence source immediately upstream of the check valve, is estimated to be 16 degrees based on Phase I research (Ref. 1). The disc oscillation frequencies, based on free body flow equilibrium method and the eddy frequency method, are calculated to be 2.65 hz and 1.58 hz. The high amplitude motion and impacts are most likely to occur near the lower of the two frequencies, based on comparisons between theory and actual tests on the three- and six-inch valves tested under Phase II. The peak stress at the base of the stud due to this level of disc motion is estimated to be 24 ksi, which falls in the low cycle fatigue range for the material used. Fatigue analysis results show that there is a very high propensity to failure due to disc stud fracture, and the analytical predictions are in the same range as the observed failure life of a few months when operated in this flow velocity range.

SUMMARY OF CHECK VALVE REVIEW METHODOLOGY

As stated in the introduction of this report, one of the major goals of the Phase II research was to develop a method to predict the behavior of swing and tilt disc check valves. Specifically, we are interested in predicting several common modes of check valve degradation so that potentially troublesome installations can be identified before the valve causes a plant problem. We believe the techniques described here, combined with the large amount of data presented in Reference 1, go a long way toward meeting this goal. In this section, we will present a summary of the method to be followed in predicting check valve degradation. We believe the predictive methodology outlined below is of particular merit both because of what it does do and, just as importantly, for what it does not do. The ability to identify and quantify, in advance, a check valve's propensity for accelerated degradation should be the aim of any review and analysis technique. The methodology described here does this.

Many check valve reviews depend on determining whether the V_{min} requirements are met for each valve application. It is very easy to create a maintenance nightmare if open-and-inspect decisions are based solely on the results of V_{min} calculations since 70 percent to 80 percent of all check valves will fail this single criterion and will end up with recommendations to be opened and inspected. This is what our methodology does *not* do.

Overview of Check Valve Review and Analysis Procedure

1. Calculate minimum velocity, V_{min}, requirements (Ref. 3).
2. Determine C_{up} factor and calculate modified V_{min} (Ref. 1).
3. Do not get discouraged when 70 percent to 80 percent of valves fail to meet V_{min} requirements. Most will prove to be in satisfactory condition.
4. Calculate hinge pin wear and, if necessary, disc stud fatigue potentials using the predictive models described in this report.
5. Disposition the valve based upon analysis results *and* any available maintenance records.

These steps will be reviewed in more detail in the following sections.

V_{min} Calculation

The important first step in the review process is determination of the valve minimum velocity requirements. In the absence of actual test data *on the specific valve in question*, the V_{min} formula described in Ref. 3 should be used.

This formula has been proven many times to provide an excellent estimate of V_{min} requirements for many swing and tilt disc check valves if certain constraints are followed. Figure 29 presents the results of seventeen valve tests compared with their V_{min} predictions calculated using the EPRI guideline formula.

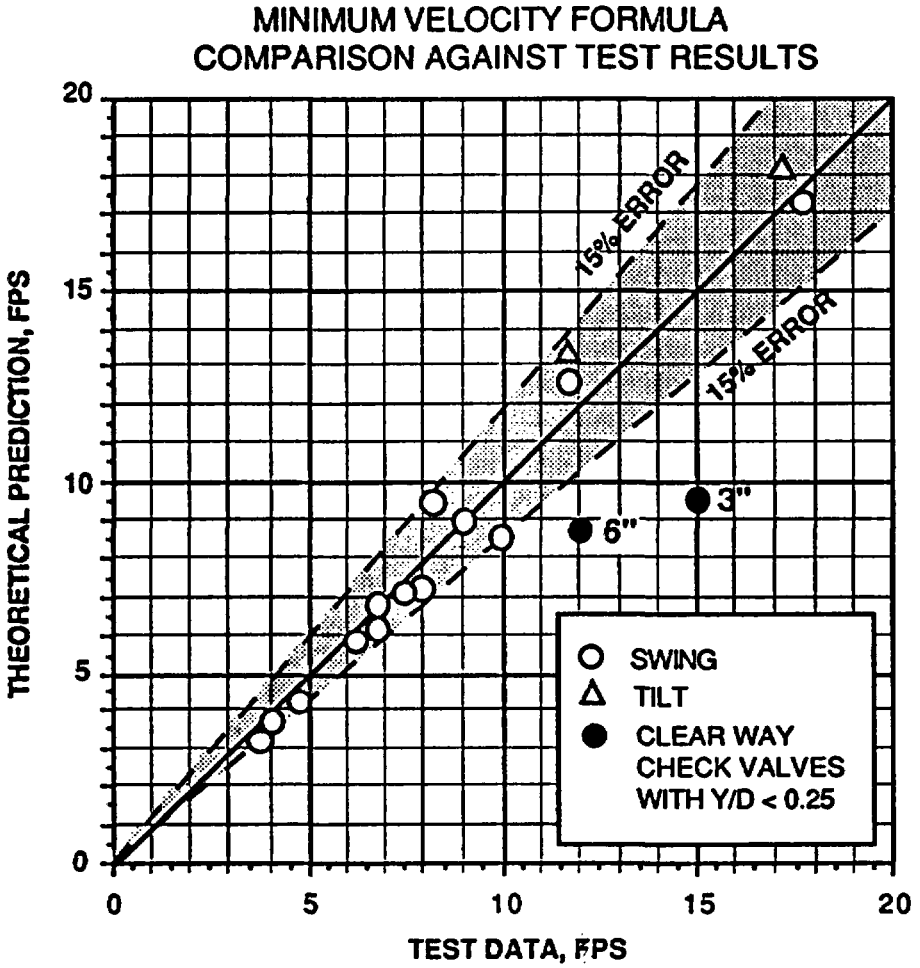

Figure 29

Minimum Velocity Formula Comparison Against Test Results

As can be seen, there is excellent correlation between the measured and predicted values, except for two data points. These two points illustrate the first important constraint of the V_{min} formula. As previously noted in Ref. 3, when the disc projection, Y, into the flow stream is less than about 25 percent of the valve size, d, the predicted results will begin to deviate from test results. This Y/d ratio is illustrated in Figure 30. Both valves have a disc angle, θ, with respect to the flow stream of 65 degrees; however, Valve A has a Y/d of 25 percent and Valve B has a Y/d of almost zero. Valve B is typical of what are generally classified as clearway swing check valves, and the V_{min} formula will underestimate the flow velocity requirements by as much as 50 percent for valves of this type. In Figure 29, the two data points labeled three-inch and six-inch are, in fact, clearway swing checks with Y/d ratios of zero and 0.14 respectively. While the fluid impingement angle, θ, is an important factor in the V_{min} calculation, it must be recognized that the Y/d ratio is an independent factor which can significantly affect the accuracy of the V_{min} estimate. If this important fact is recognized, then judicious adjustments can be made to estimate a more realistic V_{min} for a clearway valve. Refinement of the V_{min} formula is possible to take

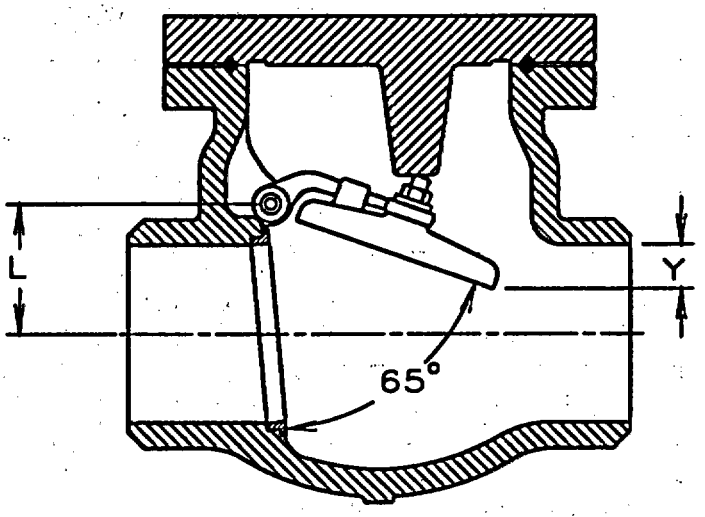

Geometry A, Y/D = 0.25

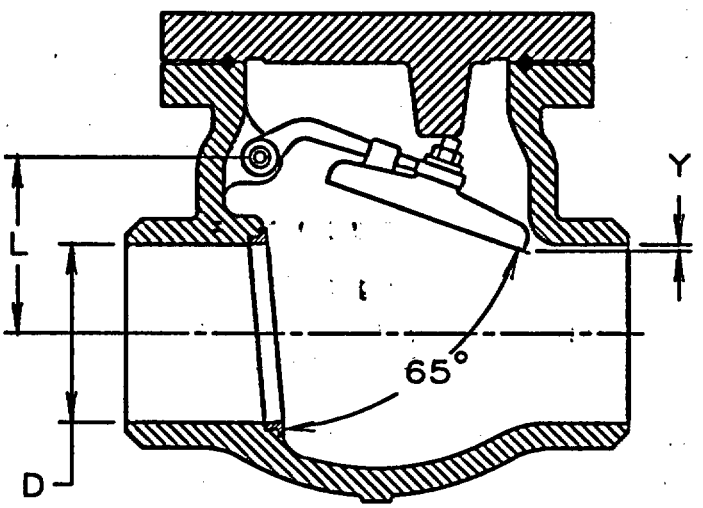

Geometry B, Y/D ≅ 0

Notes:

(1) V_{min} and disc stability are seriously affected by independent parameter "Y"

(2) When Y/D < .25, actual V_{min} may be much higher than predicted by generalized V_{min} equation, and disc stability may not be achievable with velocity increase

Figure 30

Significance of Disc Projection (Y/D) on Performance

into account the Y/d ratio. Preliminary work has shown the validity of an approach presently under development. However, systematic testing is needed to properly quantify the effect of this important factor.

In addition to the Y/d ratio, care must be exercised in the following areas when applying the V_{min} formula:

1. *Fluid impingement angle, θ, and seat angle, α.*
   Most valves have an inclined seat with angle, α. Some will have an angle as high as 30 degrees or more. In most cases this *will not* affect the net fluid impingement angle, θ. A good illustration of this is in Plant Correlation Example 1, discussed earlier. These valves have seat inclination angles of 20 degrees, yet the inlet of the valve is straight and horizontal. The seat angle by itself *will not* alter the flow direction through the valve to any appreciable extent. Therefore, the fluid impingement angle will equal β, the angle the disc makes with the pipe axis when fully open. Accounting for the full value of α in the net impingement angle can result in grossly underestimating the flow velocity requirements of a valve. For those valves which have both an inclined seat *and* a deliberately inclined inlet geometry leading into the seat, some contribution to the net impingement angle can be taken into account. Typically, this additional amount is in the area of 3 to 10 degrees.

2. *Reduced Inlet Port Geometry*
   Related very often to the previous discussion are concerns about valves with reduced inlet ports. This design feature is usually incorporated in an attempt to increase the flow velocity through the seat and, in effect, reduce the V_{min} requirements based on the flow velocity in the (larger) piping system. Unfortunately, there are often detrimental side effects which accompany the velocity increase. For example, the fluid often undergoes a severe directional change while passing through the valve or, after passing through the reduced seat area, expands abruptly upon entering the valve body. In these cases, one has in effect created a self-contained flow disturbance that may very well eliminate any beneficial effect of the increased seat velocity. In these situations, a valve which has only straight pipe for 10d upstream and would otherwise be treated as having no upstream disturbance, might best be modeled for V_{min} purposes as having a low turbulence source at 0d.

3. *Effective Disc Diameter*
   As recommended in Ref. 3, the disc diameter used to calculate the disc flow impingement area, A, should not exceed 110 percent of the valve seat diameter. Significant errors will often result if the disc diameter is assumed to be equal to the basic valve size.

Calculation of Modified V_{min} using C_{up}

After determining the generalized minimum velocity, the effects of any upstream disturbances must be accounted for. These disturbances will *always* serve to increase the V_{min} requirements above those calculated using the basic V_{min} formula. A table of V_{min} modification factors for upstream disturbances is included in Reference 1. These were determined from the extensive set of tests performed as part of that research. While every

conceivable disturbance type cannot be covered, engineering judgment can be used to make sound and conservative judgments based on the test data at hand.

Having completed this V_{min} calculation, it is not uncommon to find that 70 percent or more of all check valves in nuclear power plants systems do not meet V_{min} requirements. Technically these valves are misapplied, yet it is clear from industry records that serious problems do not exist with this large population of valves. Only a small percentage of the so-called misapplied valves suffer from accelerated degradation. The problem for the utility engineer becomes one of determining which of these misapplied check valves will turn out to be the truly "bad apple" likely to be suffering from accelerated wear and degradation. Knowledge of the valve V_{min} is necessary; but it is insufficient information to progress further. The following steps must be completed before making this determination.

Wear and Fatigue Calculations

The techniques developed in this Phase II work form the basis for predicting two of the most important check valve degradation processes: hinge pin wear and disc stud fatigue. Only after these calculations have been performed can one make an informed decision with respect to the need to open and inspect a valve, and with what frequency. Our experience has shown that by applying these techniques, using conservative estimates where information may be lacking (valve dimensions, typically), the majority of valves which do not meet V_{min} requirements are found to have very low predicted hinge pin wear rates and, often, *no* predicted disc stud fatigue problems. These valves are operating under sub-optimal conditions and their behavior must be quantified unless a massive plant-wide open-and-inspect program is desired. This is where the Phase II work can be used to predict hinge pin wear and disc stud fatigue. As shown in the plant correlation examples, considerable engineering judgment must be exercised in certain areas. Nevertheless, the methodology will greatly reduce the number of valves in need of inspection.

Conclusions

This Phase II research has resulted in quantitative techniques that can be used to predict the performance of swing check valves and help identify those valves most likely to suffer premature degradation from hinge pin wear and/or disc stud fatigue. Predictive models for hinge pin wear and disc stud fatigue have been presented with experimental verification as well as correlation to actual plant examples.

REFERENCES

1. M. S. Kalsi, Todd Horst, J. K. Wang. *Prediction of Check Valve Performance and Degradation in Nuclear Power Plant Systems*, NUREG/CR 5159, prepared for the U.S. Nuclear Regulatory Commission as Phase I SBIR Research, May 1988.

2. *Check Valve Failures or Degradation*, Significant Operating Experience Report No. 86-3, Institute of Nuclear Power Operations, Atlanta, GA, October 1986.

3. *Application Guidelines for Check Valves in Nuclear Power Plants*, EPRI NP-5475, January 1988.

4. *Aging and Service Wear of Check Valves Used in Engineered Safety-Feature Systems of Nuclear Power Plants*, NRC NUREG/CR-4302, Vol. 1, December 1985.

5. *Loss of Power and Water Hammer Event at San Onofre Unit 1 on November 21, 1985*, NRC NUREG-1190.

6. Chong Chiu and M. S. Kalsi. *Failure Analysis of Swing Check Valves - San Onofre Nuclear Generation Site - Unit 1*, NRC Docket No. 50-206, April 1986.

7. Chong Chiu and M. S. Kalsi. *Plant Availability Improvement by Eliminating Disc Vibrations in Swing Check Valves*, ASME Paper No. 86-JPGC-NE-6, October 1986.

8. M. S. Kalsi. *Analysis of the 4-Inch Tilting Disc Check Valve Problems and Proposed Modifications*, Kalsi Engineering, Inc. report (3.10.2) to Southern California Edison Company, 1986.

9. Todd Horst and M. S. Kalsi. *Integrating the Check Valve Application Review with Preventive Maintenance Programs*, ASME Paper No. 89-JPGC/NE-2, October 1989.

10. E. Rabinowicz. **Friction and Wear of Materials**, John Wiley & Sons, 1964.

11. **Wear Control Handbook**, edited by Peterson & Winer, ASME Publication, New York, 1980.

12. J. F. Archard. "Wear Theory and Mechanisms," **Wear Control Handbook**, ed. by Peterson and Winer, p. 35, ASME Publications, New York, 1980.

13. J. P. Tullis and W. J. Rahmeyer. *Performance Tests on Feedwater Check Valves for San Onofre Nuclear Power Plant, Phase A and Phase B*, Utah State University Foundation Report, April 1986.

14. S. L. Collier, C. C. Hoerner, and C. E. Davila. *Behavior and Wear of Check Valves*, ASME Paper 82-PET-12.

15. D. J. Trimble and T. A. Galisto. *Selection of a Non-Cobalt Alloy for Sliding Wear Service in a Nuclear (Check) Valve*, Wear of Materials, edited by Rhee, Ruff, and Ludena, p. 219, ASME Publication, New York, 1981.

16. W. J. Love. *Value Bushing Wear in the Atwood-Morrell Co. Check Valves CV-3, CV-5, PCSV-202, UNI-WJL-1*, March 10, 1977, UNC Nuclear Industries, Richland, Washington.

17. John E. Sununu. *Wear in Check Valves Due to Flow Induced Motion*, Master's Thesis, Massachusetts Institute of Technology, May 1987.

18. J. O. Hinze. Turbulence, McGraw-Hill, New York, 1959.

19. Laufer, The Structure of Turbulence in Fully Developed Pipe Flow, 1954.

20. K. T. Patton. *Tables for Hydrodynamic Mass Factors for Translational Motion*, ASME 65-WA/UNT-2.

21. *Criteria of the ASME Boiler and Pressure Vessel Code for Design by Analysis in Section VII and VIII, Division 2.* Published by ASME, 1969.

APPENDIX A
IMPACT AND FATIGUE PREDICTION METHODS

APPENDIX A

IMPACT AND FATIGUE PREDICTION METHODS

A.1. PEAK DISC STUD IMPACT FORCE ESTIMATION

The peak impact force estimates in the disc stud can be based upon the disc velocity before impact using the energy balance relationships. The disc/disc stop assembly may be considered as a simple mass-spring system where the disc is the moving mass and the combined assembly has an equivalent stiffness as in a simple spring. During the impact, a majority of the kinetic energy of the moving mass is converted to the elastic strain energy in the spring with a small energy loss due to friction, vibration, or small contact deformation. Neglecting the energy loss, the upper bound elastic strain energy in the system at the peak of impact where the disc movement stops momentarily can be expressed as

Kinetic Energy of Disc = Elastic strain energy in the assembly

For a small amplitude of disc oscillation, the kinetic energy of the disc before impact can be estimated as:

$$K.E. = \frac{1}{2} m V^2 \ (in-lb)$$

where

m = Disc mass, $\frac{lb\text{-}sec^2}{in}$

V = Linear velocity of disc before impact, in / sec

The equivalent stiffness of the assembly can be approximated without resorting to a detailed stiffness analysis. As shown in most swing check valve designs, the most flexible element in a disc/disc stop assembly is the disc stud. Assuming that the disc stud is the spring element which absorbs all the kinetic energy during the impact and the disc and disc stop are rigid, the total strain energy in the stud is

Stud Strain Energy = Strain energy in compression + strain energy in bending

$$= \frac{F\,\delta}{2} + \frac{M\,\theta}{2}$$

$$= \frac{F^2\,L}{2\,AE} + \frac{M^2 L}{2\,EI}$$

$$= \frac{F^2}{2}\left(\frac{L}{AE} + \frac{e^2\,L}{EI}\right)$$

where

F = uniform axial force on stud, lb

L = Stud length, in

A = Average stud cross-sectional area, in^2

M = Uniform bending moment on stud, in-lb
= Fe

e = Eccentricity of axial force, in

δ = Axial deformation of disc stud

θ = Angular deformation of disc stud

The upper peak impact force can be estimated based upon the kinetic energy to the strain:

$$\frac{1}{2} m V^2 = \frac{F^2}{2} \left(\frac{L}{AE} + \frac{e^2 L}{EI} \right)$$

$$F = V \sqrt{\frac{m}{\left(\frac{L}{AE} + \frac{e^2 L}{EI} \right)}}$$

A.2. PEAK FORCE ESTIMATION FOR THE SIX-INCH INSTRUMENTED DISC

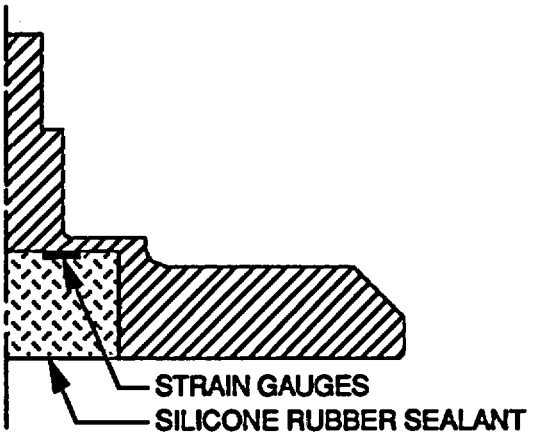

Figure A.1
Instrumented Disc Cross-Section

Figure A.1 shows the cross-section sketch of the instrumented disc modified from a six-inch disc design to accommodate the strain gauge installation for the axial impact force measurements. The axial stiffness of the disc was precisely analyzed by the finite element method and found to be 1.0×10^6 lb/in. The combined disc weight plus one-half of the hinge weight is 10.19 pounds. The peak impact force under a straight axial impact can be estimated using the above derived equation as

$$F = V \sqrt{\frac{m}{\left(\frac{L}{AE} + \frac{e^2 L}{EI}\right)}}$$

$$= V \sqrt{\frac{m}{\frac{1}{k}}}$$

$$= \sqrt{\frac{10.19}{386.4} \times 1.0 \times 10^6}\ V$$

$$F = 162.4\, V \text{ lb}$$

The tested valve has a hinge length of 5.04 inches. Therefore, the disc angular velocity versus impact force can be expressed as

$$F = 162.4 \times 5.04 \times \frac{\pi}{180}\ \omega$$

$$= 14.285\ \omega$$

where ω = Disc angular velocity before impact, deg / sec

The input force varies linearly with the disc angular velocity. For convenience, the table below shows the magnitude of angular/linear disc velocity vs. impact force.

Disc Angular Velocity, deg/sec	*Disc Linear Velocity, in/sec*	*Impact Force lb*
2	0.1759	29
4	0.3519	57
6	0.5278	85
8	0.7037	114
10	0.8796	143
12	1.055	171
14	1.232	200
16	1.407	229
18	1.583	257
20	1.759	286
24	2.111	343
28	2.463	400
32	2.815	457
36	3.167	514
40	3.519	571
45	3.958	643
50	4.398	714
55	4.838	786
60	5.278	857
70	6.158	1,000
80	7.037	1,143
90	7.917	1,286
100	8.796	1,429
150	13.195	2,143
200	17.593	2,857

Table A.1

Magnitude of Angular/Linear Disc Velocity vs. Impact Force

A.3. ESTIMATION OF DISC OSCILLATION FREQUENCY

Disc oscillation frequencies may vary with many factors such as the types of upstream disturbance, fluid media, and disc positions (disc opening angles). The actual disc frequency for a specific case is based on comparison against available test data from references (Refs. 1, 6, 7, 17, 18, 19) and engineering judgment. The three methods discussed below have been used in estimating disc oscillation frequencies: (1) the free body flow equilibrium method, (2) the eddy frequency method, and (3) the pendulum frequency method based upon the disc mass and hinge length.

A.3.1. Free Body Flow Equilibrium Method

The natural frequency of a single degree of freedom spring-mass system is given by:

$$f_n = \frac{1}{2\pi}\sqrt{\frac{K_{stiff}}{W/g}}$$

where

f_n = Natural frequency, hertz

K_{stiff} = System spring rate, lb/in

W = Effective disc weight, lb
$= W_{disc} + 0.5\,W_{hinge} + 1/3\,\rho\,(d_{disc})^3$

g = Gravitational acceleration, in/sec^2
$= 386.4$

d_{disc} = disc diameter, in

ρ = Fluid weight density, lb/in^3

For the check valve, effective spring rate can be expressed as the force required to open the disc to some equilibrium angle, θ. An expression for this force, as developed in Reference 3, is:

$$F = \frac{2\,k\,A\,\rho\,V^2}{g}\sin\theta\,\frac{\sin\theta}{2}$$

where

F = Fluid force acting on the disc, lb

k = an empirical constant dependent on valve geometry
$= 2.0$ (average value)

A = Disc area, in^2

V = Fluid mean velocity, in/sec

θ = Fluid impingement angle (see Fig. 1 in report), deg

$$K_{stiff} = \frac{1}{R}\frac{dF}{d\theta} \quad \text{where } R = \text{radius from hinge pin to disc } \mathit{CL}, \text{ in}$$

$$\therefore\ K_{stiff} = \frac{2}{R}\,\frac{K\,A\,\rho\,V^2}{g}\,\frac{d}{d\theta}\left(\sin\theta\,\sin\frac{\theta}{2}\right)$$

$$K_{stiff} = \frac{2KA\rho V^2}{Rg}\left(\cos\theta \sin\frac{\theta}{2} + \frac{1}{2}\cos\frac{\theta}{2}\sin\theta\right)$$

Finally

$$f_n = \frac{1}{2\pi}\sqrt{\frac{2KA\rho V^2 Z}{RW}}$$

where

$$Z = \left[\cos\theta \sin\frac{\theta}{2} + \frac{1}{2}\cos\frac{\theta}{2}\sin\theta\right]$$

A.3.2. Eddy Frequency Method

As shown in Reference 17, the eddy frequency of the fluid can be estimated as

$$f_{eddy} = \frac{0.08\,V}{V_s}$$

where

f_{eddy} = Eddy frequency, Hz

V = Flow velocity, in/sec

V_s = Nominal valve size, in

A.3.3. Pendulum Frequency Method

The pendulum frequency is most suitable for disc frequency estimations for low flow conditions where discs are in almost vertical hanging positions. The pendulum frequency is:

$$f_{pend} = \frac{1}{2\pi}\sqrt{\frac{g}{R}}$$

where

f_{pend} = Pendulum frequency, Hz

g = Gravitational acceleration, in/sec2
= 386.4

R = Disc hinge length, in

A.4. ESTIMATION OF DISC OSCILLATION ANGLE

Different types of upstream disturbances and distances of disturbance source produce various degrees of disc fluctuation as shown in the test results in References 1 and 3. These test results can be utilized for the similar types of upstream disturbances to estimate oscillation angles for the disc fatigue and wear predictions.

A.5. ESTIMATION OF DISC STUD FATIGUE STRENGTH

The disc stud fatigue strength under disc tapping conditions may be estimated using the following steps:

i) Calculate the minimum flow velocity requirement to fully open the disc, including the velocity margin factor to account for upstream disturbances as given in References 1 and 3. If this disc is not fully open and possibly tapping, then proceed with the following steps for stud fatigue calculations.

ii) Calculate the disc oscillation frequency as discussed in Section A.3.

iii) Calculate the disc oscillation angle as discussed in Section A.4.

iv) Calculate the maximum disc velocity based on the above calculated disc frequency and amplitude as (Appendix D also provides the measured maximum disc velocity from tests):

$$V_{max} = R \times \frac{\theta}{2} \times 2\pi f$$

where

R = Hinge length, in

θ = Disc oscillating angle (peak to peak), rad

f = Disc oscillating frequency, Hz

v) Calculate the maximum impact force using the method described in Section A.1.

vi) From the above calculated peak impact force, the stud axial and bending stresses at the weakest cross-section can be calculated as:

$$\sigma_{axial} = \frac{F}{A}$$

$$\sigma_{bending} = \frac{M}{Z} = \frac{F e}{Z}$$

where

F = Peak impact force, lb

A = Cross-Section area, in^2

e = Load eccentricity, in

Z = Section modulus, in^3

The maximum stud surface alternating stress is:

$$\sigma_{alt} = \frac{1}{2} \times SCF \times \left(\sigma_{axial} + \sigma_{bending}\right)$$

where

SCF = Stress concentration factor at the selected cross-section

vii) Calculate fatigue usage based upon the above calculated alternating stress, hours of service, oscillation frequency, and the stud mterial fatigue curve (such as the ASME fatigue curve used in the example in Appendix C).

It should be noted that the disc oscillation angle provided in Reference 1 is the 3σ disc angle on the Gaussian distribution curve (i.e., the actual disc oscillation angles due to flow turbulence are less than the 3σ value 99.7 percent of the time). Therefore, the disc impact forces are expected to be much lower than the calculated force the majority of the time. Statistical method such as Gaussian distribution may be used to provide a more realistic estimation of the stud fatigue usage. Detailed calculations are given in the example in Appendix C.

APPENDIX B
CALCULATION OF V_{MIN}, FLOW VELOCITY, AND WEAR RATE FOR PLANT CORRELATION EXAMPLE 1

APPENDIX B
CALCULATION OF V_{MIN}, FLOW VELOCITY, AND WEAR RATE FOR PLANT CORRELATION EXAMPLE 1

B.1. DATA USED IN CALCULATIONS

Dimensions

Valve ID	:	15.75"
Disc Diameter	:	15.875"
Disc & Hinge Weight	:	200 lbs
Hinge Length	:	11.375"
Hinge Pin Diameter	:	1.625"
Hinge Pin Wear Length	:	4.38" (This is accounting for both pairs of bushings, namely, the disk-shaft bushings and the trunnion bushings, that the shaft can slide in.)
Fluid Impingement Angle	:	20°

Materials

Bushings	:	Stellite-6/Stoody-6
Hinge Pin	:	Haynes Alloy 25
Hinge Pin Hardness	:	38 R_C

Installation

Valve Orientation	:	Horizontal
Upstream Disturbance	:	Side discharge dead end line tee at 2 ft
Fluid	:	Water

Operating Conditions

Flow Rate	:	12,500 gpm
Operating Temperature	:	530°F
Operating Pressure	:	1,875 psi
Valve Usage per Year	:	70%

B.2. V_{MIN} AND FLOW VELOCITY CALCULATIONS

$$V_{min}|_{generalized} = \left[\frac{g\,C\,W_{eff}\cos\theta}{K\,\rho\,A\sin^2\theta}\right]^{0.5}$$

g = Acceleration due to gravity = 32.2 ft/sec^2

C = Bouyancy factor = 0.9 for water

W_{eff} = Weight of disc-hinge arm assembly = 200 lbs

θ = Impingement angle = 20°

K = Empirical construct = 2.0

ρ = Density of constant water (operating fluid) at 530°F (operating temperature) = 46.9 lb/ft^3

$$A = \text{Disc Area} = \frac{\pi}{4}\times\left(\frac{15.875}{12}\right)^2 \text{ft}^2 = 1.3745\,\text{ft}^2$$

$$\Rightarrow V_{min}|_{generalized} = 19.0 \text{ ft/sec}$$

Since the upstream disturbance is a medium turbulence source,

C_{up} = 1.2 to 1.4 → Table 3, pg. 20, NUREG/CR-5159

$$\therefore V_{min} = C_{up}\times V_{min}|_{generalized}$$

$$= 1.2\times 19.00$$

$$V_{min} = 22.8 \text{ fps}$$

Determination of Flow Velocity Under Operating Conditions

Operating Flow Rate : 12,500 gpm

Valve ID : 15.75"

$$\Rightarrow \text{Cross-Sectional Area} = \frac{\pi}{4}\times(15.75)^2 = 194.8\,\text{in}^2$$

$$\Rightarrow \text{Flow Velocity (fps)} = 12{,}500\frac{\text{gal}}{\text{min}}\times 231\frac{\text{in}^3}{\text{gal}}\times\frac{1\,\text{min}}{60\,\text{sec}}\times\frac{1}{194.8\,\text{in}^2}\times\frac{1\,\text{ft}}{12\,\text{in}}$$

$$\text{Flow Velocity} = 20.59 \text{ fps}$$

This flow velocity is less than V_{min}; accounting for upstream disturbance.

B.3. WEAR CALCULATIONS

The wear equation is

$$W = \frac{K L d}{H}$$

where

K = Wear coefficient

L = Effective weight of disc = (W_{disc} + W_{arm}) + bouyancy factor

d = Total distance traveled by the hinge pin

H = Penetration hardness

Determination of Wear Coefficient, K

The geometric average of the wear coefficient of a compatible metal combination under poorly lubricated conditions (1×10^{-4}) and an unlubricated condition (5×10^{-4}) is:

$$K = 10^{\Re}$$

where $$\Re = \left[\frac{\log_{10}\left(1 \times 10^{-4}\right) + \log_{10}\left(5 \times 10^{-4}\right)}{2} \right]$$

$$\Rightarrow \quad K = 2.236 \times 10^{-4}$$

Determination of L, the Effective Disc Weight

Disc Weight = 200 lbs

Bouyancy Factor = 0.9 (for water)

$\Rightarrow$ Effective Disc Weight = 0.9 x 200 lbs = 180 lbs

L = 180 lbs

Determination of Sliding Distance, d

$$d = \theta \times \frac{\pi}{180} \times 2 \times f \times \phi \times 0.5 \times t \times s$$

where

θ = Oscillating angle

f = Frequency of oscillation

t = Total time over which wear is calculated

s = Statistical factor

The side discharge dead end tee line is a medium turbulence source. In NUREG/CR-5159, page 58, Figure 30, the disc fluctuation angle is seen to be approximately 8 degrees for a medium turbulence source.

$$\theta = 8^\circ$$

The equation described in Section A.3.1, page 6 of Appendix A, the frequency of oscillation is given by

$$f_n = \frac{1}{2\pi}\sqrt{\frac{2KA\rho V^2 Z}{RW}}$$

where $$Z = \left[\cos\theta \sin\frac{\theta}{2} + \frac{1}{2}\cos\frac{\theta}{2}\sin\theta\right]$$

K = an empirical constant dependent on valve geometry

= 2.0 (average valve)

$$A = \text{Area of seat port} = \frac{\pi}{4} \times \frac{(15.875)^2}{144}\,ft^2 = 1.3745\,ft^2$$

V = Flow velocity = 20.6 fps (computed in Appendix B, Section 2)

θ = Impingement angle = 20°

ρ = Fluid density = 46.9 lb/ft3 at 530°F

R = Hinge arm length = 11.375" = 0.948 ft

$$W = 200 + \frac{1}{3}\rho D_{disc}^3 = 200 + \frac{1}{3} \times 624 \times \left(\frac{15.875}{12}\right)^3 = 248 \text{ lbs}$$

$$\Rightarrow f = 1.97 \text{ Hz}$$

$$f_n = \frac{1}{2\pi}\sqrt{\frac{2 \times 2 \times 1.3745 \times 46.9 \times (20.6)^2 \times 0.3316}{0.948 \times 248}}\ \sqrt{\frac{ft^2}{ft} \times \frac{lb}{ft^3} \times \frac{ft^2}{sec^2}}$$

$$Z = \left[\cos 20 \sin 10 + \frac{1}{2}\cos 10 \sin 20\right] = 0.3316$$

$$\Rightarrow f = 2.0 \text{ hz}$$

ϕ = Hinge pin diameter = 1.625"

Total Valve Usage per Year = 70%

$$\Rightarrow \text{Total Operating Time, } t = 0.7 \times 8{,}760 \frac{hrs}{year} \times 3{,}600 \frac{sec}{hr}$$

$$\Rightarrow t = 22{,}075{,}200 \text{ seconds}$$

For a Gaussian distribution, the statistical factor, $s \cong 0.309$ from the sum of the products of magnitude multiplied by probability.

$$\Rightarrow d = 8° \times \frac{\pi}{180} \times 2 \times 2.0 \times 1.625 \times 0.5 \times 22{,}075{,}200 \times 0.309 \text{ in}$$

$$= 3.095 \times 10^6 \text{ in}$$

Determination of Penetration Hardness, H

$$H = R_C 38 = 38 \times 14{,}232 \text{ psi}$$

$$\Rightarrow H = 540{,}810 \text{ psi}$$

$$\therefore \text{ Wear Rate} = \frac{K L d}{H} = \frac{2.236 \times 10^{-4} \times 180 \times 3.095 \times 10^6}{540{,}810}$$

$$\Rightarrow W = 0.2303 \text{ cu.in/year}$$

$$\text{Bearing Area} = \frac{\pi d}{4} \times \ell = \frac{\pi \times 1.625}{4} \times 2.69 = 3.433 \text{ in}^2$$

Total Bearing Area = Bearing area at disc to shaft bushing + bearing area at trunnion bushing = $3.433 \text{ in}^2 \times 2$

$$= 6.866 \text{ in}^2$$

$$\text{Wear Depth} = \frac{\text{Volumetric Wear Rate}}{\text{Total Bearing Area}} = \frac{0.2303 \text{ in}^3/\text{yr}}{6.866 \text{ in}^2}$$

$$\Rightarrow \text{Wear Depth} = 0.0335 \text{ in/yr}$$

APPENDIX C
CORRELATION OF FATIGUE ANALYSIS WITH AVAILABLE PLANT DATA FOR PLANT CORRELATION EXAMPLE 4

APPENDIX C

CORRELATION OF FATIGUE ANALYSIS WITH AVAILABLE PLANT DATA FOR PLANT CORRELATION EXAMPLE 4

C.1. CASE HISTORY AND AVAILABLE PLANT DATA

At San Onofre Nuclear Generating Site Unit 1, a water hammer event occurred in the pressurized water reactor horizontal feedwater line caused by failed check valves in November 1985 (RefS. 5, 6, 7). The disc stud/nut connection in these check valves had fractured due to repeated impact against the open stop, which had allowed the disc to separate from the hinge prior to this water hammer event. These valves had operated satisfactorily for several years at full power conditions. Fifteen months prior to this event, the plant was operated at approximately 85 percent reduced power. This resulted in insufficient flow velocity to fully open the disc causing disc tapping and eventually fatigue failure of the threaded connection. The specific valve and system data available from the plant are:

Valve Description	:	10" x 600# MCC Pacific swing check
Fluid Condition	:	Water @ 375°F 18.54 ft/sec @ full power 16.50 ft/sec @ reduced power
Disc Weight	:	33 lb
Hinge Weight	:	12 lb
Total Impingement Angle	:	15 deg
Disc Diameter	:	11.25 in
Upstream Disturbances	:	Control valve @ 19" Expander @ 14"
Disc Stud Diameter	:	1-1/8 in
Disc Stud Length (approx.)	:	3 in
Hinge Length	:	7.5 in
Disc Material: A217	: :	Tensile strength 70 ksi Yield strength 40 ksi

C.2. STUD FATIGUE STRENGTH CALCULATIONS

C.2.1. Minimum Required Flow Velocity

$$V_{min} = \sqrt{\frac{g\ C\ W_{eff}\ \cos\theta}{K\ \rho\ A\ \sin^2\theta}}$$

where

$$g = 32.2\ ft/sec^2$$

$$\rho = 54.56\ lb/ft^3$$

$$C = \frac{489 - \rho}{489} = 0.89$$

$$W_{eff} = W_{disc} + 1/2\ W_{hinge} = 33 + 6 + 39\ lb$$

$$K = 2.0$$

$$A = \frac{\pi}{4}(d_{disc})^2 = 0.7854\left(\frac{11.25}{12}\right)^2 = 0.6903\ ft^2$$

$$\theta = 15\ deg$$

$$V_{min} = 14.61\ ft/sec$$

Minimum required flow velocity with upstream disturbance, V'min (see Ref. 1):

$$V'_{min} = C_{up}\ V_{min}$$

The estimated C_{up} for the upstream disturbance as stated in Ref. A.7 is 1.2 to 1.4. Therefore,

$$V'_{min} = 1.2 \times 14.61 = 17.68\ ft/sec$$

$$= 1.4 \times 14.61 = 20.61\ ft/sec$$

The calculated minimum required flow velocity is approximately in the same range as the actual flow velocity under the full power condition. Therefore, the disc is not held firmly against the backstop even at full power operation. At the reduced power condition, the actual flow velocity is less than the minimum required flow velocity. Therefore, disc tapping is expected.

C.2.2. Disc Oscillating Frequency

Using the three methods given in Section A.3, we have

$$f_n = \frac{1}{2\pi}\sqrt{\frac{K_{stiff}}{W/g}}$$

where

$$K_{stiff} = \frac{2\times 2\times 0.6903\times 144\times 54.56\times(16.5\times 12)^2}{7.5\times 386.4\times 12^3}$$

$$\times\left(\cos 13.3^\circ \sin 6.7^\circ + \frac{1}{2}\cos 6.7^\circ \sin 13.3^\circ\right)$$

$$= 38.7 \text{ lb/in}$$

Note: The disc angle, θ, is calculated from the disc equilibrium position based on the actual flow velocity of 16.5 ft/sec.

$$W = W_{disc} + 0.5\, W_{hinge} + \frac{1}{3}\rho\,(d_{disc})^3$$

$$= 33 + 6 + 0.333\times 54.56\left(\frac{11.25}{12}\right)^3$$

$$= 54 \text{ lb}$$

$$\therefore\quad f_n = \frac{1}{2\pi}\sqrt{\frac{38.7\times 386.4}{54}} = 2.65 \text{ Hz}$$

$$f_{eddy} = \frac{0.08\,V}{V_s} = \frac{0.96\times 16.5\times 12}{10} = 1.58 \text{ Hz}$$

$$F_{pend} = \frac{1}{2\pi}\sqrt{\frac{g}{R}} = \frac{1}{2\pi}\sqrt{\frac{386}{7.5}} = 1.14 \text{ Hz}$$

Among the above calculated frequencies, the eddy frequency of 1.58 hz is closest to the estimates based on Phase I test data and will be used in later fatigue calculations.

C.2.3. Disc Oscillation Angle

Based on the Reference 1 test data, the estimated disc oscillation angle is 16.2 degrees (3σ disc oscillation angle). The following impact force and stress are calculated using this oscillation angle.

C.2.4. Maximum Disc Velocity

$$V_{max} = R \times 2\pi f$$

$$= 7.5 \times \frac{16.2 \times \pi}{2 \times 180} \times 2\pi \times 1.58$$

$$= 10.5 \text{ in / sec}$$

C.2.5. Maximum Impact Force

$$F = V \sqrt{\frac{m}{\left(\frac{L}{AE} + \frac{e^2 L}{EI}\right)}}$$

Assuming the loading eccentricity is 0.4-inch, then

$$F = 10.5 \sqrt{\frac{\frac{39}{386.4}}{\left(\frac{3}{\frac{\pi}{4} \times 1.125^2 \times 30 \times 10^6} + \frac{0.4^2 \times 3}{30 \times 10^6 \times \frac{\pi}{64} \times 1.125^4}\right)}}$$

$$= 6,195 \text{ lb}$$

C.2.6. Maximum Alternating Stress

$$\sigma_{alt} = \frac{1}{2} \times SCF \times \left(\frac{F}{A} + \frac{F e}{Z}\right)$$

Assuming SCF at the stud fillet radius is 2, then

$$\sigma_{alt} = \frac{1}{2} \times 2 \times \left(\frac{6,195}{\frac{\pi}{4} \times 1.125^2} + \frac{6,195 \times 0.4}{\frac{\pi}{32} \times 1.125^3}\right)$$

23,960 psi

C.2.7. Fatigue Usage

The above alternating stress calculations show that under 16.2 degrees of disc oscillation angle and impacting at the maximum disc velocity of 10.5 in/sec, the maximum peak stress in the stud is 23,960 psi. Using this conservative peak stress as the 3σ peak stress, the Gaussian distributions for peak stress are:

Gaussian Distribution	*Stress Magnitude, ksi*	*Probability, %*
3.75 - 4.00 σ	30.0 - 31.9	0.02
3.50 - 3.75 σ	28.0 - 30.0	0.02
3.25 - 3.50 σ	26.0 - 28.0	0.08
3.00 - 3.25 σ	24.0 - 26.0	0.14
2.75 - 3.00 σ	22.0 - 24.0	0.34
2.50 - 2.75 σ	20.0 - 22.0	0.60
2.25 - 2.50 σ	18.0 - 20.0	1.20
2.00 - 2.25 σ	16.0 - 18.0	2.12
1.75 - 2.00 σ	14.0 - 16.0	3.46
1.50 - 1.75 σ	12.0 - 14.0	5.34
1.25 - 1.50 σ	10.0 - 12.0	7.76
1.00 - 1.25 σ	8.0 - 10.0	10.62

Table C.1

Gaussian Distributions for Peak Stress

The fatigue usage of the stud can be estimated based on the above peak stress distributions, hours of service, oscillating frequency, and a fatigue curve such as Figure C.1 (from ASME, Section III, Fig. I-9.1, 1989 Edition). The fatigue usage in an hour's tapping can be estimated as shown in Table C.2:

Gaussian Distribution	*Avg. Peak Stress, ksi*	*Design Cycles*	*Impact Cycles /hr**	*Usage*
3.75 - 4.00 σ	31.0	2.4×10^4	0.4557	1.9×10^{-5}
3.50 - 3.75 σ	29.0	3×10^4	0.4557	1.5×10^{-5}
3.25 - 3.50 σ	27.0	3.6×10^4	1.823	5.1×10^{-5}
3.00 - 3.25 σ	25.0	4.5×10^4	3.2	7.1×10^{-5}
2.75 - 3.00 σ	23.0	6×10^4	7.7	1.3×10^{-4}
2.50 - 2.75 σ	21.0	1×10^5	13.7	1.37×10^{-4}
2.25 - 2.50 σ	19.0	1.3×10^5	27.3	2.10×10^{-4}
2.00 - 2.25 σ	17.0	2×10^5	48.3	2.42×10^{-4}
1.75 - 2.00 σ	15.0	3×10^5	78.8	2.63×10^{-4}
1.50 - 1.75 σ	13.0	5×10^5	121.7	2.43×10^{-4}
1.25 - 1.50 σ	11.0	1×10^7	176.8	1.8×10^{-5}
1.00 - 1.25 σ	9.0	∞	242.0	0
			Total	1.399×10^{-3}

* Number of impact cycles is calculated as $N = 3600/f_{eddy} \times$ Probability

Table C.2

Fatigue Usage Estimations

Therefore, the total fatigue usage in one hour of service is estimated to be 1.399×10^{-3}. It is equivalent to a stud design life of 715 hours. The actual disc stud failed within 10,000 hours of service. It should be noted that the ASME fatigue curve used in the above calculations is a design fatigue curve; i.e., a safety margin of 2 on peak stress or 20 on fatigue cycles is included in deriving the fatigue curve (Ref. 21). Therefore, the actual stud fatigue life would be more than one order of magnitude higher than the above estimated value if the actual mean fatigue curve of the material is used for the calculations.

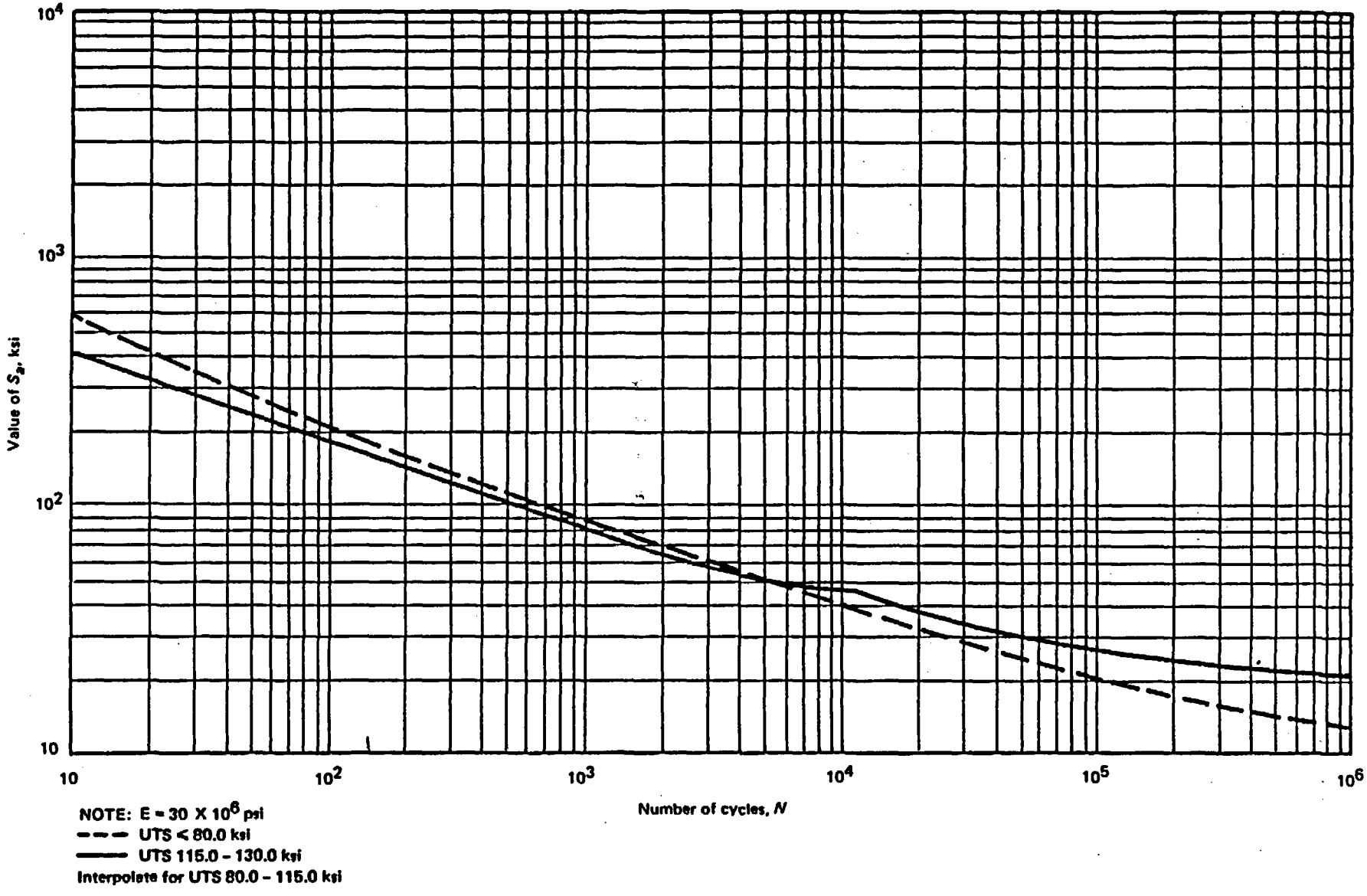

Figure C.1
ASME, Section III Design Fatigue Curves for Carbon, Low Alloy, and High Tensile Steels

APPENDIX D

PLOTS OF MEAN DISC SPEED AND 3-SIGMA DISC SPEEDS FOR THE 3-INCH AND 6-INCH TEST SWING CHECK VALVES

LIST OF FIGURES

Figure No.		Page
D.1	3-Inch Valve Mean Disk Speed(Elbow Up, 0D)	D.4
D.2	3-Inch Valve Mean Disk Speed (Elbow Up, 1D)	D.4
D.3	3-Inch Valve Mean Disk Speed (Elbow Up, 3D)	D.5
D.4	3-Inch Valve Mean Disk Speed (Elbow Up, 5D)	D.5
D.5	6-Inch Valve Mean Disk Speed (Elbow Up, 0D)	D.6
D.6	6-Inch Valve Mean Disk Speed (Elbow Up, 1D)	D.6
D.7	6-Inch Valve Mean Disk Speed (Elbow Up, 3D)	D.7
D.8	6-Inch Valve Mean Disk Speed (Elbow Up, 5D)	D.7
D.9	3- and 6-Inch Valve 3 Sigma Disk Speed (Elbow Up, 0D)	D.8
D.10	3- and 6-Inch Valve 3 Sigma Disk Speed (Elbow Up, 1D)	D.8
D.11	3- and 6-Inch Valve 3 Sigma Disk Speed (Elbow Up, 3D)	D.9
D.12	3- and 6-Inch Valve 3 Sigma Disk Speed (Elbow Up, 5D)	D.9
D.13	3-Inch Valve Mean Disk Speed (Elbow Down, 0D)	D.10
D.14	3-Inch Valve Mean Disk Speed (Elbow Down, 1D)	D.10
D.15	3-Inch Valve Mean Disk Speed (Elbow Down, 3D)	D.11
D.16	3-Inch Valve Mean Disk Speed (Elbow Down, 5D)	D.11
D.17	6-Inch Valve Mean Disk Speed (Elbow Down, 0D)	D.12
D.18	6-Inch Valve Mean Disk Speed (Elbow Down, 1D)	D.12
D.19	6-Inch Valve Mean Disk Speed (Elbow Down, 3D)	D.13
D.20	6-Inch Valve Mean Disk Speed (Elbow Down, 5D)	D.13
D.21	3- and 6-Inch Valve 3 Sigma Disk Speed (Elbow Down, 0D)	D.14
D.22	3- and 6-Inch Valve 3 Sigma Disk Speed (Elbow Down, 1D)	D.14
D.23	3- and 6-Inch Valve 3 Sigma Disk Speed (Elbow Down, 3D)	D.15
D.24	3- and 6-Inch Valve 3 Sigma Disk Speed (Elbow Down, 5D)	D.15
D.25	3-Inch Valve Mean Disk Speed(3/16" Holes, Orifice Plate at 1.5D)	D.16
D.26	3-Inch Valve Mean Disk Speed(7/8" Holes, Orifice Plate at 1.5D)	D.16
D.27	6-Inch Valve Mean Disk Speed(3/8" Holes, Orifice Plate at 1.5D)	D.17
D.28	6-Inch Valve Mean Disk Speed(1.75" Holes, Orifice Plate at 1.5D)	D.17
D.29	6-Inch Valve Mean Disc Speed (3/16" Holes, Orifice Plate at 1.5D)	D.18
D.30	6-Inch Valve 3-Sigma Disc Speed (Orifice Plate at 1.5D)	D.18
D.31	3-Inch Valve Mean Disc Speed (3/16" Holes, Orifice Plate at 2.5D)	D.19
D.32	3-Inch Valve Mean Disc Speed (7/8" Holes, Orifice Plate at 2.5D)	D.19
D.33	6-Inch Valve Mean Disc Speed (3/8" Holes, Orifice Plate at 2.5D)	D.20
D.34	6-Inch Valve Mean Disc Speed (1.75" Holes, Orifice Plate at 2.5D)	D.20
D.35	6-Inch Valve 3-Sigma Disc Speed (Orifice Plate at 2.5D)	D.21
D.36	6-Inch Valve 3-Sigma Disc Speed (Orifice Plate at 2.5D)	D.21
D.37	3-Inch Valve Mean Disc Speed (3/16" Holes, Orifice Plate at 4.5D)	D.22

D.38	3-Inch Valve Mean Disc Speed (7/8" Holes, Orifice Plate at 4.5D)	D.22
D.39	6-Inch Valve Mean Disc Speed (3/8" Holes, Orifice Plate at 4.5D)	D.23
D.40	6-Inch Valve Mean Disc Speed (1.75" Holes, Orifice Plate at 4.5D)	D.23
D.41	3-Inch Valve 3-Sigma Disc Speed (Orifice Plate at 4.5D)	D.24
D.42	6-Inch Valve 3-Sigma Disc Speed (Orifice Plate at 4.5D)	D.24
D.43	3-Inch Valve Mean Disk Speed(3/16" Holes, Orifice Plate at 10D)	D.25
D.44	3-Inch Valve Mean Disk Speed(7/8" Holes, Orifice Plate at 10D)	D.25
D.45	6-Inch Valve Mean Disk Speed(3/8" Holes, Orifice Plate at 10D)	D.26
D.46	6-Inch Valve Mean Disk Speed(1.75" Holes, Orifice Plate at 10D)	D.26
D.47	3-Inch Valve 3-Sigma Disc Speed (Orifice Plate at 10D)	D.27
D.48	6-Inch Valve 3-Sigma Disc Speed (Orifice Plate at 10D)	D.27
D.49	3-Inch Valve: Relative Severity of Various Upstream Disturbances Expressed in Terms of 3 Sigma Disc Speed	D.28
D.50	6-Inch Valve: Relative Severity of Various Upstream Disturbances Expressed in Terms of 3 Sigma Disc Speed	D.28

LIST OF TABLES

Table No.		Page
D.1A	3-Inch Valve: Mean Disc Speed vs. Flow Velocity Plots	D.3
D.1B	3-Inch Valve: 3 Sigma Disc Speed vs. Flow Velocity Plots	D.3
D.2A	6-Inch Valve: Mean Disc Speed vs. Flow Velocity Plots	D.3
D.2B	6-Inch Valve: 3 Sigma Disc Speed vs. Flow Velocity Plots	D.3

APPENDIX D
DATA BASE OF MEAN DISC SPEED AND 3-SIGMA DISC SPEEDS FOR THE 3-INCH AND 6-INCH TEST SWING CHECK VALVES

Compiled in this appendix is a series of graphs that plot mean disc speeds and three-sigma disc speeds vs. flow velocity. The graphs cover four different types of upstream disturbances located over a range of distances upstream from the valves. Data is presented for both the three-inch and the six-inch test swing check valves.

Table D.1A provides a cross-reference index linking the upstream disturbance and the distance it was located from the three-inch valve to the number of the figure in which the data of mean disc speed vs. flow velocity is plotted.

Table D.1B provides a cross-reference index linking the upstream disturbance and the distance it was located upstream of the three-inch valve to the number of the figure in which three-sigma disc speed vs. flow velocity data is plotted.

Table D.2A provides a cross-reference index linking the upstream disturbance and the distance it was located upstream of the six-inch valve to the number of the figure in which the data of mean disc speed vs. flow velocity is plotted.

Table D.2B provides a cross-reference index linking the upstream disturbance and the distance it was located upstream of the six-inch valve to the number of the figure in which the three-sigma disc speed vs. flow velocity data is plotted.

The objective of determining the mean disc speed was to estimate the average angular distance traversed by the disc per second. The scaled LVDT signal that measured the instantaneous disc angle was first differentiated in time. The resultant signal was the instantaneous velocity of the disc. Since the disc oscillates about a mean position, the direction of the disc velocity varies constantly. Because it was the magnitude of angular distance traversed by the disc and not the direction of disc travel that was of significance, the magnitude of the velocity signal was extracted by determining the absolute value of each of the data points in the velocity signal. The average of the resulting signal was the disc speed, a number that represented the angular distance traveled by the disc per second.

This value has been determined for both the three- and six-inch valves for a variety of disturbances located at several different upstream distances from the test valve and for a wide range of flow velocities.

The objective of determining the three-sigma disc velocity was to estimate the maximum possible velocity at which an impact of the disc stud against the disc stop could occur. The mean standard deviation and the mean of the mean disc speed signal was first computed. The three-sigma disc velocity was equal to the sum of mean and thrice the standard deviation of the mean disc speed data. Figures 49 and 50 are used to summarize an overall trend that is observed from the 3σ disc speed data presented in this appendix. The dependence of 3σ disc speed on the level of severity of the turbulence source and its proximity to the valve is clearly noticeable.

Upstream Distance	*Elbow Up*	*Elbow Down*	*Upstream Distance*	*Severe Turbulence*	*Medium Turbulence*
0D mean	1	13	1.5D mean	25	26
1D mean	2	14	2.5D mean	31	32
3D mean	3	15	4.5D mean	37	38
5D mean	4	16	10D mean	47	44

Table D.1A

3" Valve: Mean Disc Speed vs. Flow Velocity Plots

Upstream Distance	*Elbow Up*	*Elbow Down*	*Upstream Distance*	*Severe Turbulence*	*Medium Turbulence*
0D 3 Sigma	9	21	1.5D mean	29	29
1D 3 Sigma	10	22	2.5D mean	35	35
3D 3 Sigma	11	23	4.5D mean	41	41
5D 3 Sigma	12	24	10D mean	47	47

Table D.1B

3" Valve: 3 Sigma Disc Speed vs. Flow Velocity Plots

Upstream Distance	*Elbow Up*	*Elbow Down*	*Upstream Distance*	*Severe Turbulence*	*Medium Turbulence*
0D mean	5	17	1.5D mean	27	28
1D mean	6	18	2.5D mean	33	34
3D mean	7	19	4.5D mean	39	40
5D mean	8	20	10D mean	45	46

Table D.2A

6" Valve: Mean Disc Speed vs. Flow Velocity Plots

Upstream Distance	*Elbow Up*	*Elbow Down*	*Upstream Distance*	*Severe Turbulence*	*Medium Turbulence*
0D 3 Sigma	9	21	1.5D mean	30	30
1D 3 Sigma	10	22	2.5D mean	36	36
3D 3 Sigma	11	23	4.5D mean	42	42
5D 3 Sigma	12	24	10D mean	48	48

Table D.2B

6" Valve: 3 Sigma Disc Speed vs. Flow Velocity Plots

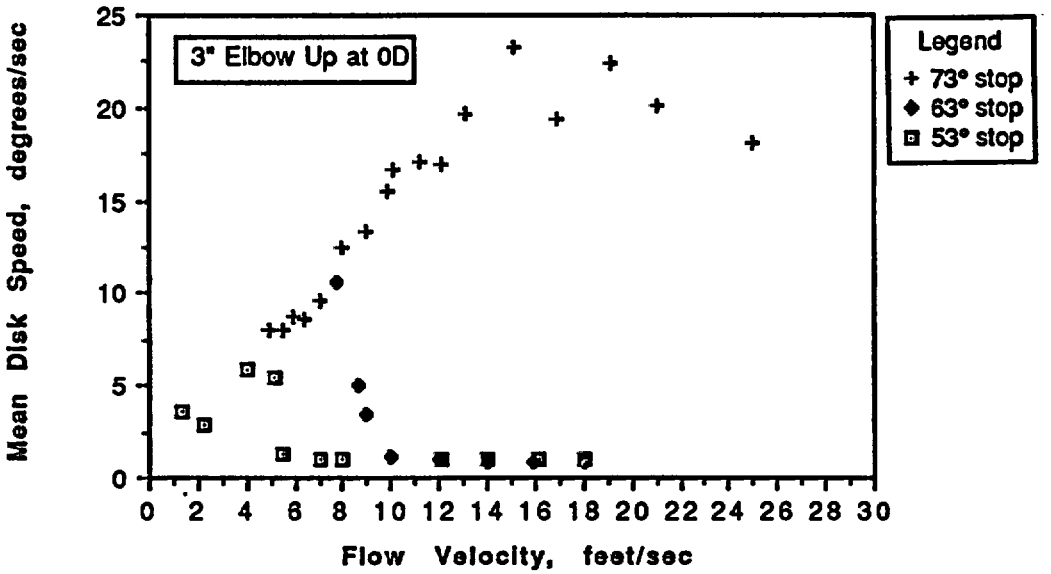

Figure D.1
3-Inch Valve Mean Disk Speed
(Elbow Up, 0D)

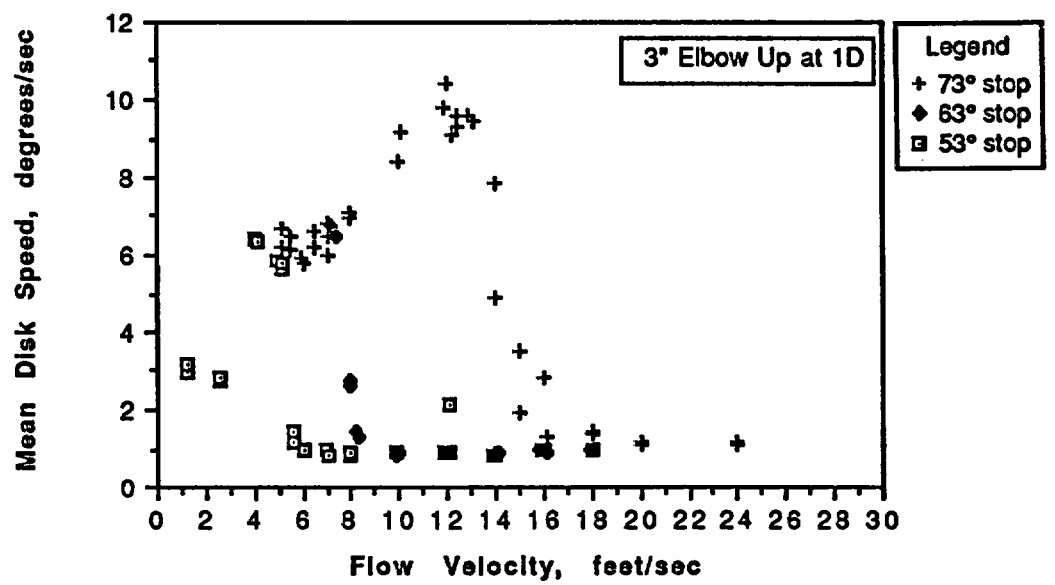

Figure D.2
3" Valve Mean Disk Speed
(Elbow Up, 1D)

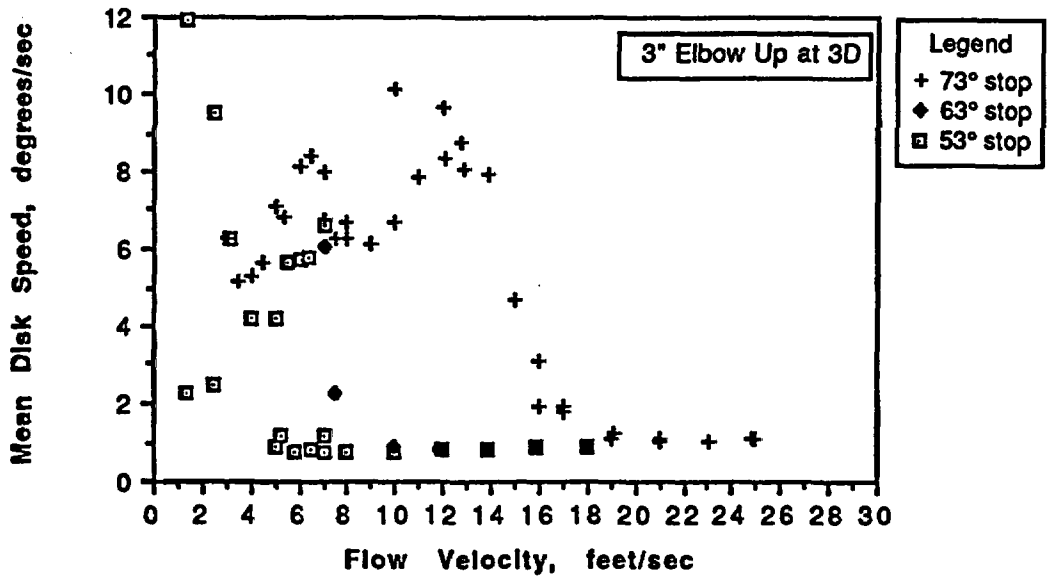

Figure D.3
3" Valve Mean Disk Speed
(Elbow Up, 3D)

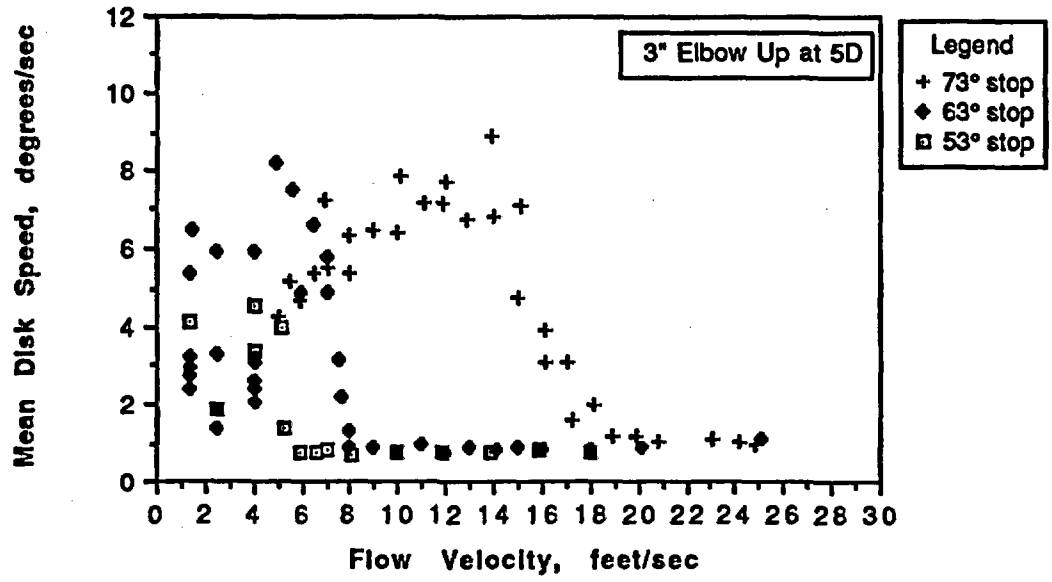

Figure D.4
3" Valve Mean Disk Speed
(Elbow Up, 5D)

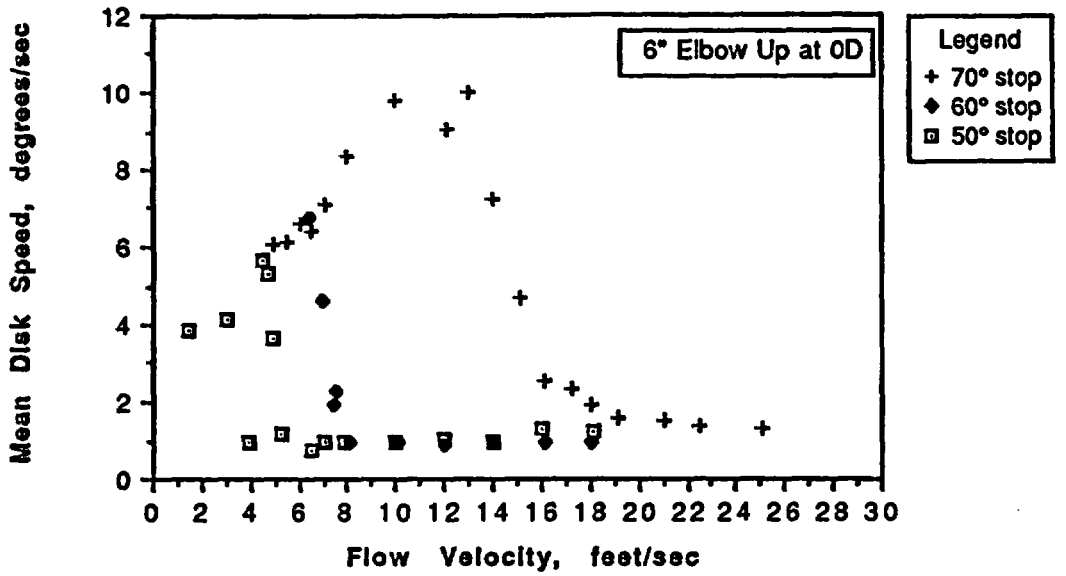

Figure D.5
6" Valve Mean Disk Speed
(Elbow Up, 0D)

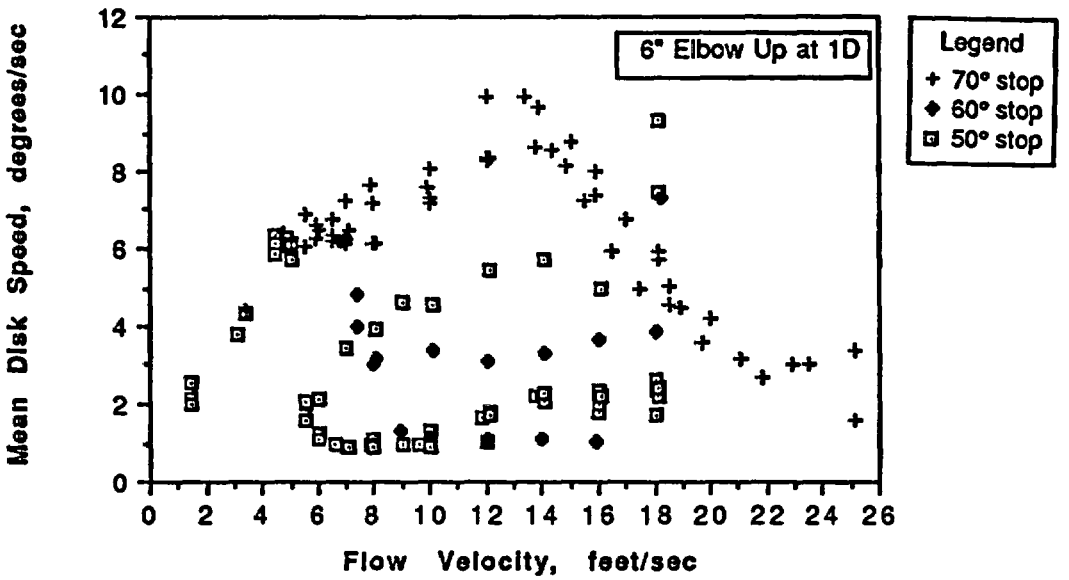

Figure D.6
6" Valve Mean Disk Speed
(Elbow Up, 1D)

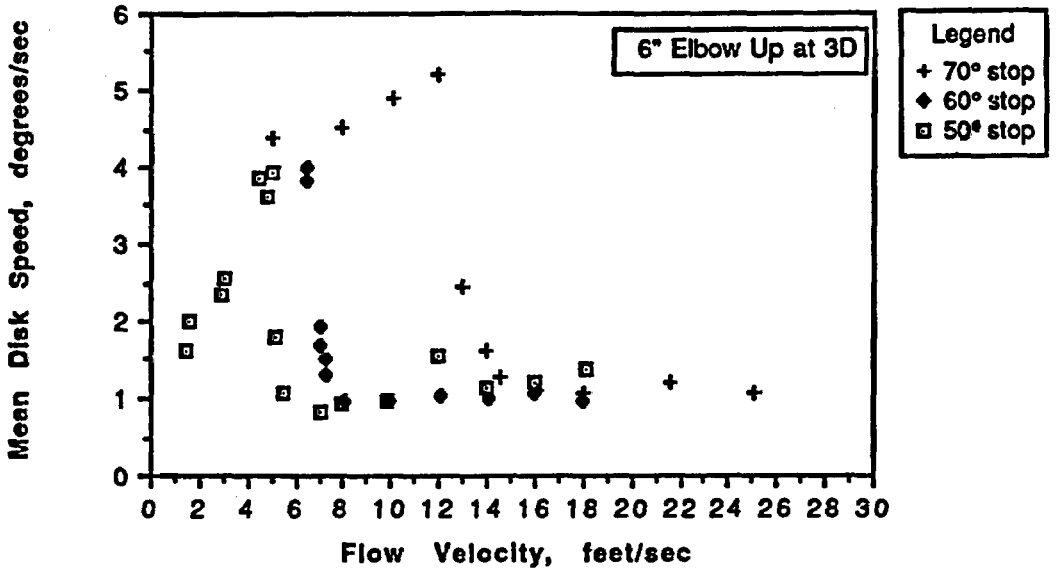

Figure D.7
6" Valve Mean Disk Speed
(Elbow Up, 3D)

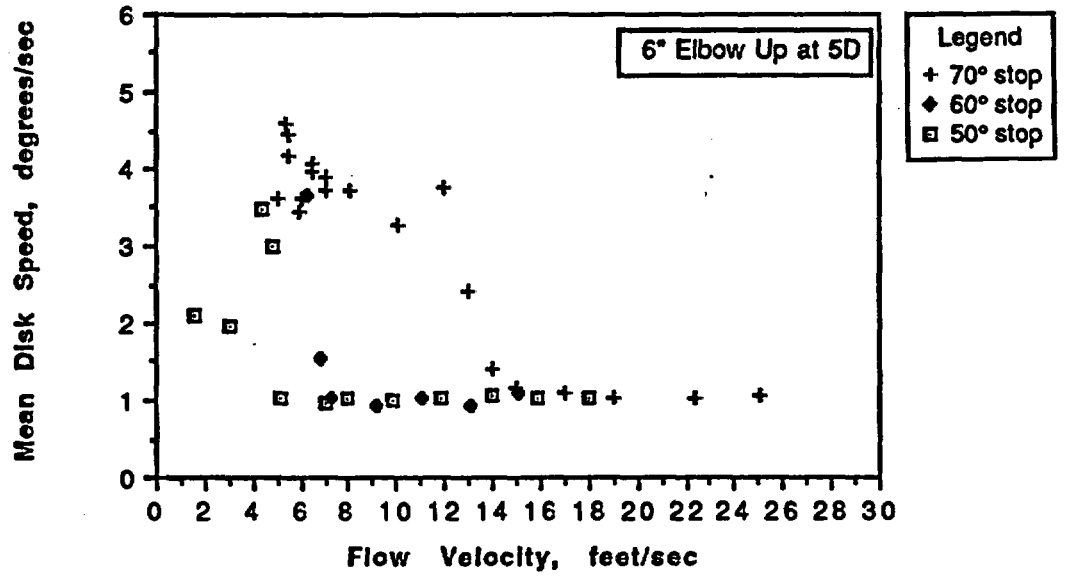

Figure D.8
6" Valve Mean Disk Speed
(Elbow Up, 5D)

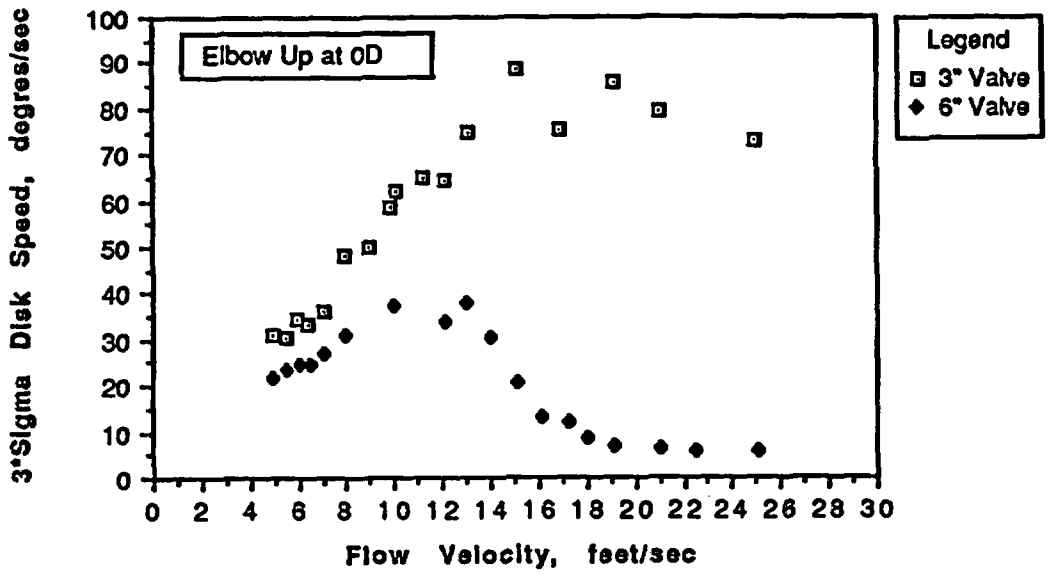

Figure D.9
3" and 6" Valve 3-Sigma Disc Speed
(Elbow Up, 0D)

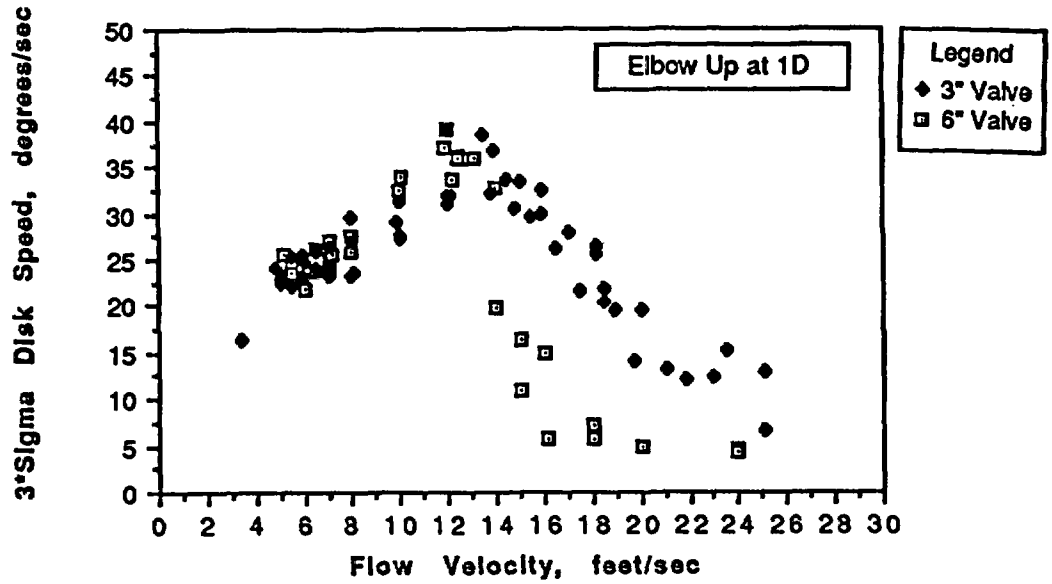

Figure D.10
3" and 6" Valve 3-Sigma Disc Speed
(Elbow Up, 1D)

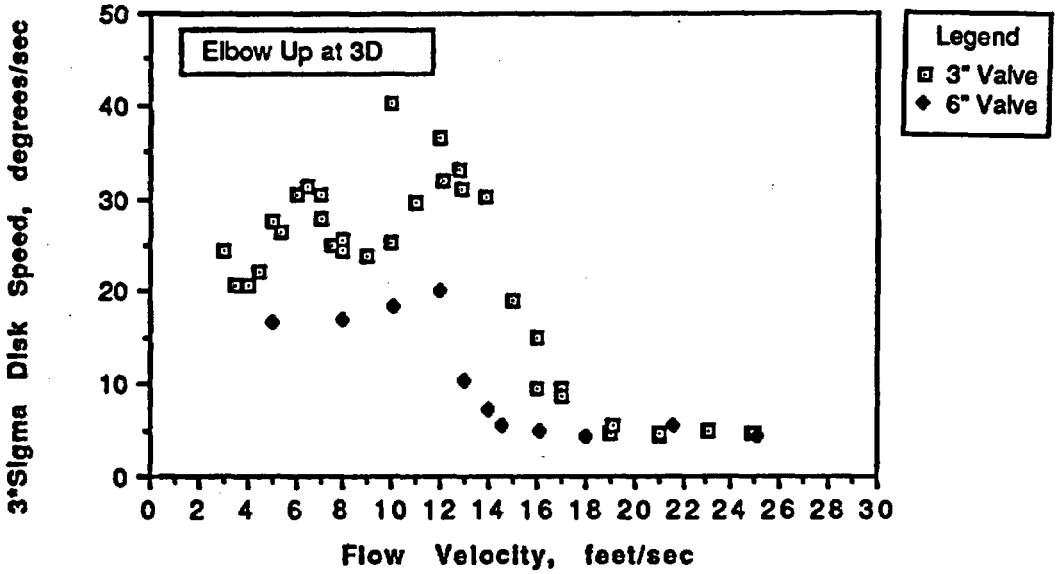

Figure D.11
3" and 6" Valve 3-Sigma Disc Speed
(Elbow Up, 3D)

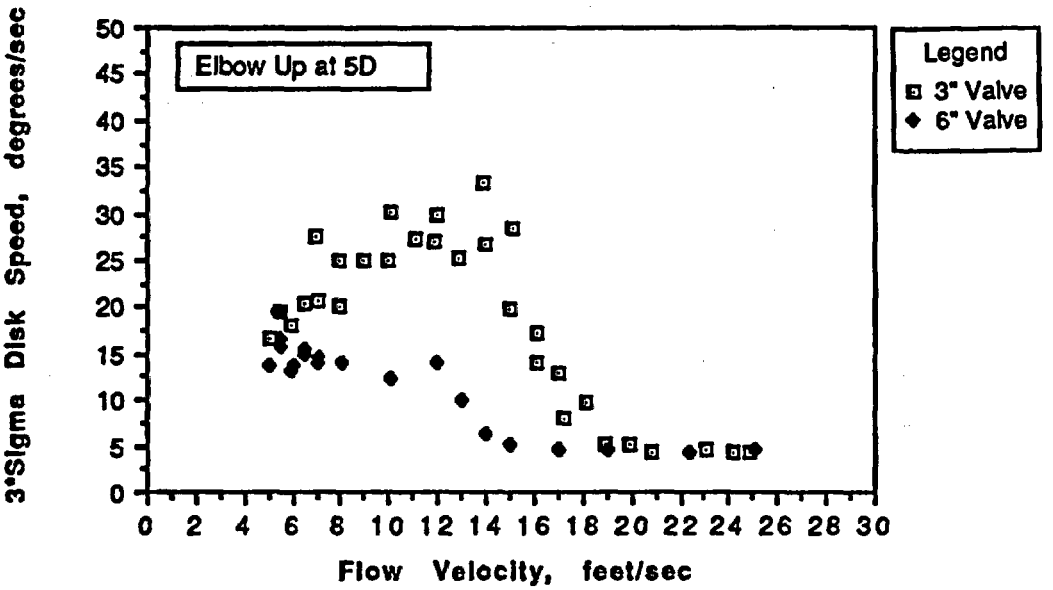

Figure D.12
3" and 6" Valve 3-Sigma Disc Speed
(Elbow Up, 5D)

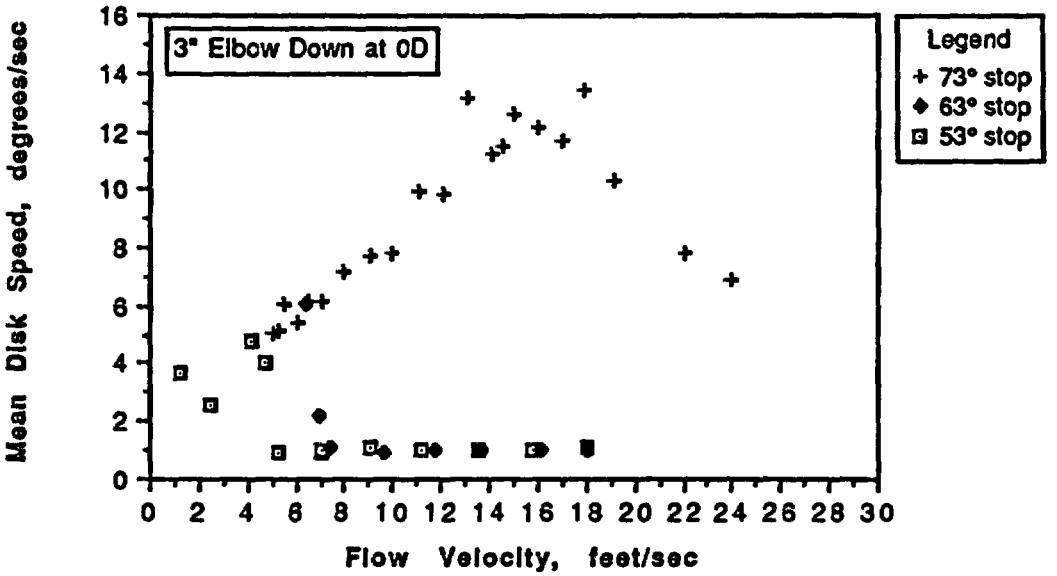

Figure D.13
3" Valve Mean Disc Speed
(Elbow Down, 0D)

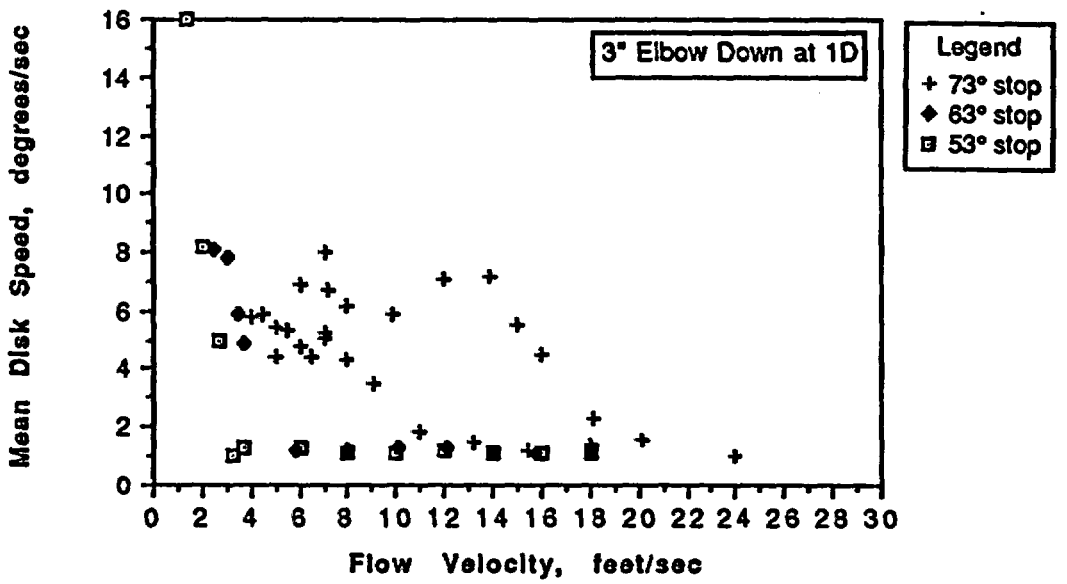

Figure D.14
3" Valve Mean Disc Speed
(Elbow Down, 1D)

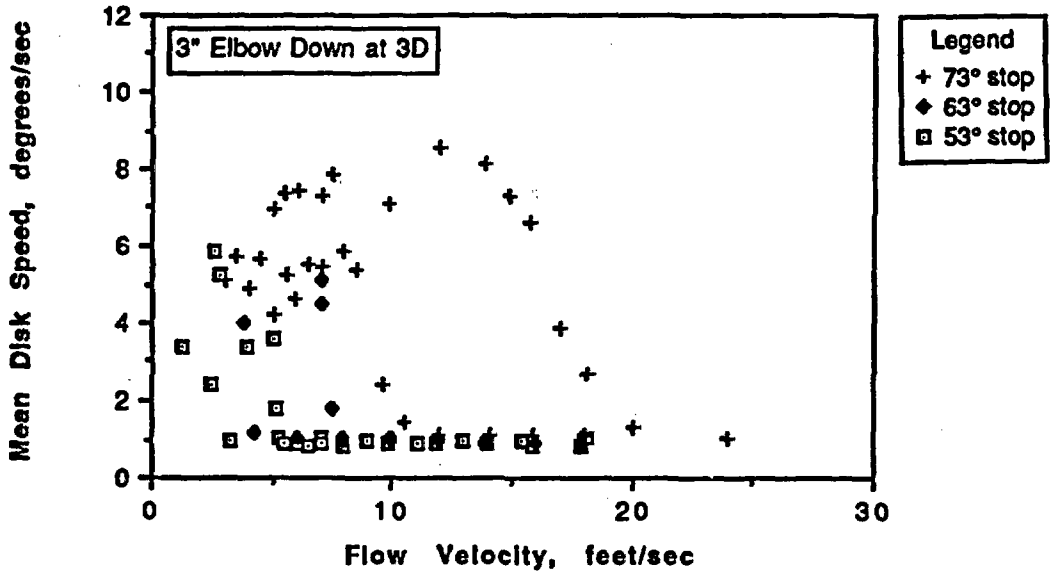

Figure D.15
3" Valve Mean Disc Speed
(Elbow Down, 3D)

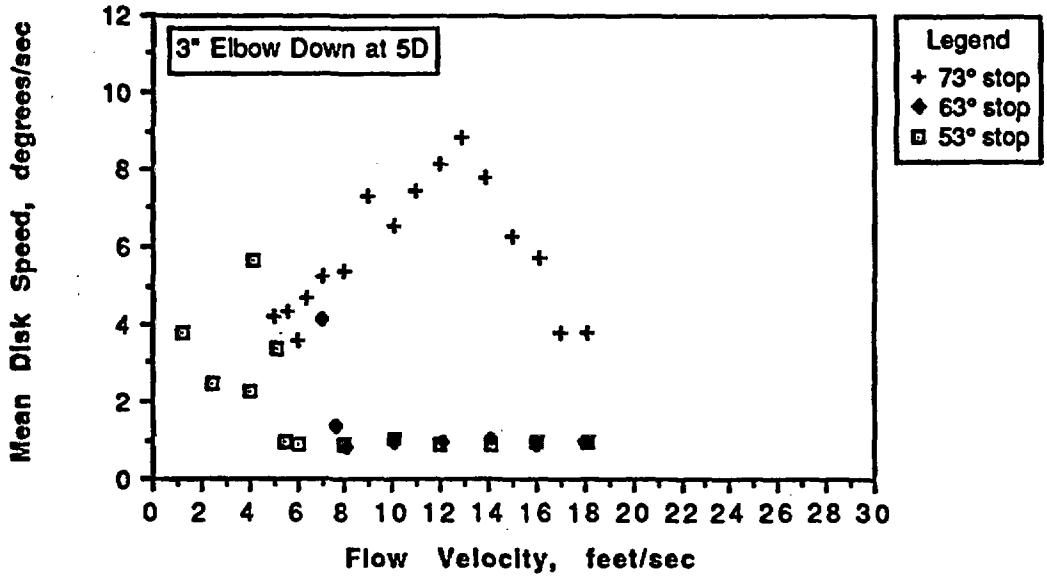

Figure D.16
3" Valve Mean Disc Speed
(Elbow Down, 5D)

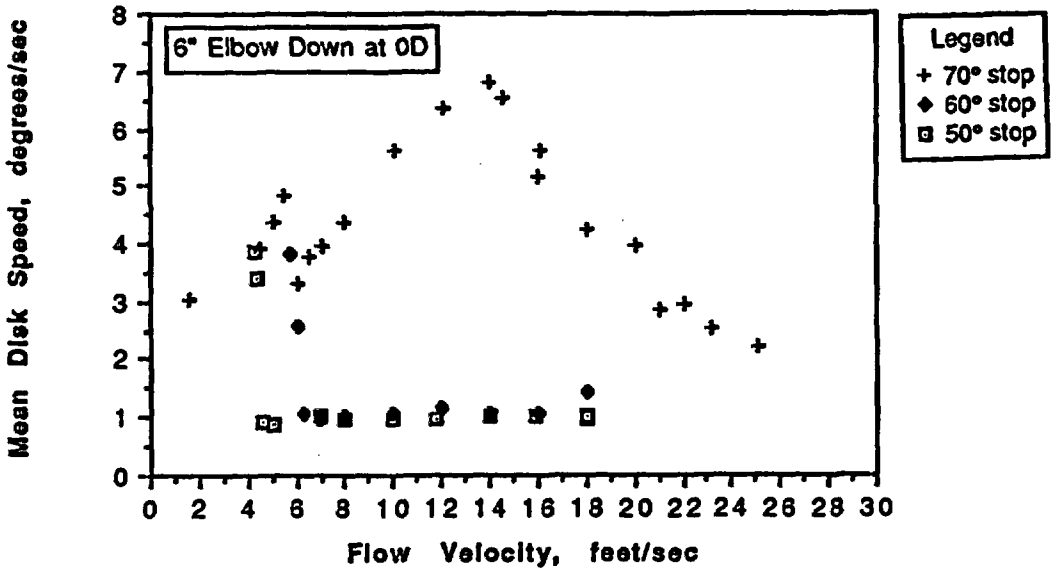

Figure D.17
6" Valve Mean Disc Speed
(Elbow Down, 0D)

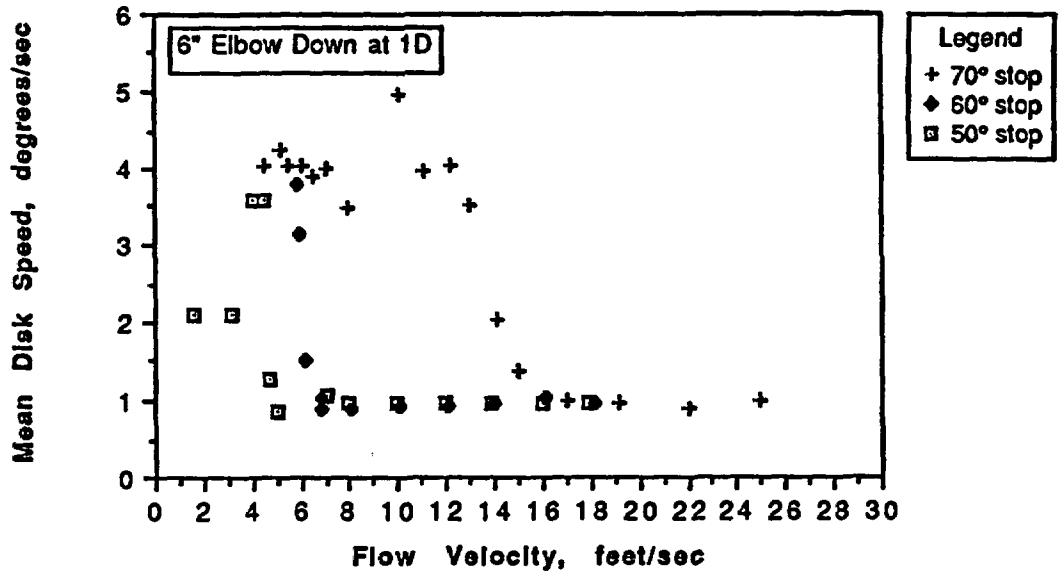

Figure D.18
6" Valve Mean Disc Speed
(Elbow Down, 1D)

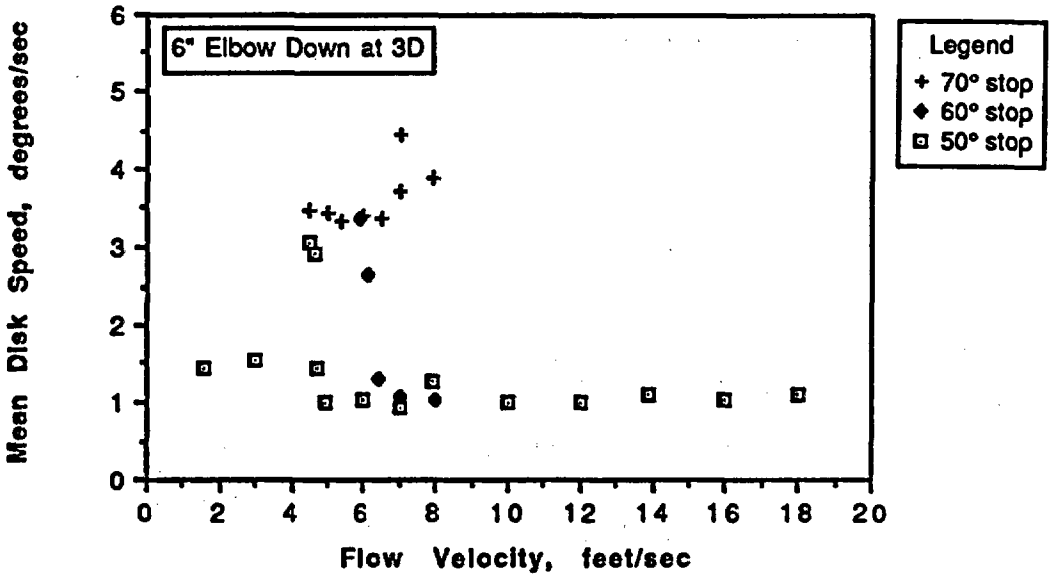

Figure D.19
6" Valve Mean Disc Speed
(Elbow Down, 3D)

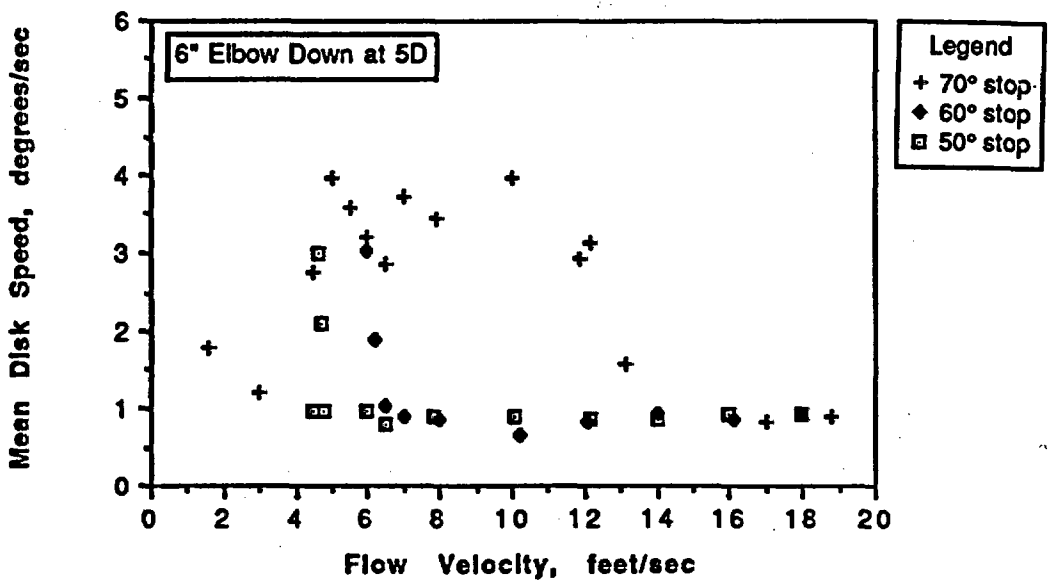

Figure D.20
6" Valve Mean Disc Speed
(Elbow Down, 5D)

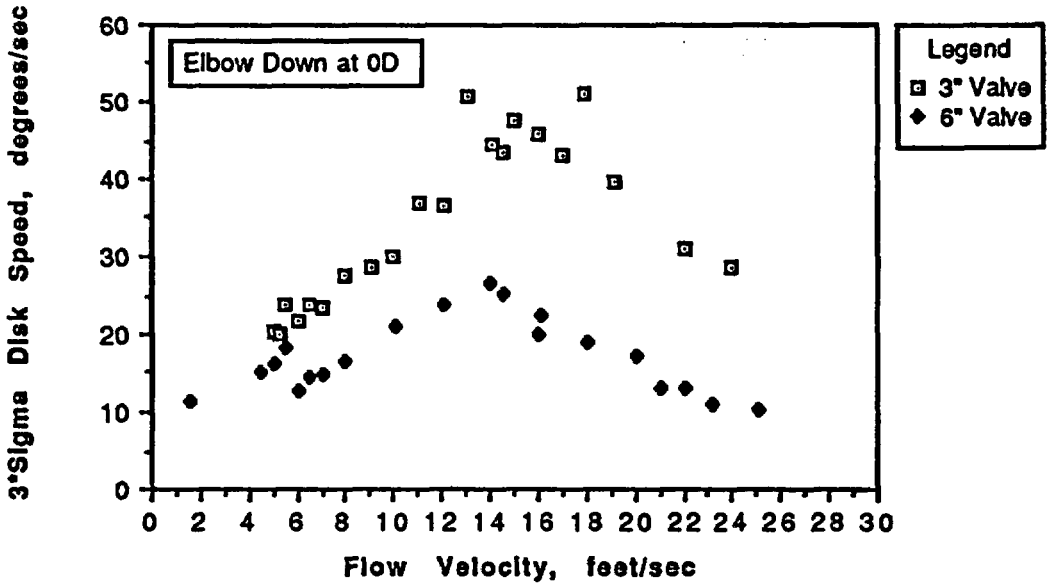

Figure D.21
3" and 6" Valve 3-Sigma Disc Speed
(Elbow Down, 0D)

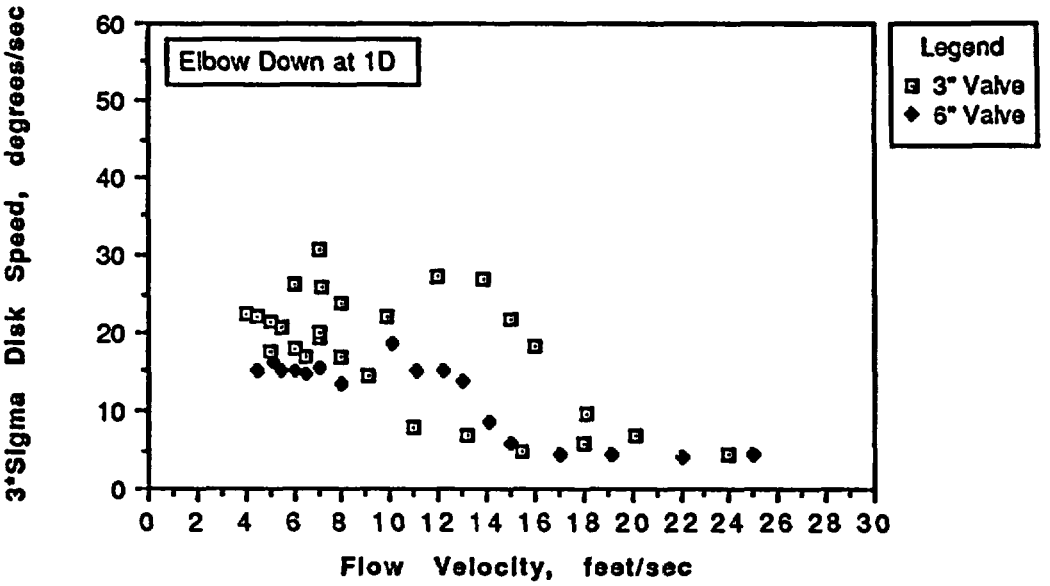

Figure D.22
3" and 6" Valve 3-Sigma Disc Speed
(Elbow Down, 1D)

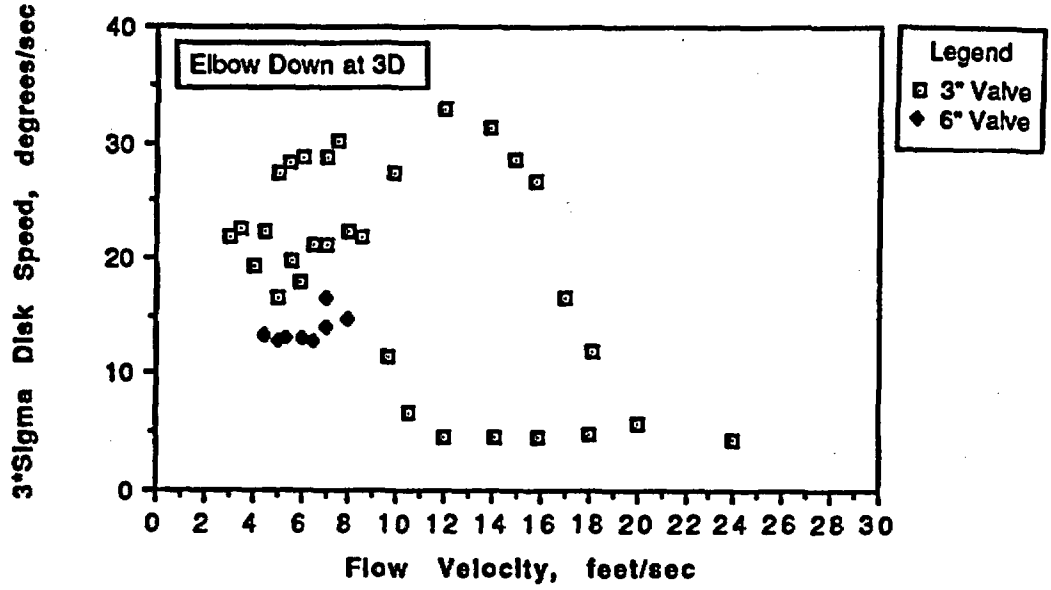

Figure D.23
3" and 6" Valve 3-Sigma Disc Speed
(Elbow Down, 3D)

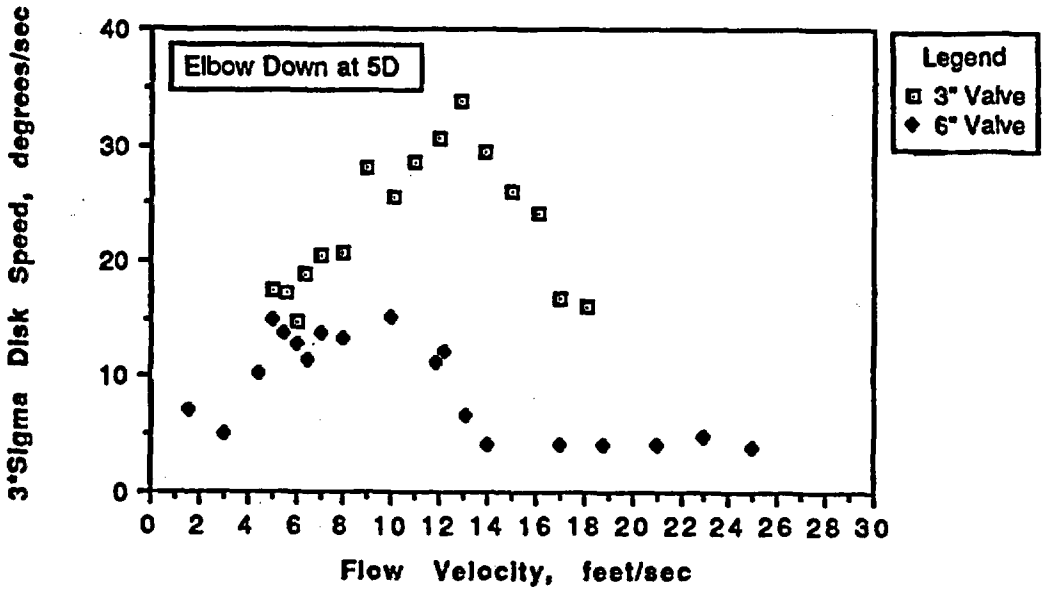

Figure D.24
3" and 6" Valve 3-Sigma Disc Speed
(Elbow Down, 5D)

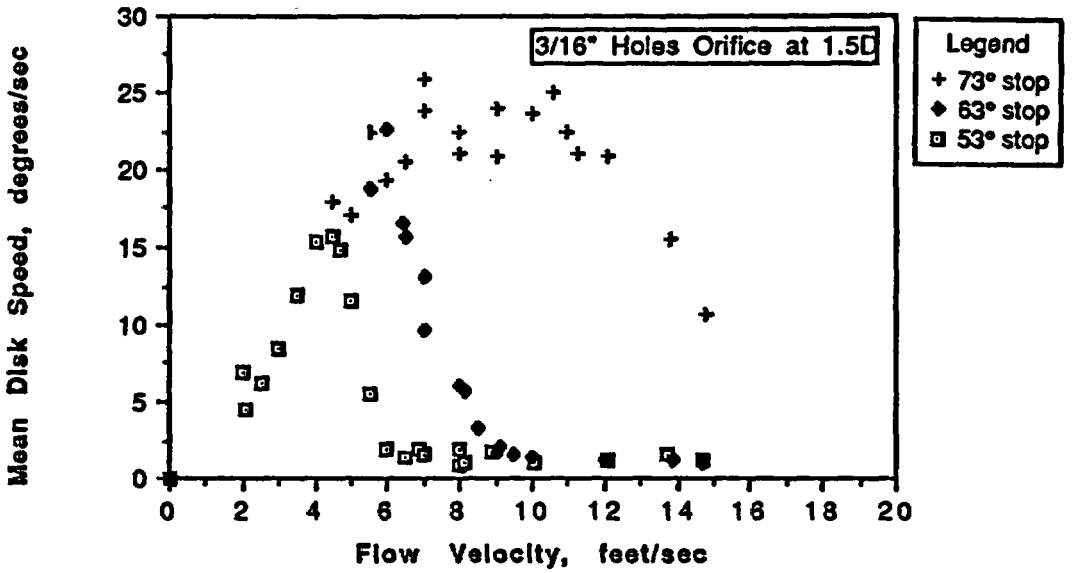

Figure D.25
3" Valve Mean Disc Speed
(3/16" Holes, Orifice Plate at 1.5D)

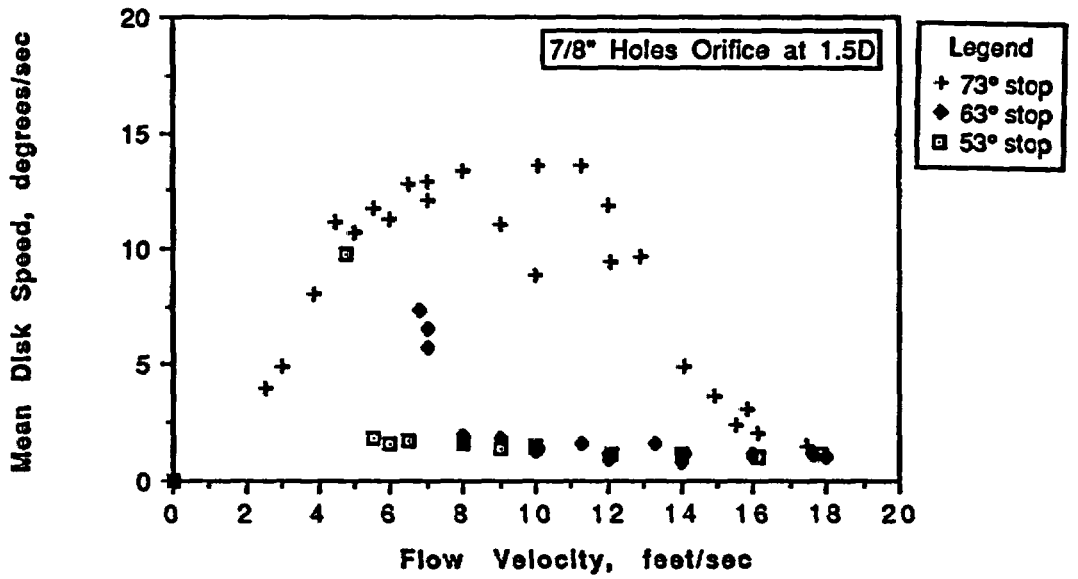

Figure D.26
3" Valve Mean Disc Speed
(7/8" Holes, Orifice Plate at 1.5D)

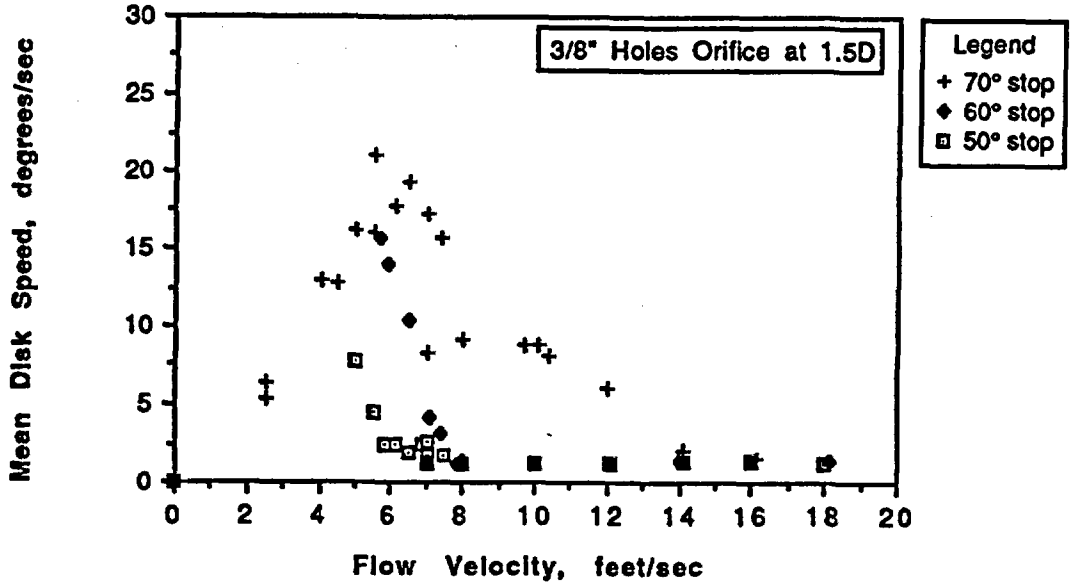

Figure D.27
6" Valve Mean Disc Speed
(3/8" Holes, Orifice Plate at 1.5D)

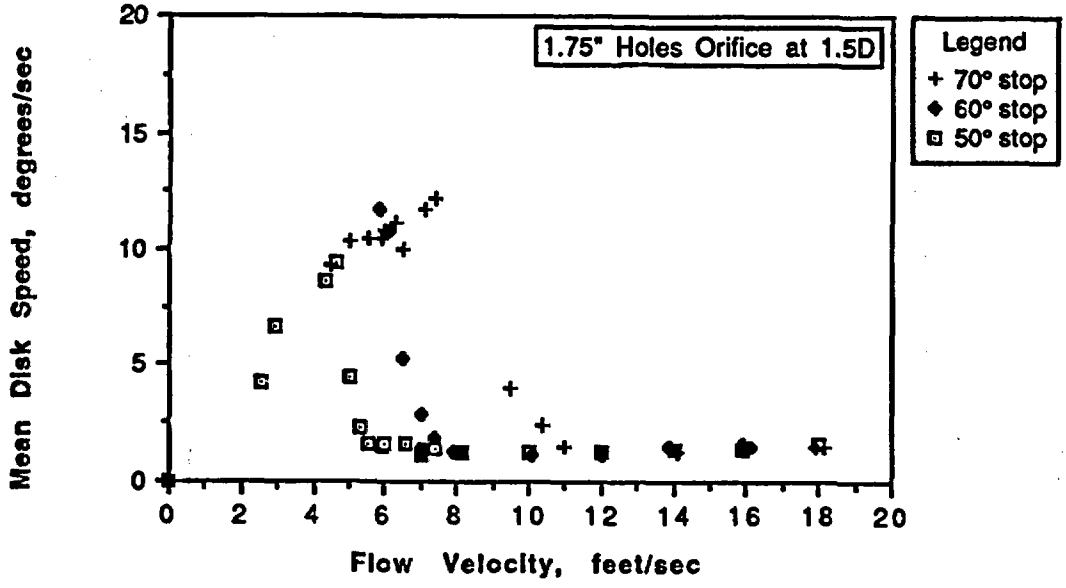

Figure D.28
6" Valve Mean Disc Speed
(1.75" Holes, Orifice Plate at 1.5D)

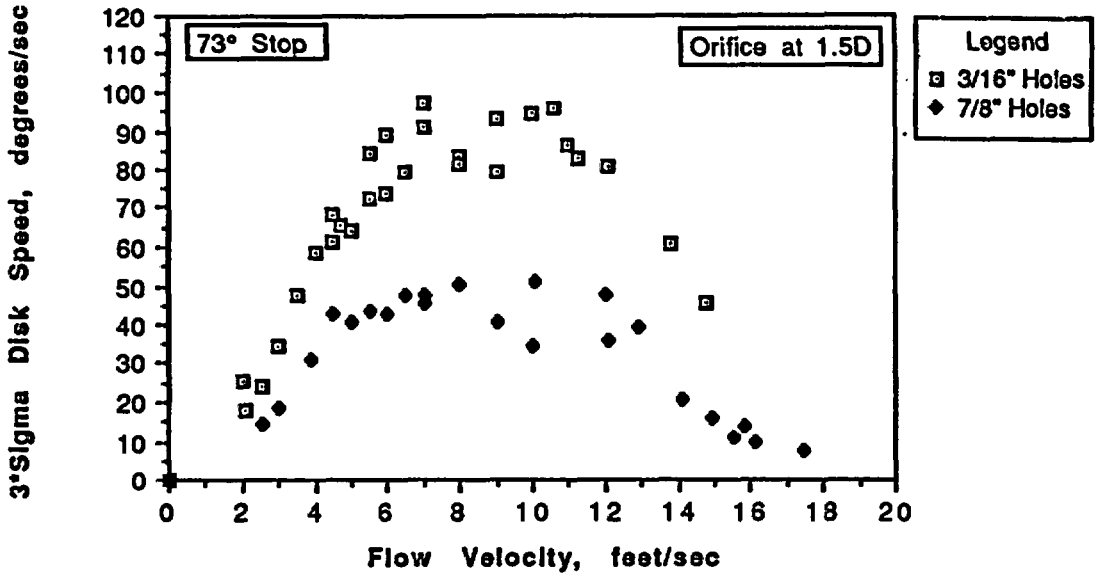

Figure D.29
6" Valve Mean Disc Speed
(3/16" Holes, Orifice Plate at 1.5D)

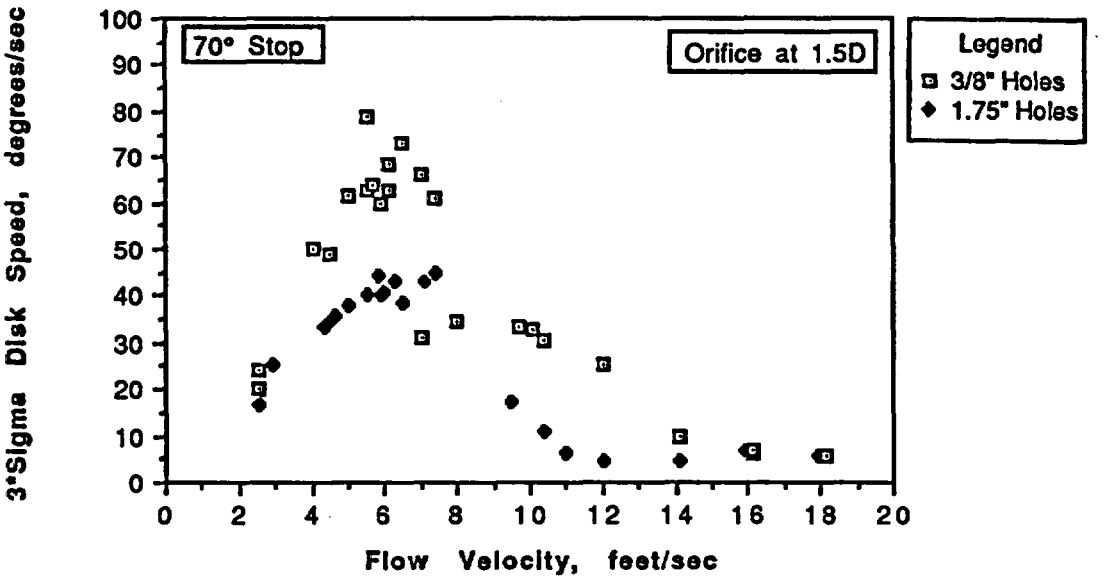

Figure D.30
6" Valve 3-Sigma Disc Speed
(Orifice Plate at 1.5D)

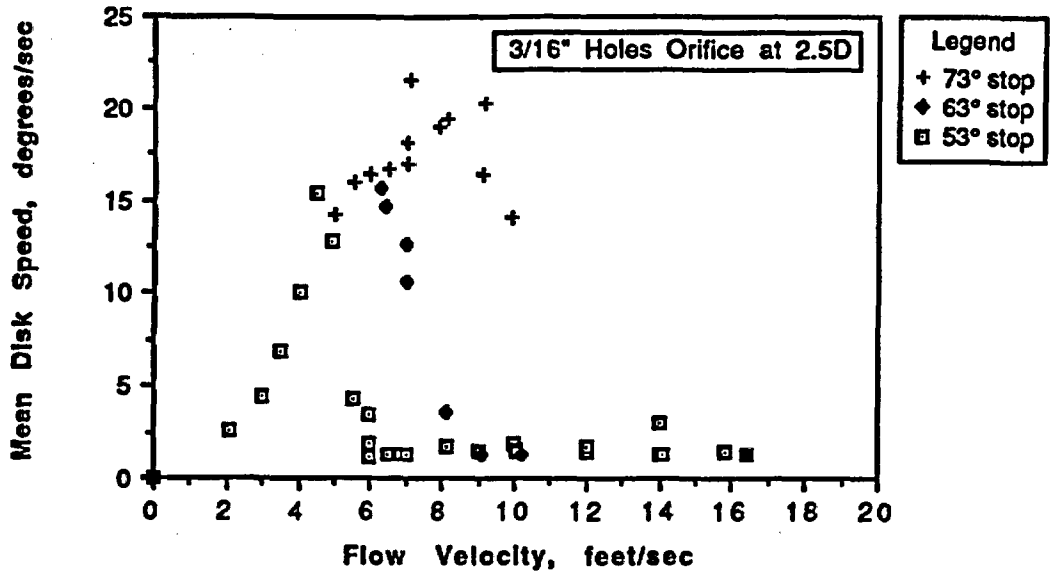

Figure D.31
3" Valve Mean Disc Speed
(3/16" Holes, Orifice Plate at 2.5D)

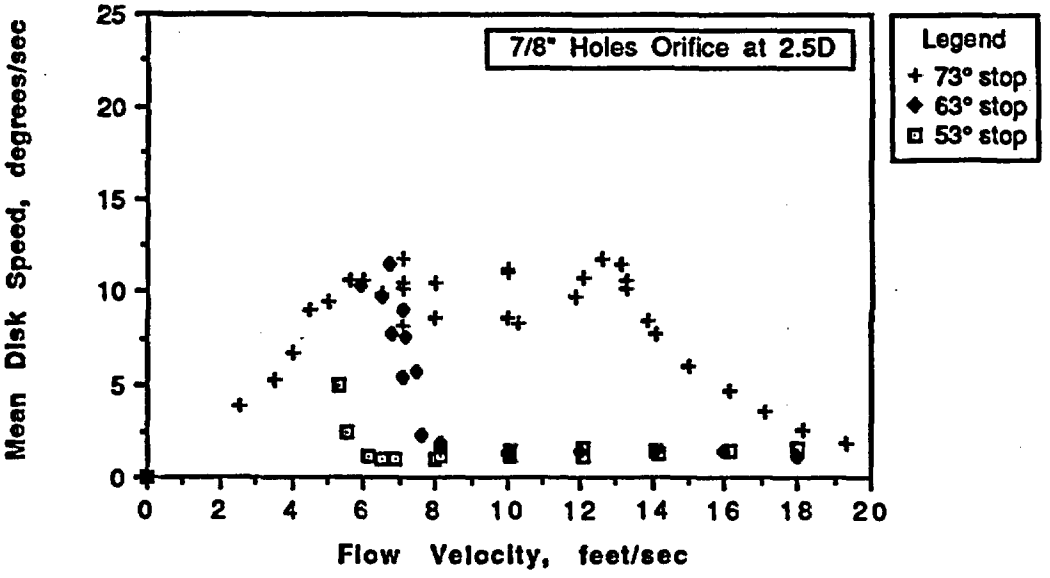

Figure D.32
3" Valve Mean Disc Speed
(7/8" Holes, Orifice Plate at 2.5D)

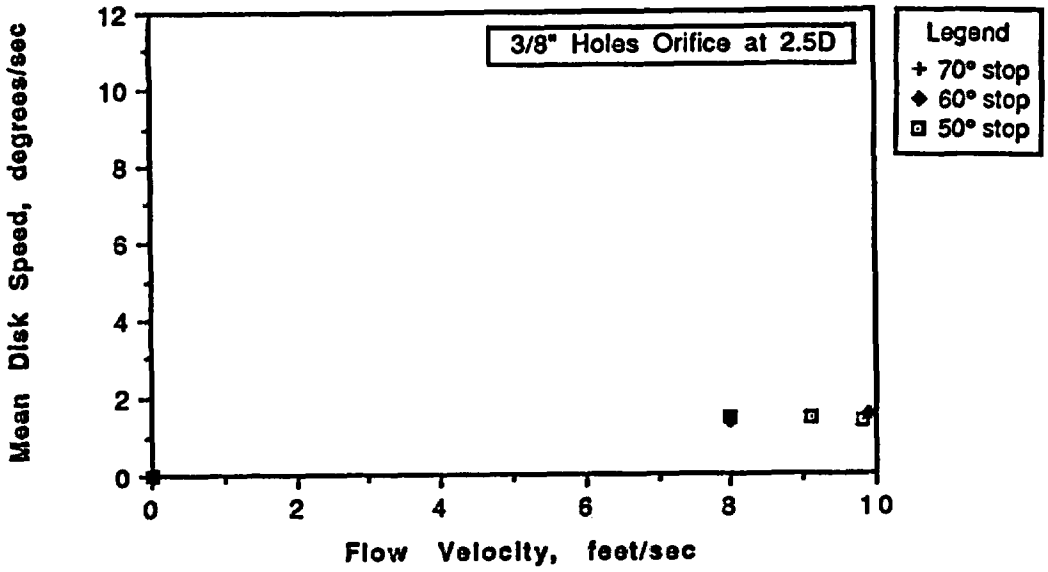

Figure D.33
6" Valve Mean Disc Speed
(3/8" Holes, Orifice Plate at 2.5D)

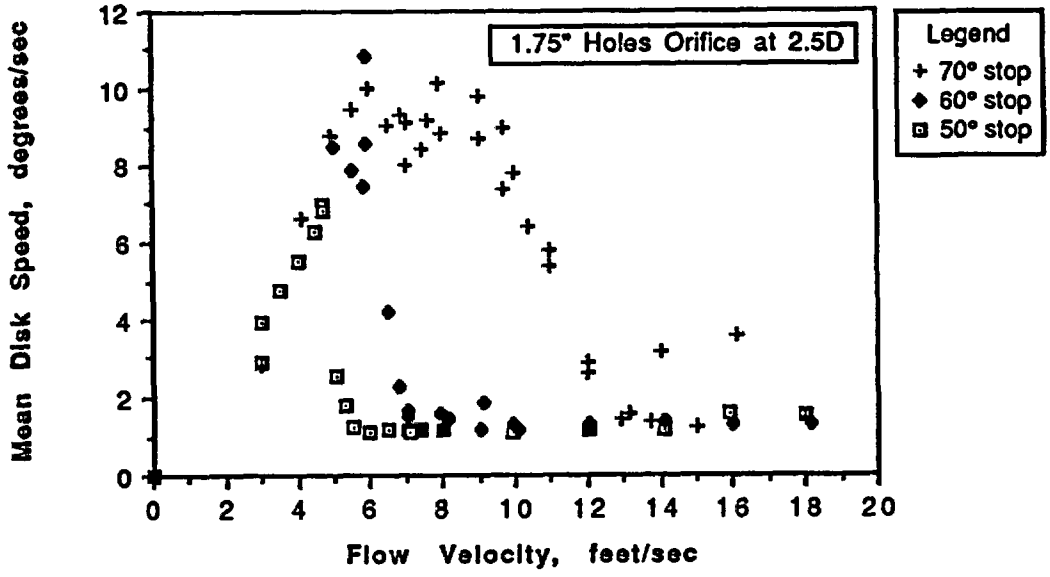

Figure D.34
6" Valve Mean Disc Speed
(1.75" Holes, Orifice Plate at 2.5D)

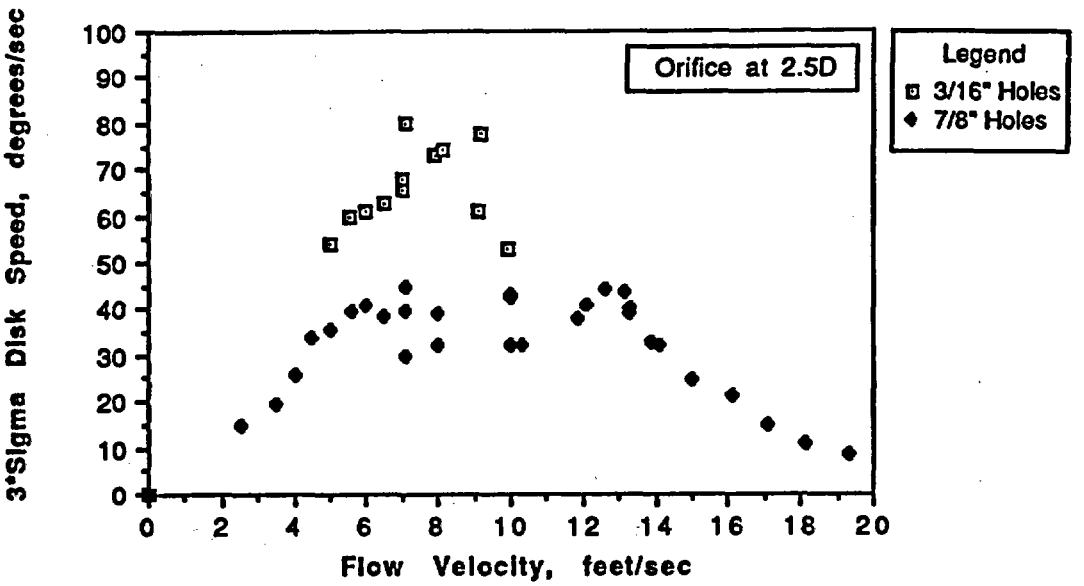

Figure D.35
3" Valve 3-Sigma Disc Speed
(Orifice Plate at 2.5D)

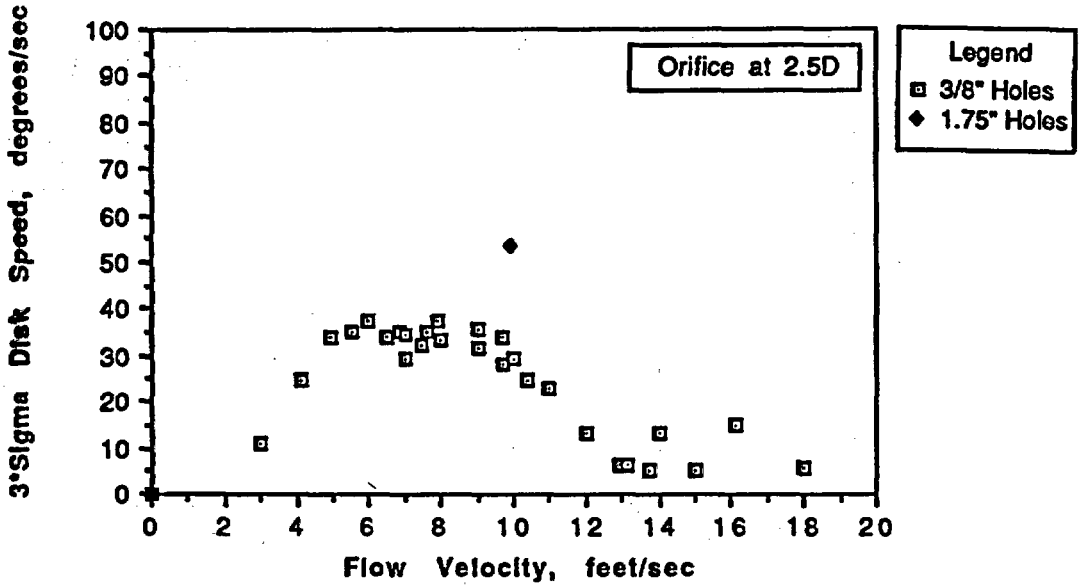

Figure D.36
6" Valve 3-Sigma Disc Speed
(Orifice Plate at 2.5D)

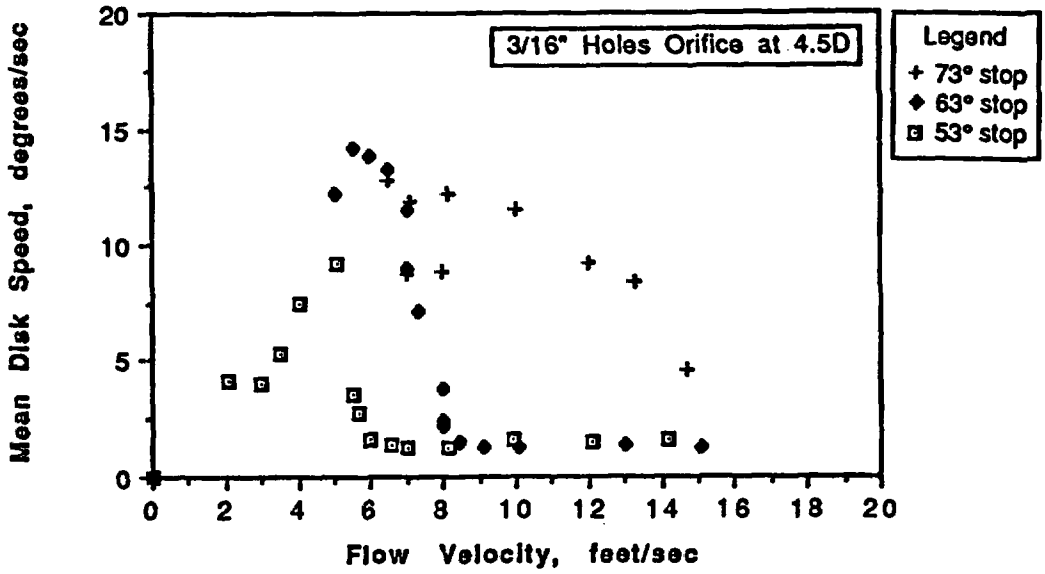

Figure D.37
3" Valve Mean Disc Speed
(3/16" Holes, Orifice Plate at 4.5D)

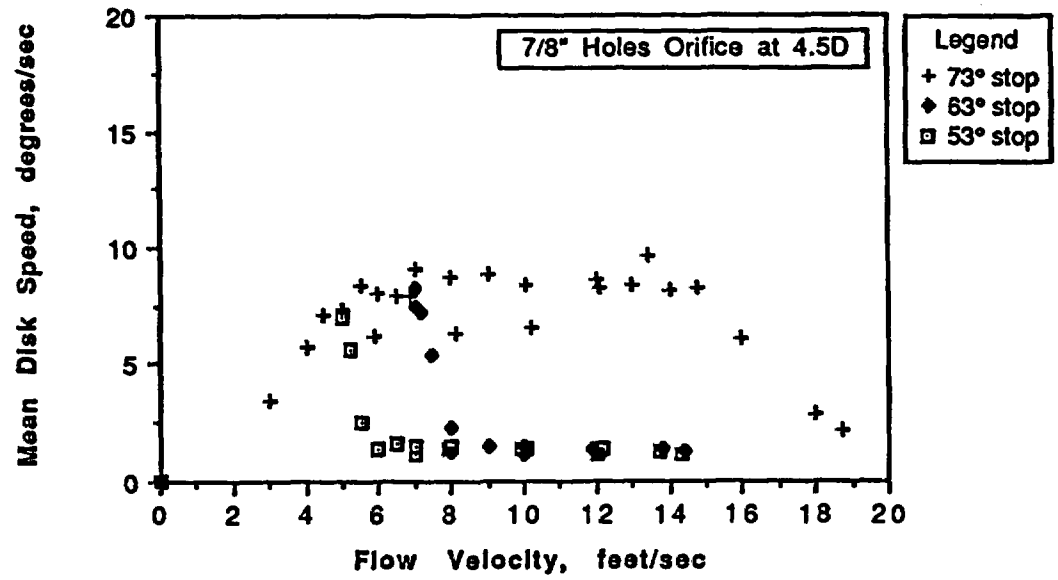

Figure D.38
3" Valve Mean Disc Speed
(7/8" Holes, Orifice Plate at 4.5D)

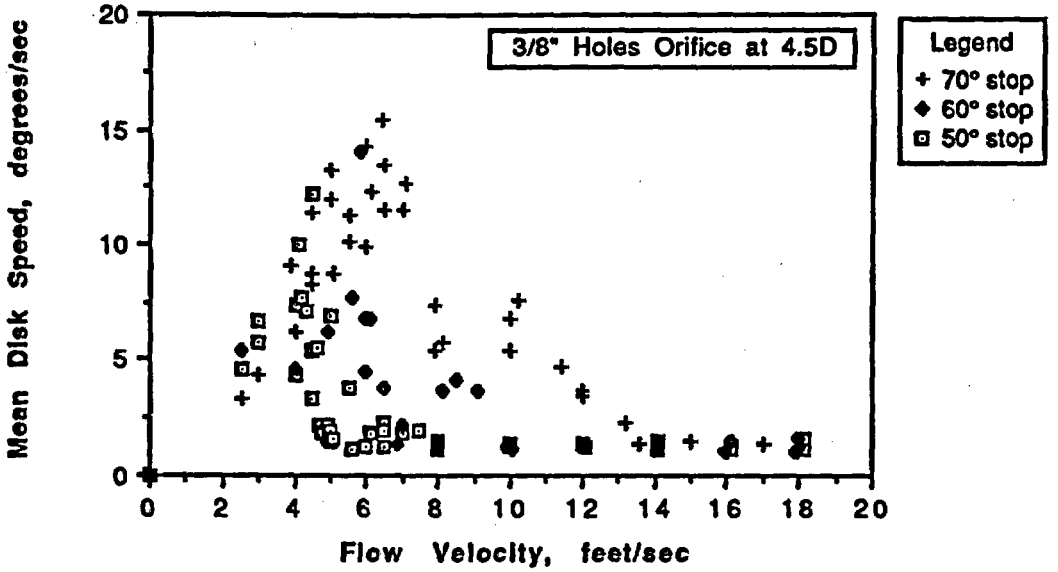

Figure D.39
6" Valve Mean Disc Speed
(3/8" Holes, Orifice Plate at 4.5D)

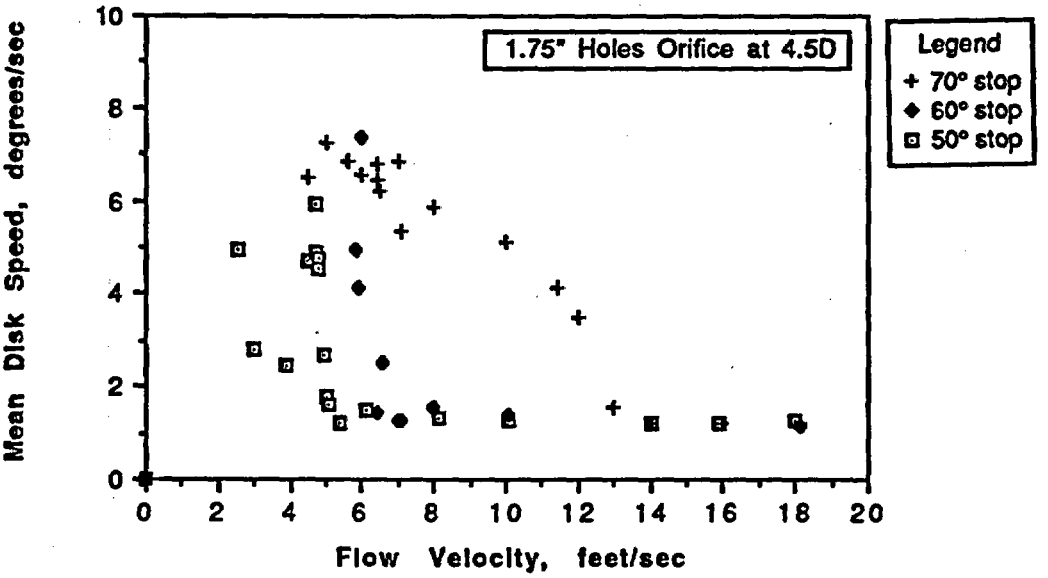

Figure D.40
6" Valve Mean Disc Speed
(1.75" Holes, Orifice Plate at 2.5D)

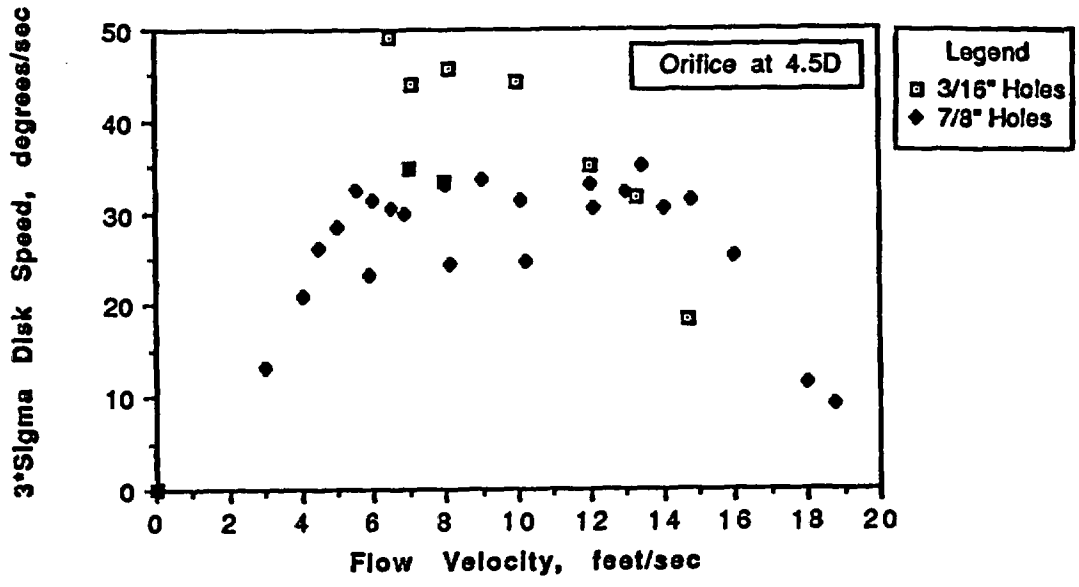

Figure D.41
3" Valve 3-Sigma Disc Speed
(Orifice Plate at 4.5D)

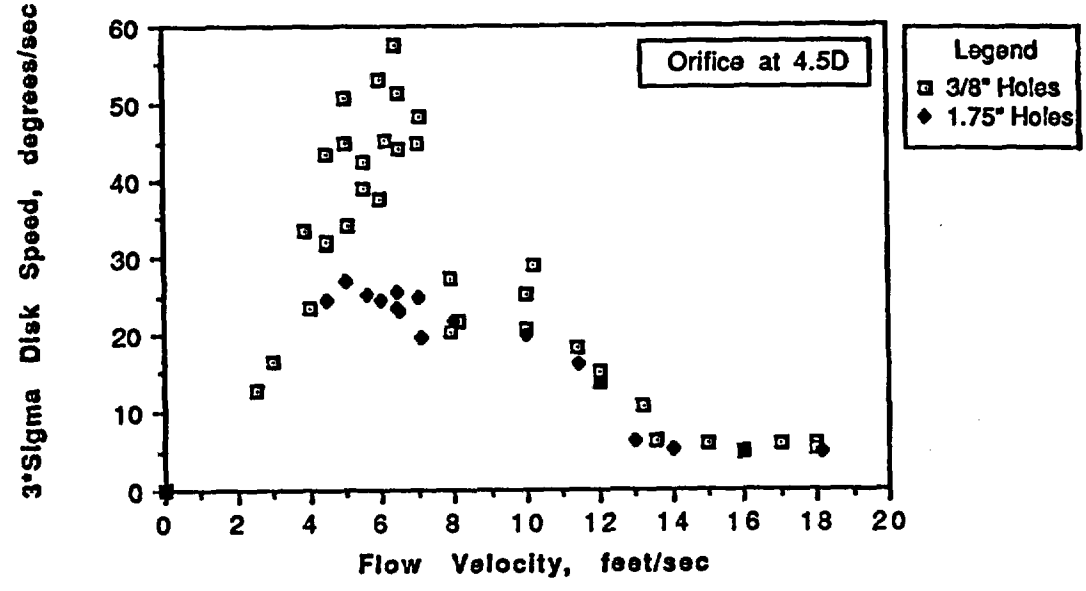

Figure D.42
6" Valve 3-Sigma Disc Speed
(Orifice Plate at 4.5D)

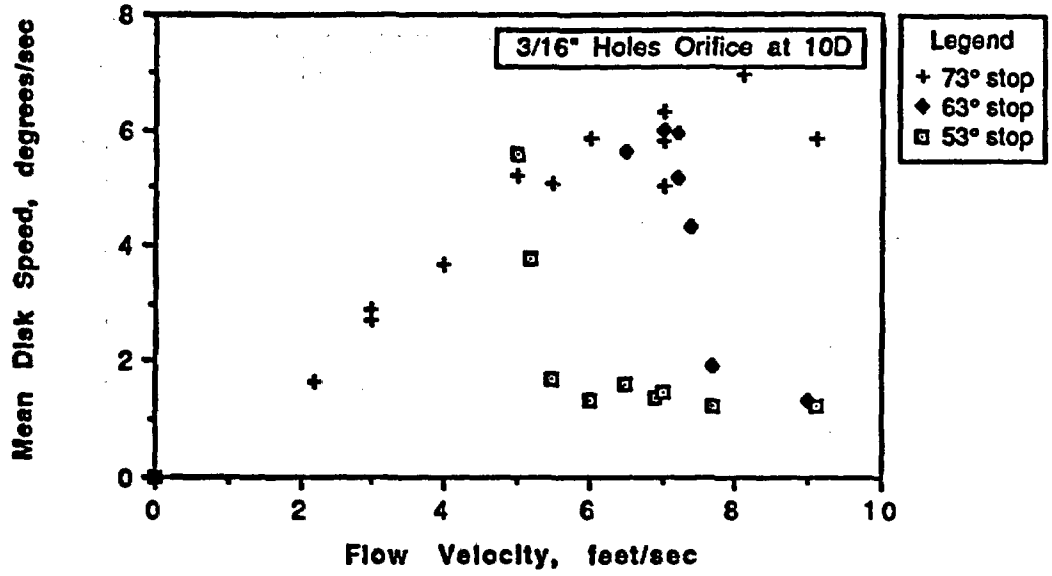

Figure D.43
3" Valve Mean Disc Speed
(3/16" Holes, Orifice Plate at 10D)

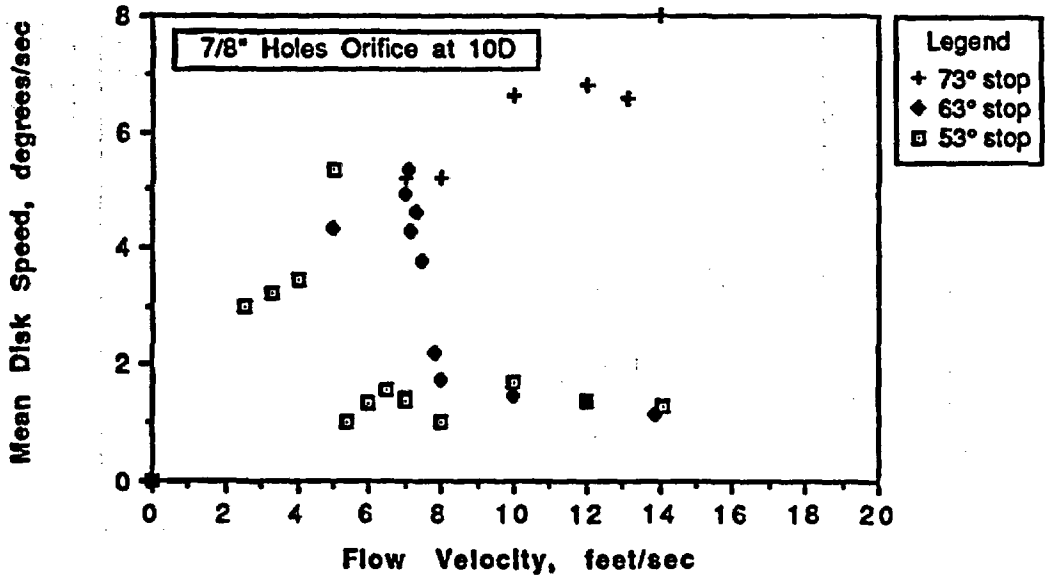

Figure D.44
3" Valve Mean Disc Speed
(7/8" Holes, Orifice Plate at 10D)

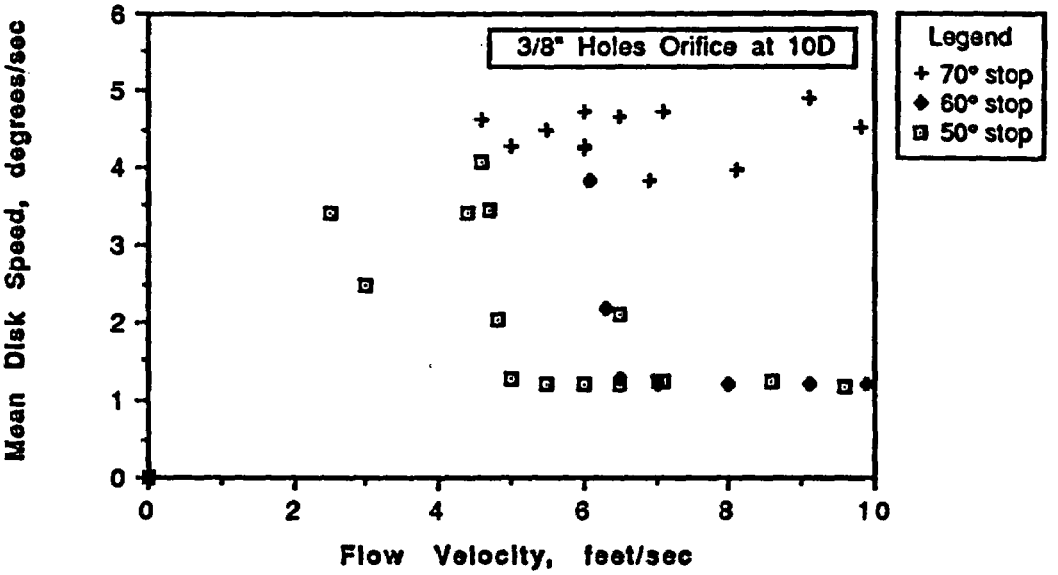

Figure D.45
6" Valve Mean Disc Speed
(3/8" Holes, Orifice Plate at 10D)

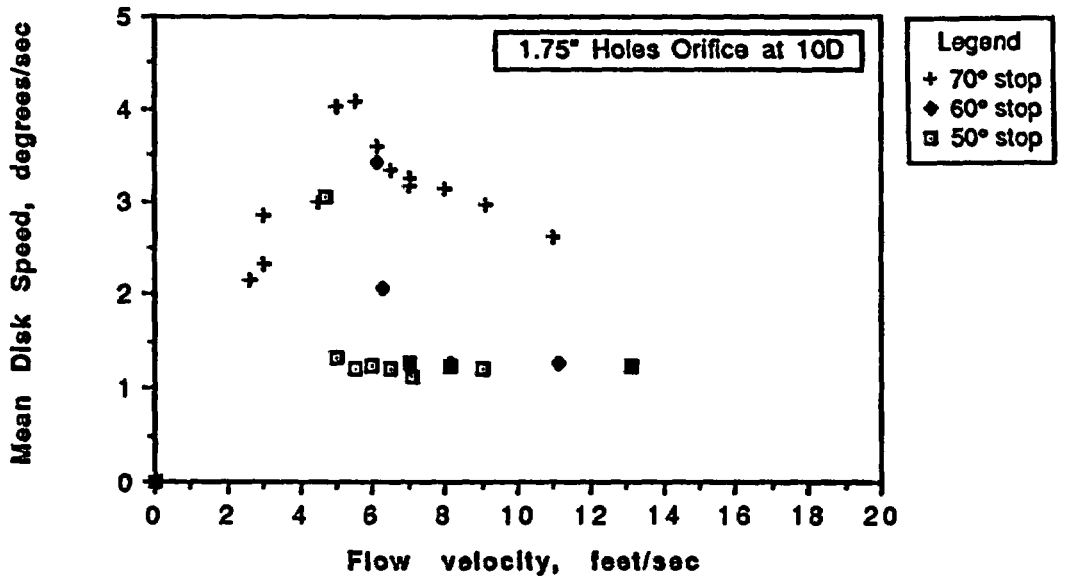

Figure D.46
6" Valve Mean Disc Speed
(1.75" Holes, Orifice Plate at 10D)

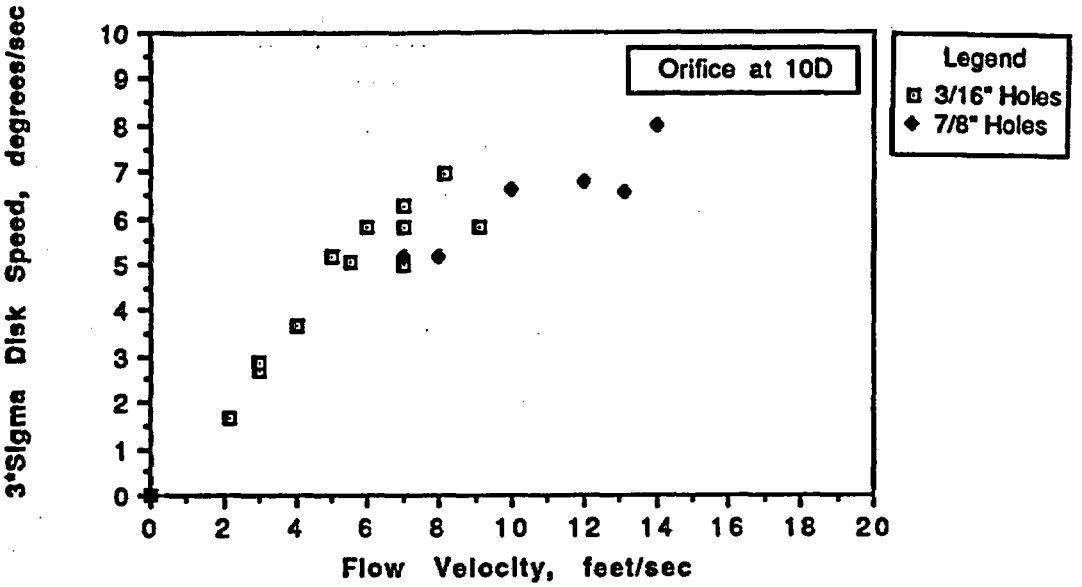

Figure D.47
3" Valve 3-Sigma Disc Speed
(Orifice Plate at 10D)

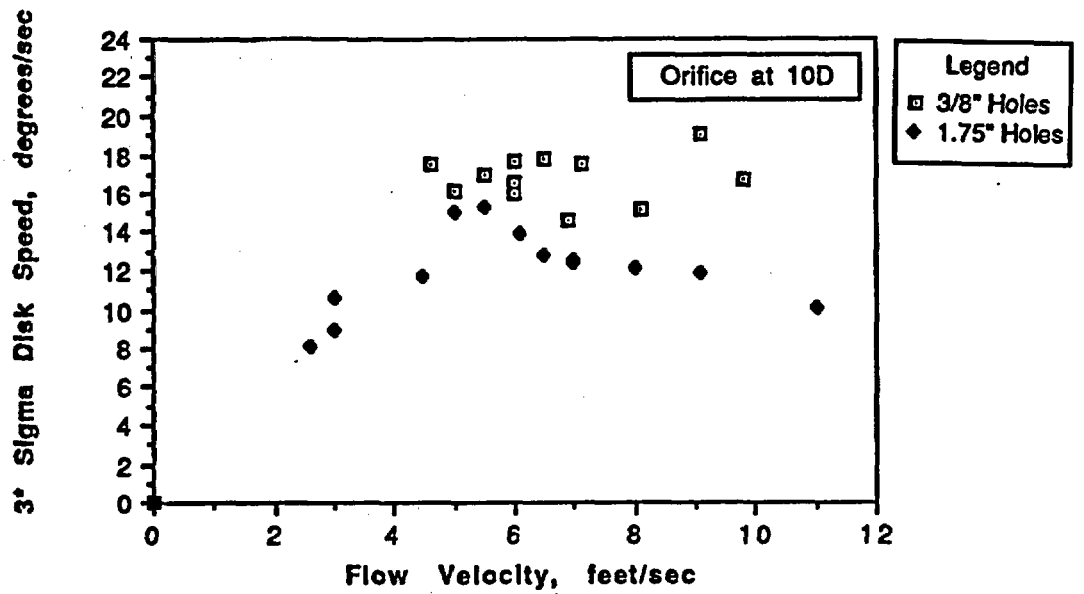

Figure D.48
6" Valve 3-Sigma Disc Speed
(Orifice Plate at 10D)

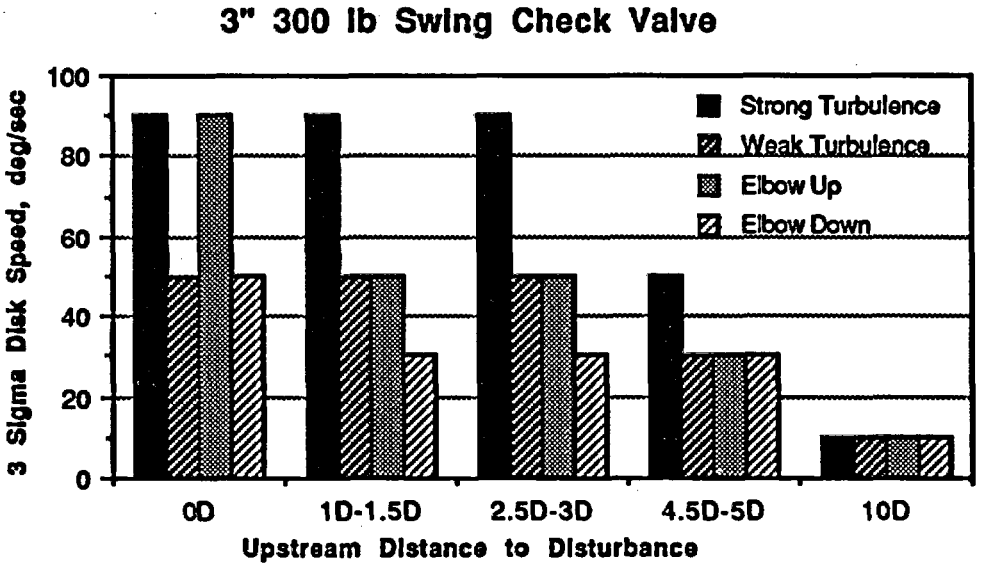

Figure D.49

3-Inch Valve: Relative Severity of Various Upstream Disturbances Expressed in Terms of 3 Sigma Disc Speed

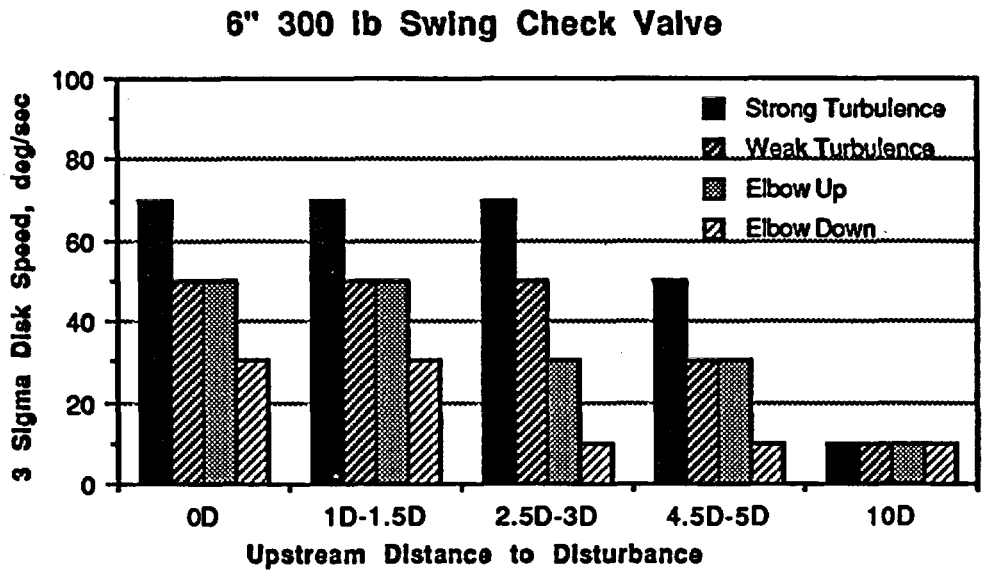

Figure D.50

6-Inch Valve: Relative Severity of Various Upstream Disturbances Expressed in Terms of 3 Sigma Disc Speed

NRC FORM 335 (2-89) NRCM 1102, 3201, 3202

U.S. NUCLEAR REGULATORY COMMISSION

BIBLIOGRAPHIC DATA SHEET

(See instructions on the reverse)

1. REPORT NUMBER (Assigned by NRC, Add Vol., Supp., Rev., and Addendum Numbers, if any.)

NUREG/CR-5583
KEI No. 1656

2. TITLE AND SUBTITLE

Prediction of Check Valve Performance and Degradation in Nuclear Power Plant Systems -- Wear and Impact Tests

3. DATE REPORT PUBLISHED

MONTH: August | YEAR: 1990

4. FIN OR GRANT NUMBER

D2510

5. AUTHOR(S)

M.S. Kalsi, C.L. Horst, J.K. Wang, V. Sharma

6. TYPE OF REPORT

Technical

7. PERIOD COVERED *(Inclusive Dates)*

9/88 - 4/90

8. PERFORMING ORGANIZATION – NAME AND ADDRESS *(If NRC, provide Division, Office or Region, U.S. Nuclear Regulatory Commission, and mailing address; if contractor, provide name and mailing address.)*

Kalsi Engineering, Inc.
745 Park Two Drive
Sugar Land, Texas 77478

9. SPONSORING ORGANIZATION – NAME AND ADDRESS *(If NRC, type "Same as above"; if contractor, provide NRC Division, Office or Region, U.S. Nuclear Regulatory Commission, and mailing address.)*

Division of Engineering
Office of Nuclear Regulatory Research
U.S. Nuclear Regulatory Commission
Washington, DC 20555

10. SUPPLEMENTARY NOTES

11. ABSTRACT *(200 words or less)*

Check valve failures in nuclear power plants have led to safety concerns as well as extensive damage and loss of plant availability in recent years. Swing check valve internals may experience premature degradation if the disc is not firmly held open against its stop and significant flow disturbances are present upstream within 10 pipe diameters. The objective of the current Phase II research was to develop and experimentally verify a quantitative methodology for predicting swing check valve performance and the degradation of internals caused by hinge pin wear or disc stud impact. Phase I research had focussed on investigating the stability of the swing check valve disc at different flow velocities for a wide variety of upstream flow disturbances located within 10 pipe diameters of the check valve. Valve performance predictions based on methodology developed as a result of Phase I and II research correlate well with actual valve operating history at plants. The conservative guidelines provided by this methodology, tempered and refined by actual performance history and integrated with preventive maintenance activities, have the potential for significantly improving the overall reliability of check valves in nuclear power plants.

12. KEY WORDS/DESCRIPTORS *(List words or phrases that will assist researchers in locating the report.)*

check valve behavior
check valve degradation
aging research
wear and impact on check valves

13. AVAILABILITY STATEMENT

Unlimited

14. SECURITY CLASSIFICATION

(This Page) Unclassified

(This Report) Unclassified

15. NUMBER OF PAGES

16. PRICE

UNITED STATES
NUCLEAR REGULATORY COMMISSION
WASHINGTON, D.C. 20555